URODYNAMICS

The Mechanics and Hydrodynamics of the Lower Urinary Tract

Second Edition   **D J GRIFFITHS**

$$p = p(\gamma)$$

Pressure

p_0 a

p b   c

ICS
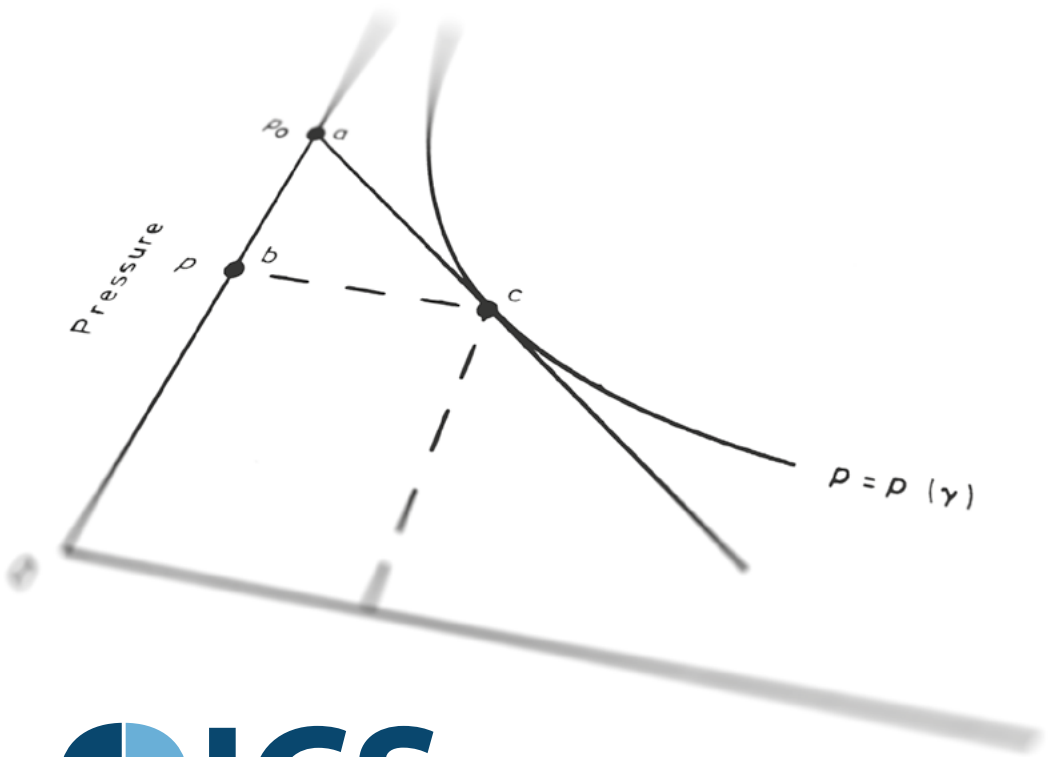
Urodynamics
The Mechanics and Hydrodynamics of the Lower Urinary Tract
D J Griffiths
Erasmus University, Rotterdam

Contents

About The Author

Derek earned his PhD in physics at St Andrews University, and regularly commuted from Exeter to the Middlesex Hospital in London in the early 1970's, where he analysed many urodynamic studies and collaborated with the Urology Research Fellows Patrick Bates and subsequently, Ted Arnold.

Derek established a productive cooperation with Paul Abrams in Bristol.

He studied pressure and flow in elastic tubes and wrote 'Urodynamics: the mechanics and hydrodynamics of the lower urinary tract' (1980)

He helped to refine the urethral resistance into concepts relating to the urethra and the bladder: the Urethral Resistance Relation and the Bladder Output Relation to describe the biomechanical balance during voiding. In collaboration with Paul Abrams they developed the well-known Abrams-Griffiths nomogram, in defining whether a slow flow rate indicated obstruction or poor detrusor contractility.

He moved to the Erasmus Hospital in Rotterdam to the Clinical Physics Department working with Ron Van Mastrigt and others, before moving again, to Edmonton, Canada. He held appointments there and in Pittsburgh latterly working in the brain imaging field.

From 1977 to 1987, while working in the Academic Hospital and the Erasmus University in Rotterdam, he made important contributions to basic and clinical urodynamics. When he moved to Rotterdam he already was well known for his description of the principle of the "collapsible tube" which is crucial for the understanding of "subvesical obstruction". He developed the bladder contractility parameter $W_{(max)}$ and the urethral resistance parameter URA. These parameters could be expressed on a continuous scale, unlike the categorical Abrams-Griffiths nomogram and the Schäfer-grades.

Derek Griffiths and Roel Scholtmeijer, a pediatric urologist from Rotterdam, described the association between detrusor instability (overactivity) and vesico-ureteric reflux (VUR) in children. VUR could now be categorized in two entities: active and passive reflux. This had important implications for the choice of treatment.

Derek Griffiths served on several ICS standardization committees and as a basic scientist on the scientific committee on several occasions.

He has clarity of thought and could explain difficult physics concepts to clinicians - not an easy task. He has taught regularly in courses aimed to improve the standard of urodynamic studies all around the world. Through an interest in children with enuresis and voiding dysfunction and subsequently with geriatric patients and incontinence, he went on to focus on central neuro-physiological tests and in particular functional MRI studies, in patients with lower urinary tract symptoms.

He has been a regular contributor at ICS meetings.

His contribution to understanding and to the ICS has been enormous.

Adapted from ICS History 1971-2010 Ted Arnold, Eric Glen, Norman Zinner

Foreword to Second Edition

When I became interested in the late 1970s in the mechanics and hydrodynamics of the lower urinary tract, I was astonished to find that clinician researchers were making measurements of mechanical quantities and interpreting them clinically with only the flimsiest of theoretical bases. The behaviour of pressures and flows, especially during voiding, seemed to be quite extraordinary and urgently to require explanation. It appeared to me then that whenever unexpected behaviour was encountered, a new "reflex" would be invented to account for it, whereas I was convinced that there must be a purely mechanical explanation for the basic features of the behaviour.

The work described in this book was thus my attempt to shore up the theoretical foundations of what the publishers insisted on calling by the new-fangled term "urodynamics." The first edition became the first real urodynamics textbook. It was aimed at students of physics interested in clinical medicine and was quite highly mathematical, but to my surprise it was purchased by nearly every physician with a serious interest in the field. Subsequently it has been out of print for many years.

Since the first edition appeared 34 years ago I have gathered much more experience of performing and teaching urodynamics, and if I wrote the book now I would show more extensively how the theoretical arguments actually work out in clinical practice. Further, the theory of flow through collapsible or distensible tubes has been extended to cover viscosity-dominated flow (as opposed to the inviscid-fluid flow on which this book is based), and in particular peristaltic flow through the ureter. In addition some of the terminology has been superseded. Those critical locations where the flow through a distensible tube potentially is controlled, named

"elastic constrictions" or "compressive zones" in the book, were renamed "flow-controlling zones" by the late Tage Hald. This descriptive if slightly misleading name (because the control is only *potential*) seems to have stuck. The rather light-hearted description of the different flow regimes as "sonic", "subsonic" or "supersonic" has been replaced by the more prosaic "critical", subcritical" and "supercritical." The terms "periurethral sphincter" and "distal intrinsic urethral sphincter," used in the book, might more properly be "striated urethral sphincter," or "urethral sphincter mechanism" (if the smooth muscle of the proximal urethra were to be included). With these exceptions, however, the book has stood the test of time remarkably well, and I am delighted that the ICS has issued this second edition. Apart from correction of a few typographical and scanning errors it is a reprinting of the first edition. It remains to be seen whether a modern urological/gynaecological audience will appreciate the mathematics as much as their predecessors did. At the very least they may be glad to know that "there's science beneath those confusing urodynamic measurements."

I am grateful to Chris Chapple and Adrian Wagg for pursuing this project, and especially to Dominic Turner, Roger Blackmore and Ashley Brookes for digitizing the first edition and helping to edit the resulting text.

D J Griffiths

Edmonton, Alberta

Preface to First Edition

The editors of a recent book on clinical urodynamics (Turner-Warwick and Whiteside 1979) suggest that 'We are so far from real understanding of so many things that, for the time being, we should... accumulate accurate clinical observations on the one hand, keeping them quite separate from our concepts of function on the other... Advance comes as a result of developing hypotheses, best conceptually held in the right hand, and continually testing them against observed facts in the left.'

If theirs is a left-handed book, full of the observed urodynamic facts, this book is its right-handed complement, an attempt to show how far the facts can be accounted for by simple mechanical concepts. While writing it I have had in mind a student of physics, interested in the subject but without much medical or physiological knowledge. I have tried to lead him (or her) to the point where he can himself intelligently interpret urodynamic measurements and communicate with clinical colleagues. On the way he will have learned something about the peculiarities of flow in highly distensible tubes and the mechanical behaviour of smooth muscle.

I cannot possibly mention all who have helped me during twelve years of urodynamics. I am especially grateful to the colleagues in Exeter and London who encouraged me at the beginning, to my students, to my present colleagues in Holland and Belgium, and to my wife.

D J Griffiths

1 The Lower Urinary Tract

1.1 Anatomy and Function

1.1.1 Introduction

The human urinary tract is a system of tubes, valves and reservoirs which guides and propels urine from the kidneys to the outside world. In the kidneys urine is formed continuously, so that the body's fluid and chemical balance is maintained.

Figure 1.1 is a diagram of the system in a girl. Each kidney is connected to a ureter, a long muscular tube through which the urine passes into the bladder. Normally the ureter remains closed for much of the time; every few seconds a bolus of urine passes along it and into the bladder, propelled by a wave of muscular contraction in the ureteral wall.

The urine gradually accumulates in the bladder. The urethra, the tube which leads from the bladder to the outside world, is kept shut by muscular contraction. The degree of fullness of the bladder is sensed by the nervous system. When a considerable volume has accumulated, up to 350-500 ml, and at a socially convenient moment, micturition occurs. That is, the muscular walls of the bladder are voluntarily made to contract so that it acts as a pump and expels the urine through the urethra into the air. Simultaneously the urethra relaxes to allow the urine to pass. The rate of outflow rises typically to about 25 ml s^{-1}. Backflow ('reflux') into the ureters is normally prevented by a non-return valve at the junction of each ureter with the bladder. When the bladder has been emptied its wall relaxes and it returns to its storage function. The urethra closes again.

This complicated system not only transforms the automatic, continuous production of urine into an intermittent, voluntary expulsion, but also protects the delicate structure of the kidneys both from excessive back-pressure and from infection. Urine is normally sterile, but because it consists of a solution of waste products in water it can become colonised by bacteria. The urethra is the first line of defence against bacterial invasion from outside. Should urine in the bladder become infected, the non-return property of the ureters prevents infection from reaching the kidneys.
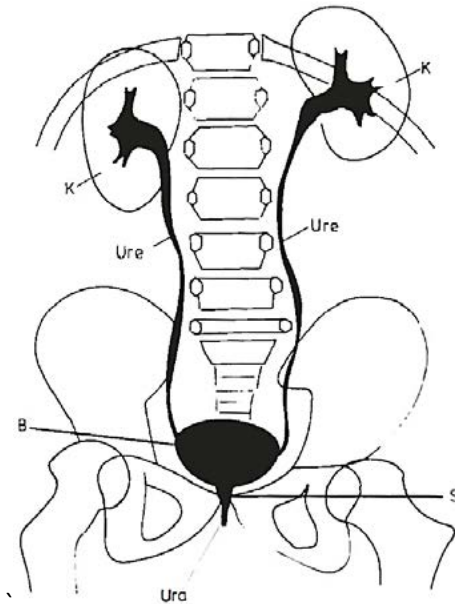
Figure 1.1 The urinary system of a girl, as seen from the front on x-ray. Both upper and lower tracts are shown as if filled with contrast medium (black). **K**, kidneys; **Ure**, ureters; **B**, bladder; **Ura**, urethra; **S**, symphysis pubis. The individual vertebrae of the lumbar part of the spinal column are visible. The sacral column lies just above and also behind the bladder, and has less distinct vertebrae. The thoracic column begins at the top of the figure.

The kidneys, the ureters and the bladder all lie inside the abdomen, the body cavity which contains also the stomach, intestines and rectum. It is bounded by sheets of partly muscular tissue: at the top by the diaphragm and at the bottom by the pelvic floor and urogenital diaphragm. The urethra passes through the urogenital diaphragm and so lies partly inside and partly outside the abdomen. The base of the bladder lies just above the pelvic floor/urogenital diaphragm and is usually roughly level with the upper edge of the bony structure known as the *symphysis pubis*, which therefore forms a convenient reference point and a landmark which is visible on x-rays (figure 1.1).

This book is concerned only with the lower urinary tract: the bladder and the urethra, alternately a reservoir with a closed outlet, and a pump emptying through a tube. Both organs are muscular, so that their mechanical behaviour is altered and coordinated by the nervous system. The bladder wall consists of smooth muscle; the urethral wall and surrounding muscles contain two types of muscle, both smooth and striated. Typical smooth muscles, such as the muscle of the stomach, are slow-acting and slow to fatigue; they contract and relax automatically, without conscious control. The smooth muscle of the bladder is unique because, although its intermittent contractions are automatic in babies, conscious control of micturition is normally learned during childhood. Typical striated muscles, such as the biceps, are under conscious control and are faster acting; they are quicker to fatigue, so that they cannot so easily maintain tension for long periods.

Accounts of the anatomy of the lower urinary tract are given by Tanagho (1971) and Gosling (1979). Very clear anatomical pictures may be found in Netter (1965).

1.1.2 The bladder

The bladder is, very approximately, a hollow sphere with an internal radius of up to about 5 cm. The total volume of tissue in the wall

remains very nearly constant, independent of the internal radius, so that the thickness of the wall depends on the radius. It is typically a few mm. Obviously the bladder cannot remain spherical right down to zero internal volume: below about 100ml the wall begins to fold up. The volume of urine remaining inside the bladder when it has contracted as far as possible is probably only one or two ml. Thus in normal micturition the bladder empties essentially to completion.

The wall of the bladder consists mainly of one smooth muscle, the detrusor. It is pierced by the urethra near the centre of its base and also by the two ureteral orifices, which lie one on each side near the back of the base (see figures 1.3 and 1.4). The triangular region between these three orifices is lined with an anatomically different smooth muscle, the trigone. The functional differences between the detrusor and the trigone are not entirely clear, but the mechanical properties of the bladder are essentially those of the detrusor.

The separate muscle fibres are easily visible in the detrusor. They run mainly tangentially within the bladder wall in overlapping whorls. Thus at a given point around the circumference of the bladder there are fibres running in several tangential directions. When a muscle fibre contracts it develops a longitudinal tension. The resultant of the individual tensions in a contracting bladder is therefore an approximately uniform 'surface tension' within the wall, isotropic in the two tangential dimensions. This 'surface tension' generates a uniform pressure within the approximately spherical bladder, just as surface tension gives rise to the excess pressure within a soap bubble.

Near the opening into the urethra the fibres of the detrusor are arranged in oriented layers in a more ordered manner. Together with some parts of the trigone and of the urethral smooth muscle they form the structure called the bladder neck, the most proximal part of the urethra, as shown in figures 1.3 and 1.4. Clearly the disposition of these fibres may be of importance for the opening of the bladder neck

when the detrusor contracts for micturition. This function of the bladder neck is discussed further in §§6.3 and 9.5.

If the bladder is idealised as a thin-walled sphere of radius R, having a tangential surface tension T' per unit width, then the total tension T in the whole circumference, as shown in figure 1 .2, is

$$T = 2\pi RT'. \tag{1.1}$$

Static equilibrium of forces demands that the excess pressure within the bladder, over that of its surroundings, is given by

$$\pi R^2 p_{det} = T \tag{1.2}$$
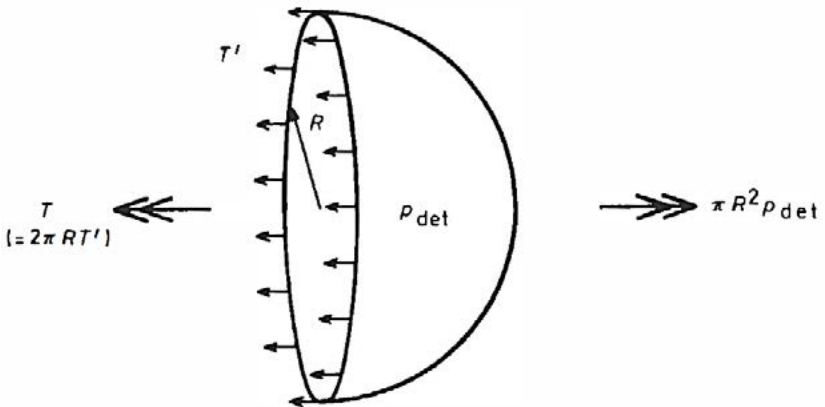
Figure 1.2 Equilibrium of forces for a half-bladder.

(Drolet and Kunov 1975). The symbol p_{det} indicates that this pressure is developed by tension in the detrusor. Its origin and properties are discussed in §2.2 and in Chapter 10. It will be assumed that equation (1.2) is valid even when fluid is flowing out of the bladder, when in fact there are small departures from static equilibrium.

1.1.3 The urethra

The structure of the urethra is different in the two sexes. The male urethra has an additional sexual function.

In both sexes the urethra is a distensible, partly muscular, curved tube. At rest the walls are folded up and it is closed. The crannies between the folds are sealed with a sticky, viscous fluid secreted by the urethral lining, the mucous membrane, so that the urethra is watertight when shut. During micturition it opens. The cross-section is not circular and is different in different parts of the urethra, but its effective diameter is a few mm.

1.1.3.1 The female urethra. The female urethra is about 4 cm long; the walls of the urethra proper are up to about 5 mm thick (see figure 1.3). Much of the inner part of the wall is composed of smooth muscle. Most of the fibres run in a longitudinal direction, but there is a thin outer layer of circularly oriented fibres. The smooth muscle is surrounded, especially at the front and sides of the urethra, by a layer of striated muscle fibres which runs within the urethral wall in a circular (tangential) direction.

The function of these muscles is disputable. In the past it was commonly believed that there was an 'internal urethral sphincter', a ring-shaped smooth muscle which, by sustained contraction, kept the resting urethra shut. Figure 1.3 shows, however, that there is no smooth muscle well placed to perform this function. The smooth muscle near the bladder neck is mainly associated with the bladder,
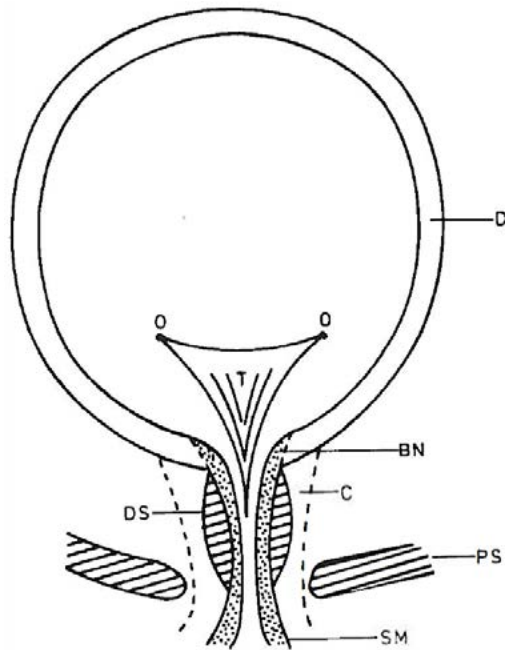
Figure 1.3 Schematic diagram of a section through female bladder and urethra, viewed from the front. **D**, detrusor smooth muscle; **T**, trigone; **SM**, urethral smooth muscle; **DS**, distal intrinsic urethral sphincter (striated muscle) ; **PS**, periurethral sphincter (striated muscles of the pelvic floor/urogenital diaphragm); **C**, connective tissue; **BN**, bladder neck; **O**, ureteral orifices. (After Gosling 1979.)

and therefore presumably contracts not at rest but during micturition. The smooth muscle near the middle of the urethra is mostly longitudinal in orientation, whereas a circular orientation would be expected for a sphincter. It seems more likely that the circularly oriented striated muscle layer acts as a sphincter, by sustained contraction at rest. Although typical striated muscles fatigue quickly,
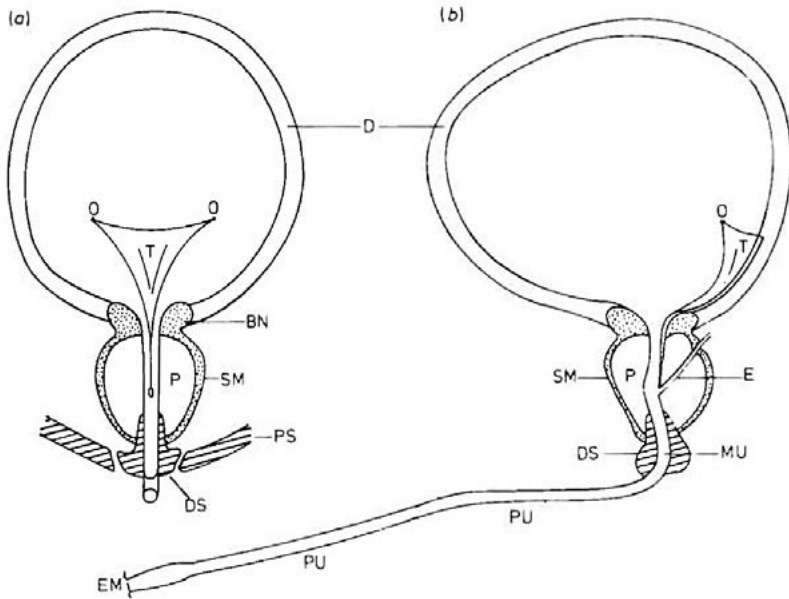
Figure 1.4 Schematic diagrams of sections through male bladder and urethra, viewed (a) from the front, and (b) from the left side. **O**, detrusor smooth muscle; **T**, trigone; **SM**, urethral smooth muscle; **OS**, distal intrinsic urethral sphincter (striated muscle); **PS**, periurethral sphincter (striated muscles of the pelvic floor/urogenital diaphragm); **BN**, bladder neck; **P**, prostate gland; **MU**, membranous urethra: **PU**, penile urethra; **EM**, external meatus: **E**, ejaculatory duct; **O**, ureteral orifices. (After Gosling 1979.)

this particular muscle is of a type which fatigues less readily. It may be called the distal intrinsic urethral sphincter.

Outside the urethral wall proper, the middle part of the urethra is surrounded by the periurethral striated muscles of the pelvic floor and urogenital diaphragm. These muscles probably can exert a sustained contraction, as well as a briefer, easily fatigued contraction which can be used to shut the urethra during micturition or to hinder undesired

leakage if the bladder should involuntarily contract. This fast action is usually assigned to the 'external urethral sphincter', but the term is potentially confusing (Turner-Warwick 1979). A better term is 'periurethral sphincter'. In addition, the pelvic floor and urogenital diaphragm support the bladder within the abdominal cavity.

1.1.3.2 The male urethra. The male urethra is much longer than that of the female, typically about 17 cm (figure 1.4). The distal part − the penile urethra and the external meatus − is mainly non-muscular. It will be considered here as a purely passive distensible conduit, although its mechanical properties can certainly be altered, as during erection. The more proximal parts are analogous to the female urethra.

The bladder neck is much more strongly developed than in the female. Circularly oriented smooth-muscle fibres form a pronounced ring around the urethral orifice. Distal to this, the walls of the prostatic part of the urethra are thickened to form the prostatic capsule, a partly smooth-muscular structure at the entry into the urethra of the ducts for the ejaculate. Some fibres of the detrusor are probably anchored to it. The prostatic capsule merges into the smooth muscle of the wall of the membranous urethra, where the fibres are mostly longitudinally oriented, as in the female. Here there is again an outer layer of circularly oriented fibres of striated muscle, which also extends proximally around the prostatic capsule. Periurethral striated muscles are present, as in the female. The fast action of the periurethral sphincter is much more powerful than in the female.

1.1.4 Nervous control

The muscles of bladder, urethra and pelvic floor are controlled and coordinated by the nervous system. The innervation is complicated and debatable; only a simplified account is given here (see Gosling 1979).

The nomenclature is confusing; figures 1.5 and 1.6 are an attempt to make it clearer. A detailed grasp of the material set out in this section is not at all necessary for the understanding of the rest of the book. It is however vital if one is to understand the medical literature.

In many parts of the body the striated muscles are under conscious control by the fast-acting *somatic* nervous system, while the slower-acting smooth musculature is controlled unconsciously by a separate system, the *autonomic* nervous system. The latter can in turn be divided into two branches, *sympathetic* and *parasympathetic*. Many smooth muscles show spontaneous oscillatory activity, and receive innervation from both branches, which modify the activity in different ways. These branches are sometimes referred to by the names of the chemical transmitters by which the signals are transmitted from the
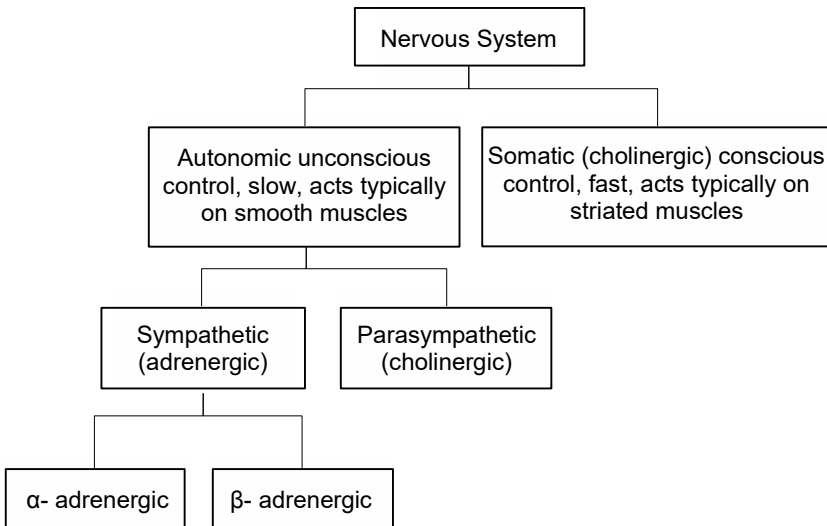
Figure 1.5 Nomenclature and organisation of the nervous system, simplified.

nerves to (e.g.) a muscle. The sympathetic system is *adrenergic* (chemical transmitter noradrenaline or a similar substance); the parasympathetic system is *cholinergic* (chemical transmitter acetylcholine or a similar substance). To add to the confusion, the somatic system is also cholinergic (see figure 1 .5). The sympathetic branch of the autonomic system can itself be divided into two sub-branches, called respectively *α-adrenergic* and *β- adrenergic*, which may have different effects or may act on different parts of the same organ.

This system carries *motor* or *efferent* nervous impulses from the central nervous system (the spinal cord and brain) to the organ, which thus may be activated, inhibited or otherwise affected. In addition there are *sensory* or *afferent* impulses which carry information about the condition of the organ back to the central nervous system, so forming feedback loops. Efferent and afferent impulses are carried by different nerve fibres, but usually follow the same nervous pathways. Thus a so-called 'nerve' is a bundle of nerve fibres which carries signals in both directions.

Like many other smooth muscles, an isolated bladder or strip of detrusor muscle shows spontaneous mechanical activity. However, a sustained and coordinated contraction does not usually occur without external stimulation.

It is generally agreed that the coordinated contraction associated with micturition is produced by stimulation of the detrusor by motor impulses from the *pelvic* nerves, which run from the lowest (sacral) part of the spine to the bladder (see figure 1 .6). These nerves form part of the parasympathetic branch. At the same time, some of the urethral and periurethral striated muscles relax so allowing flow to pass more easily. These urethral muscles also receive parasympathetic innervation via the pelvic nerves, which presumably inhibits their sustained contraction when the detrusor is stimulated to contract. The

picture is of a *micturition reflex*, a simultaneous contraction of the detrusor and relaxation of some of the (peri)urethral muscles, which is coordinated at a micturition centre in the sacral part of the spinal cord. The feedback input tending to trigger the reflex is believed to be an afferent signal in the pelvic nerve, originating from receptors in the bladder wall which are stimulated as the bladder fills with urine. If this were all, micturition would occur automatically at a certain bladder volume, when the signal from the receptors reached a certain trigger level. This may in fact be the case in babies and in people with certain types of spinal injury. However, the spinal centre coordinating the reflex is also subject to learned voluntary control, descending from the brain via the spinal cord, so that the trigger level can be voluntarily adjusted, and so the bladder volume at which micturition occurs can be controlled at will, within limits.

The bladder and urethra are also influenced by the sympathetic branch of the autonomic nervous system, via the hypogastric nerves which originate from near the middle (thoracic/lumbar) part of the spinal cord. Sympathetic efferent signals inhibit contraction of the detrusor between micturitions and keep the urethra shut by stimulation of the urethral (smooth) muscle. Both α- and β-sub-branches appear to be involved. Since there is relatively little direct sympathetic innervation of the smooth muscle of bladder or urethra, the sympathetic branch probably acts indirectly via the parasympathetic innervation, by means of interconnections between the two branches (ganglia).
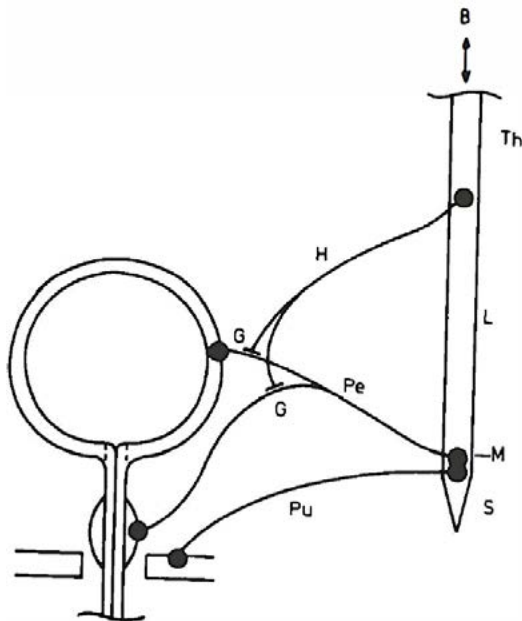
Figure 1.6 Innervation of lower urinary tract. **B**, brain; **Th**, **L**, **S**, thoracic, lumbar and sacral parts of spinal cord ; **H**, hypogastric nerve (sympathetic); **Pe**, pelvic nerve (parasympathetic); **Pu**, pudendal nerve (somatic); **M**, sacral micturition centre; **G**, ganglia. In the male there is also direct sympathetic innervation of the bladder neck and prostate, probably with sexual function.

The periurethral striated muscles, forming the periurethral sphincter, can be consciously stimulated to contract by the somatic nervous system via the pudendal nerves, which originate, like the pelvic nerves, from the sacral part of the spine. They may also play a part in the micturition reflex.

1.1.5 Functional changes

The lower urinary tract described above is clearly a far from passive system. Its mechanical properties can be altered by stimulation or inhibition of many different muscles and even by changes in blood flow. Such alterations are called functional changes. They can come about also through the mechanical influence of the structures surrounding the urinary tract.

The most important influence is that of the abdomen within which the bladder is situated. Because the bladder wall is flexible, pressure changes in the abdomen are transmitted to the urine in the bladder. The pressure in the bladder is therefore the sum of two contributions:

$$p_{ves} = p_{det} + p_{abd}. \qquad (1.3)$$

The detrusor pressure p_{det} is that contribution to the intravesical pressure p_{ves} which comes from the stresses in the bladder wall. A simple expression for it has been given in equation (1.2). The abdominal pressure p_{abd} is the contribution to p_{ves} from the surrounding abdomen. Equation (1.3) is further discussed in §2.2.

The proximal part of the urethra, above the urogenital diaphragm, is subject to abdominal pressure, while the distal parts are not. Therefore changes in abdominal pressure alter the distribution of pressure along the lumen of the urethra. Urethral pressure is considered in §2.2.5.

The abdominal pressure is lowest at rest in a supine position. It is higher in the sitting and standing positions. It increases during activities such as talking, coughing, sneezing, blowing, lifting and abdominal straining. All these activities cause functional changes of pressure in the bladder and urethra.

1.2 Pathology

1.2.1 Types of complaint

Patients come to urologists with complaints such as incontinence (unwanted leakage of urine), urgency or too frequent micturition, painful micturition, blood in the urine, a poor stream or total inability to pass water. Behind the symptoms may lie any condition from a simple mechanical defect in the urinary tract to a malfunctioning of the neuromuscular control system, alone or occurring together, and perhaps associated with an infection of the urine or a more general neurological disease.

Some of these conditions—especially incontinence—are socially disabling rather than threatening to life. They cause a great deal of unhappiness, but their treatment is not very heroic or glamorous. Probably for this reason urodynamics has been relatively neglected in the past. Some conditions however—for example, those leading to chronic urinary infection—are serious because damage to the kidneys can cause death.

1.2.2 Common non-neurological conditions

A purely mechanical weakness of the urethra is quite common in women. It results in involuntary loss of urine when the abdominal pressure is raised, as during coughing, sneezing or lifting a weight. The condition is called stress incontinence or, rather, genuine stress incontinence to distinguish it from another condition with similar symptoms, described below. It is discussed further in §6.2.

The longer and more powerful male urethra is not so subject to mechanical weakness but frequently becomes obstructed. Its resistance to flow is raised and micturition occurs with a reduced flow rate and a raised bladder pressure. The bladder may respond with

hypertrophy—the detrusor becomes more massive and stronger—and also by becoming more difficult to control, so that active contractions occur involuntarily. The symptoms may include not only a poor stream and painful micturition but also frequent micturition, waking to pass water at night, and the feeling of urgency to pass water. If such contractions can be objectively demonstrated in the clinic, the bladder may be called unstable or hyperreflexic. (The precise definitions of these terms are subtle; see Turner-Warwick 1979.) After the obstruction has been surgically removed the bladder may revert to stable behaviour. If it does not do so, the now mechanically weakened urethra may be unable to withstand the involuntary detrusor contractions, so that leakage—incontinence—occurs. Obstruction may occur at the bladder neck (seen mostly in younger men), in the prostatic urethra through growth of the prostatic capsule (in older men), in the membranous urethra (as a congenital anomaly in young boys and babies), in the penile urethra, or at the external meatus. Obstruction is considered in Chapter 9.

An unstable bladder is often found in females without obvious cause. They may complain of urgency of micturition, or of incontinence associated with urgency. They may have the symptoms of stress incontinence, since a cough (for example) may trigger an involuntary detrusor contraction and a second cough then causes a leak. Leakage of this type is discussed in §6.2.2.

1.2.3 Neurological conditions

Diseases of the nervous system, congenital abnormalities of the spinal cord and spinal cord lesions due to injuries can have drastic effects on the functioning of the urinary system (and other organs). Neuropathic bladder is a term encompassing all peculiarities of the lower urinary tract caused in this way.

The location of the damage in the nervous system is decisive in determining its effect on the bladder and urethra (see Thomas 1979). As can be seen from figure 1.6, a break in the spinal cord above the level of the sacral micturition centre destroys sensation and conscious control of micturition, but leaves the micturition reflex intact, so that automatic activity is possible. Such damage is called an upper motor neurone lesion. A lesion that destroys the sacral micturition centre itself, or interrupts its connections with the bladder and urethra, certainly destroys the coordination of detrusor and urethral musculature and may prevent all detrusor activity. This is called a lower motor neurone lesion. In practice, the lesions may be partial rather than complete, and the behaviour of bladder and urethra is complicated and may gradually change. Commonly, however, the bladder cannot be emptied completely. The residual urine forms a breeding ground for bacteria, which may lead eventually to chronic infection, kidney damage and the death of the patient.

1.3 Urodynamics

1.3.1 The aims of urodynamics

At a straightforward clinical level, urodynamic measurements have proved useful in diagnosis - for example, in distinguishing between two conditions previously regarded as one, such as genuine stress incontinence and incontinence associated with a detrusor contraction; in monitoring the progress of a disease - for example, neuropathic bladder; and in evaluating objectively the results of therapy - for example, the amount of urine lost by an incontinent patient may be measured before and after treatment, instead of relying on the patient's assurance that he or she is better (or worse), although this is also important.

Urodynamics has not so far been so successful in suggesting treatments for disease; it has produced the concept of the unstable

bladder, but there is no reliable treatment for it. The development of new treatments depends, partly, on understanding the normal and pathological behaviour of the system, and urodynamics is certainly indispensable at this research level. What it can give is an accurate understanding of the mechanical behaviour of the urinary tract, although this is not entirely straightforward because the high distensibility of the system puts it outside the range of standard engineering. The mechanical behaviour is modulated neuromuscularly in ways which are difficult to understand because of the complex anatomy and innervation. There is plenty of scope for confusion, and so a grasp of the purely mechanical behaviour is essential if progress is to be made in the neuromuscular field.

1.3.2 Outline of the book

The object of the book is to lay the foundations of such a sound mechanical understanding of the lower urinary tract, by a weaving together of theory, laboratory experiments and clinical observations. Physiological and clinical conclusions are drawn whenever possible, so as to provide a standpoint from which medical and physiological problems can be tackled.

After a short practical discussion of clinical measurements, there follows an explanation of the physics of fluid flow through a highly distensible tube, both theoretical and experimental. The theory is applied to the urethra under both normal and pathological conditions. The mechanical properties of the bladder are then outlined in a chapter which contains as much physiology as physics, since the peculiar properties of smooth muscle have to be taken into account. Clinical applications are described. Finally, the mechanical properties of urethra and bladder are put together to yield an understanding of the course of micturition.

The direction of the book is from the exact (physics) towards the inexact (the interpretation of medical observations). It therefore becomes more debatable as it goes forward. It is surely necessary, however, to travel in this direction if urodynamics is to be useful.

2 Clinical Measurements

2.1 The Urodynamic Examination

Micturition is an activity that is under conscious control, and therefore is studied in conscious patients. However, the control is exerted rather indirectly, via the autonomic nervous system (see § 1.1.4), and is easily interfered with. The very fact that measurements are being made can disturb a patient so that unrepresentative results are obtained, or none at all. This is the main difficulty in practice.

During a typical urodynamic examination, the pressure in the patient's bladder (the intravesical pressure, p_{ves}) is recorded by a fine catheter passing through the urethra or through the abdominal and bladder walls. Similarly, the pressure in the rectum or stomach is measured, and is taken to be representative of the abdominal pressure p_{abd}. The difference between the intravesical and abdominal pressure is the pressure contribution from stresses in the bladder wall, the detrusor pressure p_{det} (see equation (1 .3)).

At the beginning of the examination the patient's bladder is emptied if necessary. It is then slowly filled through a catheter with x-ray contrast medium or physiological saline solution, while the pressures are recorded (filling cystometry). Sometimes the bladder is filled with CO_2 gas, but its use will not be discussed here. Various manoeuvres may be tried in an attempt to provoke unstable contractions (§ 1.2.2). The filling catheter may then be withdrawn. The patient is asked to micturate into a device which measures and records the flow rate and the voided volume. At the same time the pressures are recorded, and the shape of the bladder and urethra may be observed and recorded (micturating cystourethrography). The patient may be asked to interrupt the stream for a few seconds before the bladder is finally
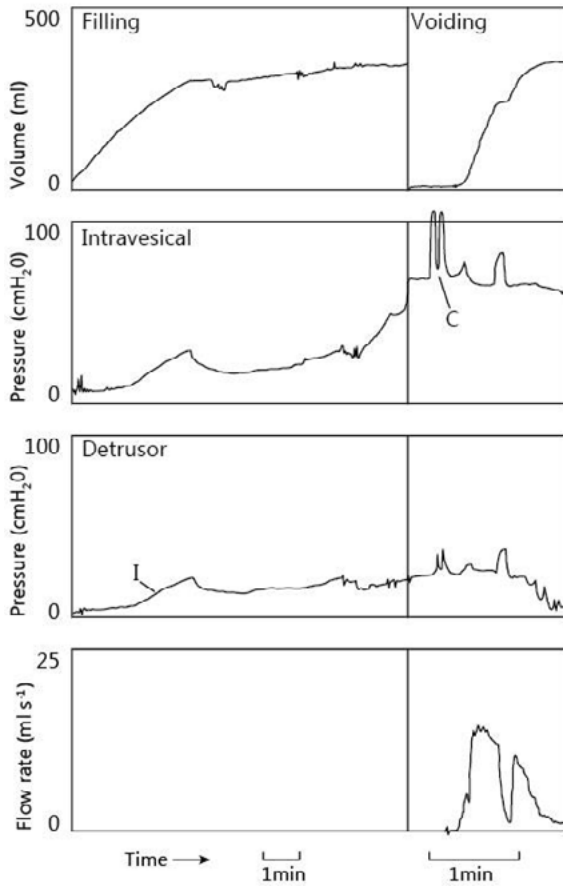
Figure 2.1 Record of pressures, flow rate and volume during urodynamic examination of a female patient, both filling and voiding. For simplicity, the record of abdominal pressure has been omitted. **I**, detrusor contraction (instability): **C**, cough. (Redrawn from Griffiths 1977 Br. J. Urol. 49 29-36, by permission of Br. J. Urol. and Longman Group Ltd.)

emptied. Figure 2.1 is a typical record of these events. Micturating cystourethrograms are shown in figure 2.2(a, b).
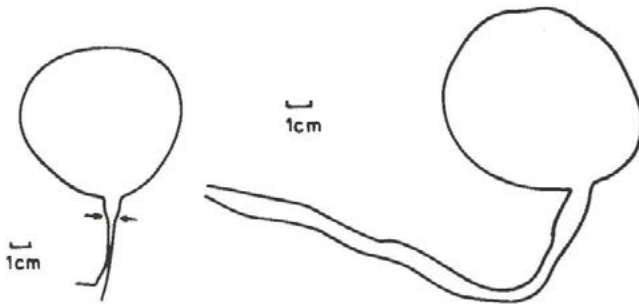
Figure 2.2 Outlines of bladder and urethra during micturition, traced from micturating cystograms of patients without urethral obstructions. a) Female (arrows mark the position of maximum urethral pressure measured at rest); b) Male (after Eyrick et al 1969).
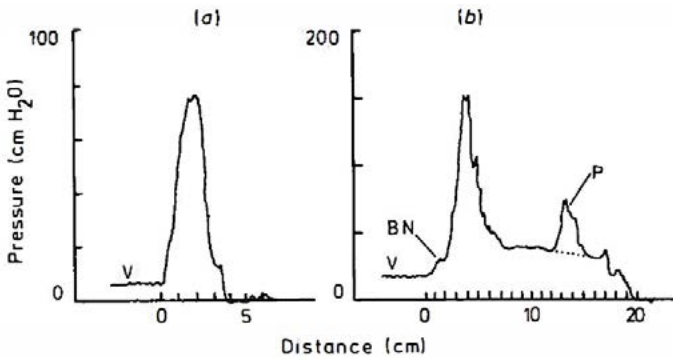
Figure 2.3 Outlines of bladder and urethra during micturition, traced from micturating cystograms of patients without urethral obstructions. a) Female (arrows mark the position of maximum urethral pressure measured at rest); b) Male (after Eyrick et al 1969).

Either before or after micturition the pressure exerted on a measuring device by the walls of the urethra may be recorded as the device is withdrawn through the urethra (the urethral closure pressure profile). Female and male urethral closure pressure profiles are shown in figure

2.3(a, b). Sometimes the electrical activity in the muscles surrounding the urethra, or elsewhere in the pelvic floor, may be measured by needles inserted into them or by superficial electrodes (the electromyogram, EMG).

The basic mechanical measurements that are made in a urodynamic study are thus extremely simple: pressure, volume and flow rate. There are however one or two peculiarities which require discussion.

2.2 Specific Measurements

2.2.1 Volume and flow rate

In giving the results of clinical measurements, volumes are expressed in ml. Flow rates are volume flow rates and are expressed in ml s^{-1} or ml min^{-1}. In theoretical calculations, where functions of volume and flow rate may occur, they should be expressed in standard SI units, m^3 and $m^3 s^{-1}$, respectively (1 ml = $10^{-6} m^3$).

During filling cystometry the volume of liquid introduced into the bladder may be measured directly. It should be remembered that additional fluid is entering the bladder from the ureters at an unknown rate (perhaps about 2 ml min^{-1}).

During micturition, the stream of voided liquid is collected by a flowmeter. Many flowmeters measure the voided volume in the first instance and calculate the flow rate by electrical differentiation of the volume signal with respect to time. The volume can be measured in many different ways. A few flowmeters measure the flow rate directly and produce a volume signal by electrical integration. In practice, most of these flowmeters perform quite similarly. They tend to have a rather long settling time (up to 1 s or more) because the liquid has to be gathered in a funnel before it is delivered to the collecting vessel. The funnel introduces variable smoothing, delay and distortion into

the measuring system. An ideal flowmeter would measure directly on the unimpeded stream, without a funnel. So far no such flowmeter exists, but the urinary drop spectrometer (§8.2) promises eventually to become one.

In addition to the flow rate, other measurements are sometimes made on the external stream, and these are considered in Chapter 8.

2.2.2 The pressure in the bladder

Pressures measured clinically are given in cm H_2O. In theoretical calculations they are expressed in Pa (1 cm $H_2O \cong 98$ Pa).

The liquid in the bladder, when in hydrostatic equilibrium, has a vertical, gravitational pressure gradient. The measured pressure must therefore be referred to a particular level. The intravesical pressure is defined as the pressure in the bladder, with respect to atmospheric pressure, measured at the level of the upper edge of the symphysis pubis (see figure 1.1). The relevant gravitational pressure differences are only a few cm H_2O, quite small compared with the micturition bladder pressure of from 20 to 100 cm H_2O.

Other pressures, measured with respect to atmospheric, may be referred to the same level. Where this is specifically intended they may be called piezometric pressures. The intravesical pressure is by definition piezometric.

How this works out in practice depends on how the pressure in the bladder is measured. A catheter-tip pressure transducer, for example, referenced to air, measures the pressure acting on the transducer (with respect to atmospheric). Its reading therefore depends on the vertical position within the bladder of the catheter tip. The position must be known if the reading is to be converted to the piezometric intravesical pressure.

Very often an external pressure transducer is used in conjunction with a liquid-filled catheter. Provided the density of the liquid in the catheter is similar to that of the liquid in the bladder, the reading is independent of the position of the catheter tip in the bladder, but does depend on the height of the external transducer. The transducer should be placed at the level of the upper edge of the symphysis pubis in order to register the intravesical pressure correctly.

2.2.3 The abdominal pressure

In § 1.1.5 the abdominal pressure was defined as the contribution to the intravesical pressure from the abdominal surroundings of the bladder:

$$p_{ves} = p_{det} + p_{abd}. \qquad [1.3]$$

Since this equation is often criticised it is worth examining it in detail. There is no doubt that in a static, fluid-filled bladder, p_{ves} exists, is easily measured and (remembering that it is piezometric) is uniform from point to point. It is a purely hydrostatic pressure without shear components. It is therefore sensible to define p_{det} and p_{abd} as purely hydrostatic pressures, averaged over the bladder so that they are uniform; p_{abd} is taken to be piezometric.

In practice, the difficulty lies in the measurement of p_{abd}. so that p_{det} can be calculated from equation (1.3). Clearly p_{abd} is an average of the stresses exerted by the surrounding structures on the bladder wall. These stresses are likely to be non-uniform and to have shear components which are to be removed by averaging. To avoid the difficulty of averaging, what is measured in practice is the hydrostatic pressure within a second cavity, inside the abdomen and as close to the bladder as practical. It is assumed that the intrinsic contribution to the pressure from the walls of the cavity can be neglected, so that the

measured piezometric pressure is in fact p_{abd} for the cavity. One hopes that this is also the value appropriate to the bladder.

Since the rectum is easily accessible (through the anus) and lies immediately behind the bladder, it is often used for the measurement of abdominal pressure. Because it does not normally contain liquid, the pressure is often measured inside a loosely fitting, water-filled balloon lying within it. With a water-filled catheter connected to an external transducer at the level of the upper edge of the symphysis pubis, a piezometric pressure is recorded.

Because of the indirect nature of the measurement, artefacts are very common. If all is well, the detrusor pressure given by equation (1.3) should be small and positive (0-10 cm H_2O) when the patient is at rest with a nearly empty, relaxed bladder. The transient response of the catheter is usually checked by asking the patient to cough. As the abdominal pressure rises and falls sharply, the excursions made by the bladder and rectal pressure measurements should be similar, corresponding to no change in p_{det}. In practice, this ideal is difficult to attain. A fairer test can be made by asking the patient to blow against his hand for a second or two. The resulting sustained rise in abdominal pressure should be registered equally in both bladder and rectum. Rectal contractions, if they occur, usually fluctuate over periods of several seconds or tens of seconds. They can be recognised as artefacts since they cause fluctuations in the apparent abdominal pressure without corresponding intravesical pressure variations.

2.2.4 The detrusor pressure

The detrusor pressure is calculated by electronic subtraction of p_{abd} from p_{ves}. It represents, to as good an approximation as possible, the contribution to the intravesical pressure from the stresses in the bladder wall, both passive (viscoelastic) and active (contractile). Its significance is best illustrated by an example, as shown in figure 2. 1.

During the slow filling of the bladder the detrusor should normally remain relaxed and the detrusor pressure should rise only slightly, by up to about 10 cm H_2O when the patient states that his bladder is full and he must pass water. In figure 2.1 an (abnormal) wave of active contraction is seen during filling (see § 10.1. 1). When the patient stands up or coughs the abdominal and intravesical pressures change, but the detrusor pressure remains approximately constant. On the command to pass water the detrusor contracts actively and raises the detrusor pressure to about 25 cm H_2O (in this case only a small rise). The detrusor pressure is maintained with little change as long as flow continues. When the patient is asked to interrupt the stream the flow rate falls and the detrusor pressure rises. When flow recommences the detrusor pressure falls back to near its previous value and the bladder is emptied to completion, as shown by the approximate equality of the introduced and voided volumes. When the bladder is empty the detrusor has ceased contracting and the detrusor pressure is once more close to zero.

2.2.5 Urethral pressure measurement

2.2.5.1 The nature of the measurement. If the lumen of the urethra is filled with liquid, stationary or perhaps in steady flow, the pressure in the liquid is in equilibrium with the normal stress exerted by the urethral walls. This stress depends on the forces, active and passive, in the walls and surrounding structures, and, in the proximal part of the urethra, on the abdominal pressure. Therefore it is subject to functional changes (§ 1.1.5). Nevertheless it is clear what is being measured.

In practice the fluid pressure in the urethra is seldom measured when
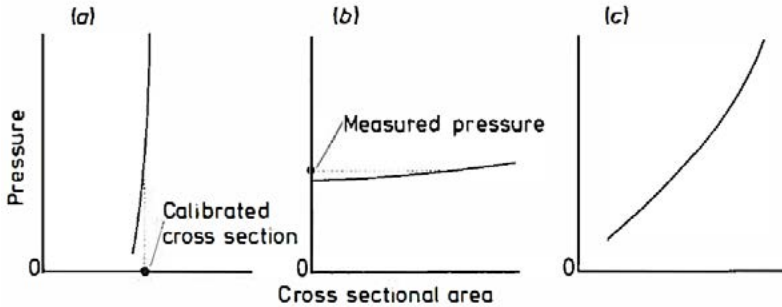
Figure 2.4 Diagrams showing how intraluminal pressure depends on cross sectional area for tubes which are (a) near-rigid ; (b) highly distensible; (c) intermediate. (Reproduced from Urol. Clin. N. Am. 6, no. 1, p147 (1979) by permission of WB Saunders Company.)

it is filled with liquid, i.e. during micturition. On the other hand, the pressure within the resting urethra is very often measured. Since the urethra is not filled with liquid under these conditions, it is at first sight difficult to understand what is measured and whether the various methods that are in use give comparable results.

A urethra is a distensible tube. If it were inflated with liquid to a given pressure, the cross sectional area of the lumen (at any point along its length) would depend on the pressure. Thus there is a mathematical relation between fluid pressure and cross sectional area.

A tube which is only slightly distensible, near-rigid in fact, has a pressure/area relation as in figure 2.4(a): under very large changes in pressure there is only a small change in cross sectional area. In this case one single pressure measurement, at an arbitrarily chosen cross sectional area, would not be useful in characterising the properties of the tube. It would be more sensible to estimate the near-constant cross sectional area, for example by determining the largest rigid

probe that could easily be inserted and withdrawn, a procedure known as calibration. A highly distensible tube, on the contrary, has a pressure/area relation as in figure 2.4(b). The pressure changes little over a wide range of cross-sectional areas. In this case a single pressure measurement at an arbitrarily chosen area is indeed representative of the mechanical properties of the tube, while a cross-section determined by calibration clearly is not. An intermediate case is shown in figure 2.4(c). Here no single measurement of either pressure or cross-sectional area is representative: the whole pressure/area relation is needed. Thus pressure measurement and calibration are appropriate to different types of tubes, and there are tubes for which neither is appropriate by itself.

In practice, calibration is performed by urologists in particular parts of the urethra (the external meatus) and in certain pathological conditions (strictures, §9.4) where the urethra is sufficiently rigid for them to obtain a result. Normally, however, most parts of the urethra appear to be quite highly distensible within their working range, with pressure/area relations like that in figure 2.4(b). Pressure measurement is therefore appropriate. Note that the natural cross-section, especially at the smaller cross-sectional areas, is certainly not circular (Huisman 1978). The probes used to measure the urethral pressure all impose to some extent their own shape on that of the urethral lumen. The size of the probe is usually specified in French gauge (Charrière). This figure is the circumference of the (round) probe in mm.

The urethral pressure varies along the length of the urethra. Its distribution—the plot of pressure against distance (figure 2.3a, b)—is called the urethral closure pressure profile.

2.2.5.2 Methods of measuring the urethral pressure.

Balloons: A cylindrical balloon, mounted concentrically on a catheter, is inflated outside the urethra to a pressure marginally above atmospheric. It is inserted into the urethra and the pressure of the fluid in the balloon measured. A true hydrostatic pressure is measured; the situation is close to the ideal of a fluid-filled urethra discussed in the previous section. If the balloon is too long (10 or 20 mm) in comparison with the axial distances over which significant pressure variations occur, it averages out the variations: the pressure profile, obtained by drawing the balloon through the urethra, is smoothed and distorted.

Provided the catheter is liquid-filled and the external pressure transducer at the right level, piezometric pressures are obtained.

Catheter-tip transducer: A small solid state pressure transducer, mounted on the side of a small round catheter, is placed in the urethra. Such a transducer measures in fact not the hydrostatic pressure, but the normal stress component on its surface. At first sight one might expect the measurements to depend on the orientation in the urethra. This would certainly be the case if the urethra were like a collapsible plastic tube. Such a tube does not seal round the catheter, but leaves small open channels. Thus in some orientations the transducer would be directly in contact with the atmospheric pressure, while in others it would be pressed upon by the tube wall. There is evidence, however, that the urethra seals quite well round a catheter (§5.2), and reports of clinical experience with these solid state transducers suggest that they give reproducible and reliable results, independent of orientation. Presumably any space between the catheter and the urethral walls is sealed with viscous mucus.

Technically this is a very easy method of measuring the urethral pressure. In principle, the measurements should be converted to piezometric pressures.

Infusion (Brown-Wickham) method: The pressure needed to force water or gas slowly out of one or more side- or end-holes in a round catheter, lying in the urethra, is measured. Since the fluid escapes along the urethra into the bladder or the atmosphere[†], this appears at first sight to be a measurement of the resistance to flow of a substantial part of the urethra, and not of the pressure exerted by the urethral wall at the site of the catheter hole. Nevertheless the measured quantity can be very close to the local urethral pressure, provided that the urethra is highly distensible (see §5.2). If the urethra is not highly distensible the measurement of urethral pressure has little point (§2.2.5. 1).

The readings must in principle be corrected for viscous pressure losses within the catheter. In practice, this is easily done by taking as the zero of pressure the reading in air when the fluid is flowing. If an aqueous liquid is used and the external pressure transducer is at the right level, piezometric urethral pressures are obtained. The basis of the method is considered in more detail in §5.2.

[†] The direction of escape is used to define the continence zone (see figure 5.2)

3 A Physical Approach to Flow through the Urethra: Uniform Tubes

3.1 The Urethra and the Hydrodynamic Problem

A urethra is a curved tube having a non-circular cross-section which differs in shape from point to point. At any one point its cross-sectional area is variable because the tube is distensible. How then should it be described mechanically? The urethral closure pressure profile (figure 2.3a,b) shows the pressure p exerted by the walls of the resting urethra as a function of the position x, when the cross-sectional area A is kept constant. The pressure depends on A as well as x (see figures 2.4 and 5.1); p is here assumed to be an increasing function of A, for given x. A further condition (3.8b) is given in §3.2. 1.

The simplest possible assumption is therefore that

$$p = p(A, x), \qquad\qquad (3.1)$$

i.e. that the pressure at a given point depends only on the local cross-sectional area, and not on the configuration at other nearby points. It is an approximation which can be tested experimentally (§§4.2.2 and 4.2.3).

The hydrodynamic problem is as follows. Given a urethra for which the function $p(A, x)$ is known, what determines (i) the flow rate for a given bladder pressure, and (ii) the degree of distension of the urethra, i.e. the shapes shown in figure 2.2(a, b)? With regard to (ii), it is striking that the mechanical properties of the female urethra (figure 2.3a) are roughly symmetrical about its midpoint, while the shape during micturition (figure 2.2a) is certainly asymmetrical. How does this difference arise?

We shall approach the problem in stages, dealing in this chapter with uniform tubes, and in the following chapter with the non-uniform case. In both chapters the rather surprising behaviour of a highly distensible tube is treated first and is then contrasted with the well-known behaviour of rigid or near-rigid tubes. The analysis is confined to steady flow.

The flowing fluid, urine, is variable in composition but its density and coefficient of viscosity are similar to those of water. The x-ray contrast medium sometimes used in clinical studies of micturition is a little denser and more viscous. Occasionally gas (air or CO_2) is used for micturition or flow studies, but its density is very much lower. In the theoretical treatment we shall, initially, neglect viscosity.

Gravity may be taken into account by taking the pressures as piezometric. This means that a physically uniform tube will not behave as uniform in our sense unless it is either horizontal or immersed in a bath of fluid of the same density as that flowing inside the tube.

3.2 Flow of an Inviscid Fluid through a Uniform Distensible Tube

3.2.1 Theory

Consider the steady flow of an inviscid, incompressible fluid, of density ρ, from a reservoir at pressure p_0 through a straight and uniform distensible tube. The fluid velocity v is uniform over the cross-section and is parallel to the axis. The fluid pressure p (with respect to atmospheric) is uniform and is given by

$$p = p(A), \hspace{3cm} (3.2)$$

where A is the cross-sectional area of the tube. The volume flow rate Q through the tube is given by

$$Q = vA. \tag{3.3}$$

Because of our assumptions the Bernoulli equation is satisfied:

$$p(A) + \tfrac{1}{2}\rho v^2 = p_0. \tag{3.4}$$

Therefore, eliminating v,

$$Q^2 = [p_0 - p(A)]2A^2/\rho. \tag{3.5}$$

Since A is unknown, Q cannot be calculated from this equation. Imagine, however, that A varies while p_0 remains fixed; Q is then zero when A is zero, and also when A satisfies the equation

$$p(A) = p_0. \tag{3.6}$$

Between these two limits, equation (3.5) possesses a real and positive solution for Q, since $p(A)$ is an increasing function of A. Therefore the variation of Q with A is as shown in figure 3.1. It has a maximum value Q_{max} for a certain value of A. Provided there is no other limitation on the flow rate (and this is discussed further in §3.2.7 and Chapter 4), Q_{max} will be the flow rate that is realised.
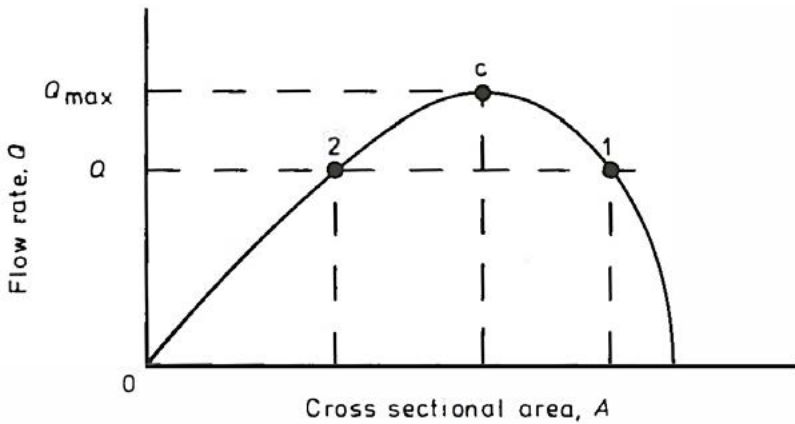
Figure 3.1 Dependence of flow rate on cross-sectional area at a fixed pressure head, as given by equation (3.5). When the flow rate has its maximum value the flow speed is sonic (point c). For a flow rate $Q < Q_{max}$ two solutions are possible: subsonic (point 1), or supersonic (point 2).

In order to find the maximum, equation (3.5) is differentiated:

$$\mathrm{d}Q^2/\mathrm{d}A = [p_0 - p(A)]4A/\rho - (\mathrm{d}p/\mathrm{d}A)2A^2/\rho. \qquad (3.7)$$

The rhs is equal to zero when $A = 0$, which is of no interest, and when

$$p_0 - p(A) = \tfrac{1}{2}A \, \mathrm{d}p/\mathrm{d}A, \qquad (3.8a)$$

which corresponds to a maximum of Q, provided that

$$A^2 \mathrm{d}^2 p/\mathrm{d}A^2 + 3A \, \mathrm{d}p/\mathrm{d}A > 0. \qquad (3.8b)$$

We assume for the time being that this condition is satisfied. It is examined further in §§ 3.2.3 and 8.2. Equation (3. 8a) may be solved for the cross-sectional area corresponding to Q_{max}, if $p(A)$ is known.

From equations (3.5) and (3.8a), Q_{max} is then given by

$$Q^2_{max} = (A^3/\rho) \, dp/dA. \qquad (3.9)$$

The corresponding value of the fluid speed v is, using equation (3.3),

$$v = [(A/\rho) \, dp/dA]^{1/2} = c_0. \qquad (3.10)$$

Thus, when $Q = Q_{max}$, the fluid speed has the characteristic value c_0, which depends on the elastic properties $p(A)$ of the tube and the density of the fluid. c_0 is not a constant, however, but varies with the cross-sectional area A. Its significance is discussed further in §3.2.5.

3.2.2 Example

Suppose that

$$p(A) = G + HA^n, \qquad (3.11a)$$

where G, H and n are constants. n and H are non-zero and have the same sign, so that dp/dA is positive. Condition (3.8b) implies that

$$Hn(n + 2) > 0. \qquad (3.11b)$$

Therefore, since $Hn > 0$,

$$n > -2. \qquad (3.11c)$$

From equation (3.8a), $Q = Q_{max}$ when

$$p_0 - G - HA^n = \frac{1}{2}nHA^n, \qquad (3.12)$$

that is,

$$A = \left[\frac{2(p_0 - G)}{(n+2)H}\right]^{1/n}. \qquad (3.13)$$

The corresponding fluid speed is, from equation (3.10),

$$v = c_0 = (nHA^n/\rho)^{1/2}, \qquad (3.14)$$

and the flow rate Q_{max} is

$$Q_{max} = c_0 A = (nH/\rho)^{1/2}A^{(n+2)/2}. \qquad (3.15)$$

The relation between the flow rate $Q = Q_{max}$ and the pressure head p_0, the resistance relation, is found by eliminating A from equations (3.13) and (3.15):

$$Q = \left(\frac{nH}{\rho}\right)^{1/2}\left[\frac{2(p_0-G)}{(n+2)H}\right]^{\frac{1}{2}+\left(\frac{1}{n}\right)}. \qquad (3.16)$$

Equation (3.16) is valid for $p_0 > G$. If $p_0 < G$ the equation has, in general, no real solution. Reference to equation (3.11a) shows that p_0 is then less than the pressure G at which the tube opens. Therefore the tube remains shut and there is no flow. As shown in figure 3.2, then, the flow rate is proportional to $(p_0 - G)^{1/2+(1/n)}$ for $p_0 > G$, and it is zero for $p_0 < G$.
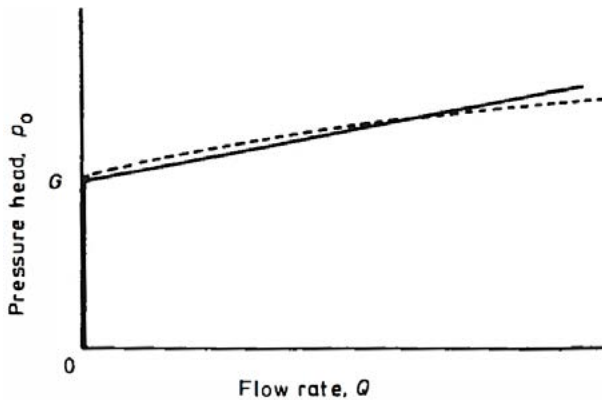
Figure 3.2 Resistance relation (equation (3.16)) between pressure head and flow rate for a distensible tube. Broken curve n = 1: full curve n = 2.

In order to make the example clearer, let us take some realistic numerical values. Let

$$G = 4 \times 10^3 \text{ Pa} \cong 40 \text{ cm } H_2O$$

$$n = 1$$

$$H = 10^8 \text{ Pa m}^{-2} \cong 1 \text{ cm } H_2O/\text{mm}^2$$

$$\rho = 10^3 \text{ kg m}^{-3} = 1 \text{ g ml}^{-3}.$$

The resistance relation is given by equation (3.16) as

$$Q = (10^8/10^3)^{1/2}[2(p_0 - 4 \times 10^3)/3 \times 10^8]^{3/2} \text{ m}^3 \text{ s}^{-1}$$
$$= 10^{-8}[(p_0 - 4 \times 10^3)/15]^{3/2} \text{ m}^3 \text{ s}^{-1},$$

where the pressure head p_0 is in Pa.

If $p_0 = 5.5 \times 10^3$ Pa $\cong 55$ cm H_2O, for example,

$$Q = 10^{-5} \text{ m}^3 \text{ s}^{-1} = 10 \text{ ml s}^{-1}.$$

The cross-sectional area of the tube is then (equation (3.13)),

$$A = 10^{-5} \text{ m}^2 = 10 \text{ mm}^2.$$

It follows from equation (3.11a) that the pressure in the tube is

$$p = 4 \times 10^3 + 10^8 \times 10^{-5} = 5 \times 10^3 \text{ Pa}$$
$$\cong 50 \text{ cm } H_2O.$$

The fluid speed is (equation (3.14)),

$$v = c_0 = (10^8 \times 10^{-5}/10^3)^{1/2} = 1 \text{ m s}^{-1}.$$

Note that

$$vA = 10^{-5} \text{ m}^3 \text{ s}^{-1} = Q.$$

3.2.3 The connection between the resistance relation and the elastic properties of the tube

In the specially chosen example (§3.2.2), the resistance relation, equation (3.16), is determined by the elastic properties of the tube, equation (3.11 a). In the general case an analytical solution is not possible, but it remains true that the resistance relation can be determined from the elastic properties, and vice versa. This is most easily carried out graphically, as follows.

We introduce a new variable, $\gamma = 1/A^2$, so that the elastic properties are represented by

$$p = p(\gamma). \tag{3.17}$$

Equation (3.8a) becomes

$$p_0 - p(\gamma) = -\gamma \, dp/d\gamma. \tag{3.18}$$

and equation (3.9) becomes (with the assumption that $Q = Q_{max}$)

$$Q^2 = -(2/\rho) \, dp/d\gamma. \tag{3.19}$$

Therefore

$$-dp/d\gamma = \tfrac{1}{2}\rho Q^2 = [p_0 - p(\gamma)]/\gamma. \tag{3.20}$$

Equations (3.20) are easily solved graphically, as shown in figure 3.3. If the curve $p = p(\gamma)$ is known, the tangent at any point c has a slope $-\tfrac{1}{2}\rho Q^2$ and the intercept on the p axis is the corresponding pressure
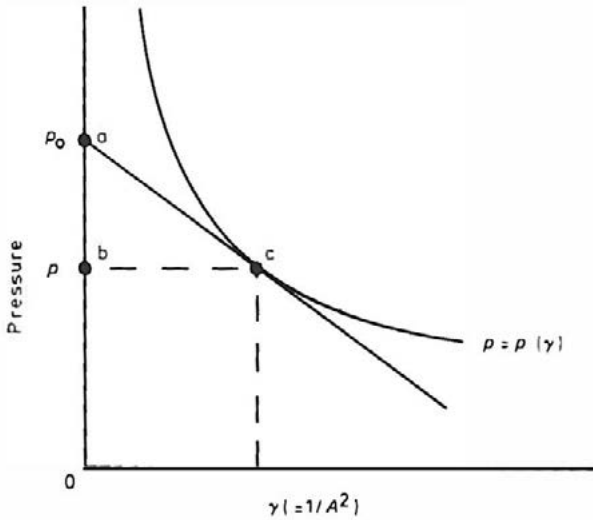
Figure 3.3 Graphical solution of equations (3.20). Tangent ac has a slope $-\rho Q^2$, where Q is the flow rate for the pressure head p_0.

head p_0. Thus each point on the curve gives a pair of corresponding values p_0 and Q, and from all the points the complete resistance relation is determined.

Conversely, if the resistance relation is known, the elastic properties of the distensible tube may be found. For each pair of values of p_0 and Q one draws through the point $(p_0, 0)$, on a p/γ plot, a straight line of slope $-\frac{1}{2}\rho Q^2$. The envelope of all such lines is the curve $p = p(\gamma)$; see figure 3.4. This is easily transformed to the function $p = p(A)$.

The coordinates of the point c at which the tangent from $(p_0, 0)$ touches the curve $p = p(\gamma)$ represent respectively the pressure p and the value of γ (i .e. the cross-sectional area) of the tube when the
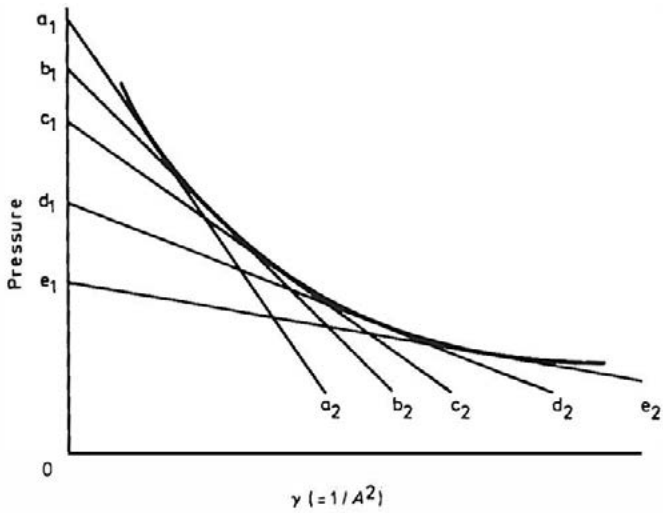
Figure 3.4 Determination of elastic properties from the resistance relation. Each of the lines a_1a_2, b_1b_2, etc has a pressure intercept p_0 and slope $-\frac{1}{2}\rho Q^2$. The envelope of the lines (bold curve) is the function $p = p\,(\gamma)$.

pressure head is p_0, the flow rate Q is equal to Q_{max} and the fluid is flowing at the characteristic speed c_0.

Equation (3.4) shows that the difference between p_0 and p is given by

$$p_0 - p = \frac{1}{2}\rho v^2 \qquad\qquad (3.21a)$$

$$= \frac{1}{2}\rho c_0^2, \qquad\qquad (3.21b)$$

since here $v = c_0$. The difference can easily be identified on the p/γ plot (figure 3.3), and so the characteristic speed c_0 can be determined graphically.

In terms of γ, the condition (3.8b) becomes

$$d^2p/d\gamma^2 > 0. \qquad\qquad (3.21c)$$

That is, the p/γ plot must be concave upwards, as in figure 3.3. What happens if condition (3.21c) is not satisfied can be understood from §8.2.

3.2.4 Exercise

Suppose that as in §3.2.2, for a certain distensible tube, $p(A) = G + HA^n$ (equation (3.11a)) with $G = 4 \times 10^3$ Pa, $n = 1$, $H = 10^8$ Pa m^{-2} and $\rho = 10^3$ kg m^{-3}. In terms of γ, equation (3.11a) becomes

$$p(\gamma) = G + H\gamma^{1/2}. \qquad\qquad (3.22)$$

(i) Plot p as a function of γ in the range

$$0.25 \times 10^{10} \text{ m}^{-4} \le \gamma \le 4 \times 10^{10} \text{ m}^{-4}.$$

(ii) Draw a tangent to the resulting curve from the point

$$p = 5.5 \times 10^3 \text{ Pa}, \qquad \gamma = 0.$$

Measure its slope.

(iii) Hence show that the flow rate Q through the tube for a pressure head of 55 cm H_2O is (approximately) 10 ml s^{-1}, in agreement with the analytical result.

(iv) Calculate, from the graph, the pressure and cross-sectional area of the tube under these circumstances, and the speed of flow of the liquid. Compare with the analytical results.

3.2.5 The characteristic fluid speed c_0

The speed c_0 (equation (3. 10)), at which the fluid flows has a special significance: it is the speed at which small-amplitude pressure waves of low frequency are propagated along the fluid-filled tube (see e.g. McDonald 1974, p253). Such waves, known as Young waves, are analogous to low-frequency sound waves. c_0 has therefore been lightheartedly christened the 'sonic' speed, although in fact it is very much smaller than the speed of true sound for a highly distensible tube, perhaps 1 m s^{-1} or less.

In order to demonstrate that c_0 is indeed the sonic speed we consider a uniform distensible tube, filled with initially stationary, incompressible fluid of density ρ, and having initially a finite cross-sectional area. Suppose that a small-amplitude pressure pulse is propagated along it in the positive x direction. Associated with the pulse are a small dilatation of the cross-sectional area and a small fluid flow. We assume that the pressure p and fluid velocity v are uniform over the cross-section and that $p = p(A)$. These assumptions are expected to be valid in the long-wavelength, low-frequency limit, where the effect of wall curvature may be neglected.

Consider a fluid element of length dx, as illustrated in figure 3.5. The net rate of inflow into it is $(- \partial Q/\partial x)$ dx, and this is equal to the rate of increase of its volume, $(\partial A/\partial t)$ dx, where t is time. Therefore

$$-\partial Q/\partial x = \partial A/\partial t$$
$$= (dA/dp)\partial p/\partial t.$$

$$(3.23)$$
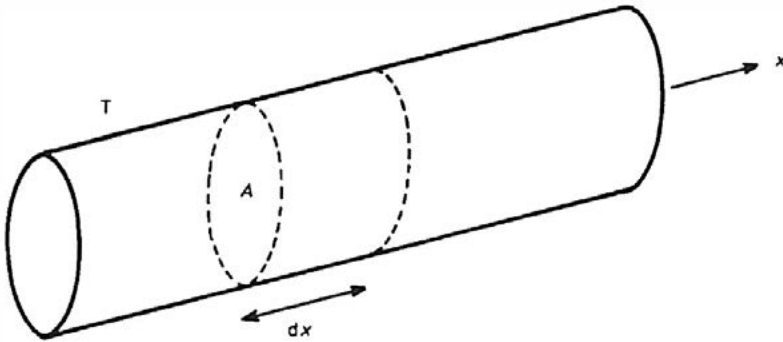
Figure 3.5 Coordinate system for calculation of the speed of pressure waves in the tube T. The flow and fluid velocity in the wave are taken to be positive in the positive x direction.

The net force on the element in the positive x direction is $-A(\partial p/\partial x)\,dx$, to first order in d$x$, which is equal to the acceleration of the element, $\partial v/\partial t$, multiplied by its mass, $\rho A\,dx$. (The inertia of the tube wall is assumed negligible.) Therefore

$$- \partial p/\partial x = \rho\,\partial v/\partial t. \qquad (3.24)$$

But

$$Q = vA \qquad (3.25)$$

and so

$$\partial Q/\partial t = v\,\partial A/\partial t + A\,\partial v/\partial t. \qquad (3.26)$$

Now v and $\partial A/\partial t$ are both proportional to the small amplitude of the pressure pulse. Therefore, to first order in small quantities,

$$\partial Q/\partial t = A \, \partial v/\partial t. \tag{3.27}$$

Substituting in equation (3.24),

$$- \partial p/\partial x = (\rho/A) \, \partial Q/\partial t. \tag{3.28}$$

If equation (3.23) is differentiated partially with respect to t, and equation (3.28) with respect to x, and if $\partial^2 Q / \partial t \, \partial x$ and $\partial^2 Q / \partial x \, \partial t$ are then set equal, it follows that

$$\partial^2 p/\partial t^2 = (A/\rho)(\mathrm{d}p/\mathrm{d}A) \, \partial^2 p/\partial x^2. \tag{3.29}$$

Some further terms of second order in small quantities have been neglected.

Equation (3 .29) is a wave equation for the fluid pressure p. It shows that, within the limitation of the analysis, a small-amplitude disturbance is propagated along the fluid-filled tube at the speed

$$c_0 = [(A/\rho) \, \mathrm{d}p/\mathrm{d}A]^{1/2}. \tag{3.30}$$

This sonic speed is also the characteristic speed of steady flow of fluid through the tube (equation (3.10)).

The speed c_0 depends on the pressure in the tube, i.e. on the cross-sectional area A. In the example discussed in §3.2.2, where

$$p(A) = G + HA^n, \tag{3.11a}$$

we showed that

$$c_0 = (nHA^n/\rho)^{1/2}. \tag{3.14}$$

For the particular case $n = 1$, c_0 is thus proportional to $A^{1/2}$.

3.2.6 Exercise

In general the dependence of c_0 on A can be complicated. Figure 3.6 shows the elastic properties of a thin-walled latex tube.
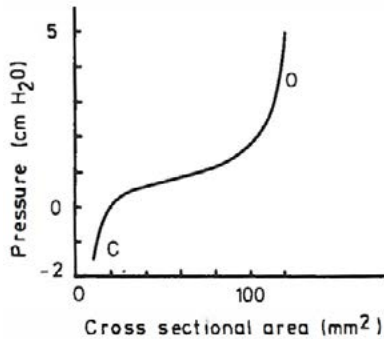
Figure 3.6 Elastic properties of thin-walled latex tube. In the region marked **O** the tube is fully open (circular cross-section). Near **C** it is collapsed and nearly flat. Negative pressures imply that the intra-luminal pressure is lower than the external pressure. (After Brower and Scholten 1975.)

(i) Comparing figure 3.6 with figure 2.4(a-c), how would you describe the elastic behaviour of the tube?

(ii) Sketch a graph showing qualitatively the variation of c_0 with A for the tube.

3.2.7 Subsonic and supersonic flows

Within our approximations, for a distensible tube, the flow rate for a given pressure head takes the value Q_{max} at which the speed of flow is sonic, provided nothing else limits the flow rate to a lower value. The qualification is important. Referring to figure 3.1, if the flow rate is limited by an external device to a value of $Q < Q_{max}$. then there are two possible cross-sectional areas for the distensible tube. One of these (point 1) is large, corresponding to a low speed of flow; the other

(point 2) is small, corresponding to a high speed. The two possible speeds are respectively less and greater than the sonic speed, i.e. sub- and supersonic.

The situation is conveniently assessed from a p/γ plot (figure 3.7). For a pressure head p_0, the flow rate Q_{max} corresponding to sonic flow is given by the slope of the tangent, as shown. The slope is $-\frac{1}{2}\rho Q^2_{max}$. If the flow rate is limited to a value below Q_{max} there are two possible solutions with small and large γ: points 1 and 2 respectively.

Consider point 1. According to equation (3.21a) the difference ($p_0 - p$),
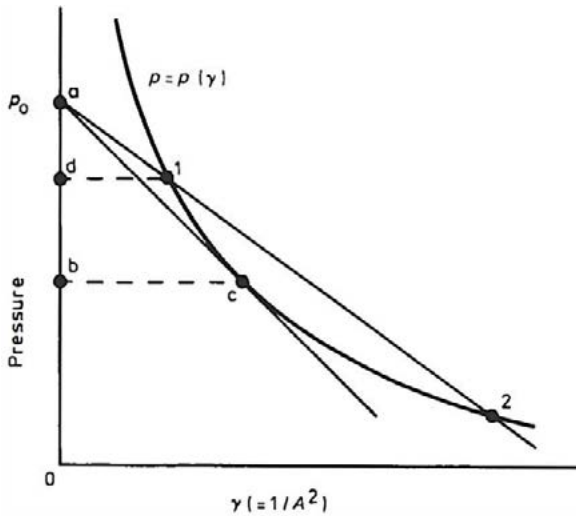
Figure 3.7 p/γ plot for sonic, sub- and supersonic flows. At the pressure head p_0 the sonic flow rate Q_{max} is given by the slope $-\frac{1}{2}\rho Q^2_{max}$ of tangent ac. If $Q < Q_{max}$, there are two solutions given by the intersections of the line a 1 2 (slope $-\frac{1}{2}\rho Q^2$) with the curve $p = p(\gamma)$. Solution 1 is subsonic: solution 2 is supersonic.

distance ad in figure 3.7, is equal to $\frac{1}{2}\rho v^2$, where v is the speed of flow. The value of $\frac{1}{2}\rho c_0^2$ for this pressure and cross-sectional area is represented by the distance ab. Thus at point 1, with the smaller value of γ and the larger cross-sectional area, v is less than c_0: the flow is subsonic. Correspondingly at point 2, with the smaller cross-sectional area, the flow is supersonic.

3.2.8 Summary

An incompressible inviscid fluid, flowing steadily through a uniform distensible tube and otherwise unrestricted as to rate, flows at a characteristic sonic speed which depends on the elastic properties of the tube and the density of the fluid. The resistance relation between the flow rate and the pressure head also depends on the elastic properties and the density. The degree of distension of the tube varies with the pressure head.

This flow rate, corresponding to sonic flow, is the maximum that is possible with a given pressure head. If the flow rate is externally restricted to a value below the maximum, two different flow regimes are possible, having respectively sub- and supersonic speeds of flow.

3.3 Effects of Viscosity on Flow through a Distensible Tube

In the theory developed in §3.2 viscosity is ignored completely. The situation at the opposite extreme, viscosity-dominated flow, has also been examined (Van Schaik et al 1977, Wild et al 1977). The flow is dominated by viscosity if the tube is long and the Reynolds number of the flow is of order 1 or smaller. The Reynolds number is given by

$$\mathrm{Re} = \rho d v / \eta \qquad (3.31a)$$

where d is a typical tube diameter and η is the coefficient of viscosity of the fluid. Using equation (3.3) and remembering that d $\cong A^{1/2}$ for a tube of roughly circular cross-section,

$$Re \cong \rho Q / \eta A^{1/2}. \qquad (3.31b)$$

Typically, for the urethra, $Q \cong 20$ ml s^{-1} = 2×10^{-5} m^3 s^{-1}, while $A^{1/2} \cong 3$ mm. For urine $\rho \cong 10^3$ kg m^{-3} and $\eta \cong 10^{-3}$ kg m^{-1} s^{-1}. Therefore Re $\cong$ 7000. The flow is certainly not dominated by viscosity. It is therefore sensible to introduce viscous effects as a correction to the inviscid-fluid theory[†].

As in the case of the rigid tube (§3.4.3), the principal effect of viscosity is to cause losses so that the pressure head decreases in the direction of flow. Figure 3.8 shows a p/γ diagram in these circumstances. The flow rate Q is determined by the lowest pressure head in the tube, that at the downstream exit. Here the speed of flow is sonic.

[†] In the clinical examination called retrograde urethrography, extremely viscous contrast fluid is injected at the external meatus and flows backwards up the urethra. Here the Reynolds number is much lower and the flow may be viscosity-dominated.
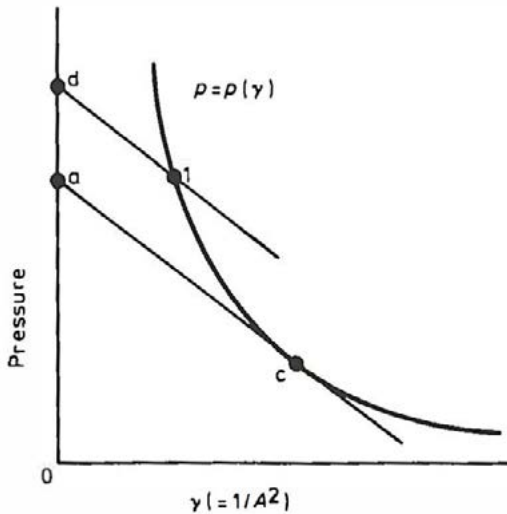
Figure 3.8 p/γ plot with viscosity. At the downstream end of the tube, the pressure head is represented by point **a**. and the flow is sonic (point **c**). Further upstream, the pressure head is higher (point **d**), but the flow rate is the same (**d1** and **ac** have same slope); the solution is given by point **1**, subsonic flow.

Further upstream the flow rate Q is the same but the pressure head is higher. Therefore $Q < Q_{max}$ locally and so two possibilities are open; sub- and supersonic flow. Since supersonic flow is unstable in this situation (§4.3.3), the flow is subsonic. Figure 3.8 then indicates that γ increases in the direction of flow. Thus the tube is widest at its upstream end and tapers to its narrowest cross-section at the exit where the flow is sonic.

At the exit the local pressure head p_0' is related to the flow rate Q by the local resistance relation

$$Q = Q(p_0') \qquad\qquad (3.32a)$$

or

$$p_0' = p_0' (Q), \tag{3.32b}$$

which is fixed by the elastic properties of the tube as described in §3.2.3. The pressure head p_0 at the entrance to the tube is therefore given by

$$p_0 = p_0' (Q) + \Delta p_0, \tag{3.33}$$

where Δp_0 is the loss, due to viscosity, of pressure head within the tube. Since Δp_0 itself depends on Q and the elastic properties of the tube, equation (3.33) is of limited value.

3.4 Flow through a Rigid or Near-rigid Uniform Tube

3.4.1 Rigid tube, inviscid fluid

A simplified outline of the well-known characteristics of flow through a rigid tube is useful, not as a starting point for understanding the urethra, but to make clear how differently a highly distensible tube behaves.

Consider an inviscid and incompressible fluid emptying through a uniform rigid tube into a space where the pressure is P_{ext}, with respect to atmospheric. Let the fluid come from a reservoir at pressure p_0 ($>p_{ext}$) and let the cross-sectional area of the tube be A_0. The Bernoulli equation is applicable at the tube exit, where the fluid pressure is equal to p_{ext}, i.e.

$$p_0 = p_{ext} + \frac{1}{2}\rho v^2. \tag{3.34}$$

Since at the exit

$$Q = A_0 v, \tag{3.35}$$

it follows that

$$Q = A_0[2(p_0 - p_{ext})/\rho]^{1/2}. \tag{3.36}$$

Equation (3.36) is the resistance relation, between flow rate Q and pressure head p_0, for the rigid tube. Not only is it different in form from that for a distensible tube (e.g. equation (3. 16)), but it involves different parameters, for example p_{ext}.

3.4.2 Near-rigid tube, inviscid fluid

Let the tube be not completely but nearly rigid, as in figure 2.4(a). Then the cross-sectional area A depends slightly on the fluid pressure p:

$$A = A(p). \tag{3.37}$$

At the exit the fluid pressure is p_{ext}; therefore

$$A = A(p_{ext}) \tag{3.38}$$

and

$$Q = A(p_{ext})\, v. \tag{3.39}$$

Equation (3.34) is valid at the exit, and so

$$Q = A(p_{ext})\, [2(p_0 - p_{ext})/\rho]^{1/2}. \tag{3.40}$$

Just as for a rigid tube, the resistance relation depends on p_{ext}. It does not depend on dp/dA or the sonic speed c_0, which are essential to the behaviour of a highly distensible tube.

3.4.3 Rigid tube, viscous fluid

The main effect of viscosity is to cause energy losses, so that the pressure head p_0 at the tube exit is less than the reservoir pressure p_0'. Equation (3.36) remains valid at the exit, approximately, provided p_0 is replaced by p_0', the local pressure head:

$$Q = A_0 \, [2(p_0' - p_{ext})/\rho]^{1/2}, \qquad (3.41)$$

where

$$p_0' = p_0 - \Delta p_0, \qquad (3.42)$$

and Δp_0 is the loss of pressure head caused by viscosity and turbulence between the reservoir and exit.

Δp_0 depends on the flow rate and on the length l of the tube, among other variables. For example, if the flow is turbulent, and if entrance effects can be neglected

$$\Delta p_0 \cong klQ^2, \qquad (3.43)$$

where k is approximately constant for a tube of given cross-sectional area. Substitution in equations (3.4 1) and (3.42) leads to

$$Q = A_0[2(p_0 - p_{ext})/\rho]^{1/2} / [1 + 2klA_0^2/\rho]^{1/2}. \qquad (3.44)$$

Thus the resistance relation still depends on the exit pressure p_{ext}. Equations (3.36), (3.40) and (3.44) all show that

$$Q \propto (p_0 - p_{ext})^{1/2} \qquad (3.45)$$

whether the tube is rigid or near-rigid, and whether the fluid is inviscid or viscous and turbulent.

3.5 When Is a Tube Distensible and when Near-rigid?

In §§3.2 and 3.4 we have given two apparently contradictory accounts of flow through a uniform tube. If the tube is treated as distensible, the flow rate depends on the elastic properties of the tube through the sonic speed, but not on the exit (external) pressure; if treated as near-rigid, it depends on the exit pressure but the sonic speed is of no significance. In the latter case, the resistance relation has a great variety of possible forms, depending on the elastic properties of the tube. How are these accounts to be reconciled?

Consider a near-rigid tube with the elastic properties shown in figure 2.4(a). The corresponding p/γ plot is shown in figure 3.9. Let the exit pressure be p_{ext} as in §3.4. According to the argument of §3.4.2 the fluid pressure p in the tube is equal to p_{ext}, and the tube takes up a cross-section $A = A\,(p_{ext})$. In terms of $\gamma = 1/A^2$,

$$p\,(\gamma) = p_{ext}. \tag{3.46}$$

The point $(p,\ \gamma)$ satisfying equation (3.46) is shown in figure 3.9. From equation (3.40), the flow rate Q satisfies

$$\frac{1}{2}\rho Q^2 = (p_0 - p_{ext})\,A^2 = (p_0 - p_{ext})/\gamma. \tag{3.47}$$

Therefore the line joining the point $(p_0, 0)$ to the point (p, γ) has a slope $\frac{1}{2}\rho Q^2$. Comparison with figure 3.7 shows that the situation is exactly as at point 1: the flow is subsonic.

The explanation is that Q is limited to below the hypothetical value Q_{max} at which the speed of flow would become sonic by the exit pressure p_{ext}. Referring to figure 3.9, the pressure p_{son} at which the flow would become sonic is very much lower than p_{ext}. Under these circumstances the flow remains subsonic and the pressure in the tube
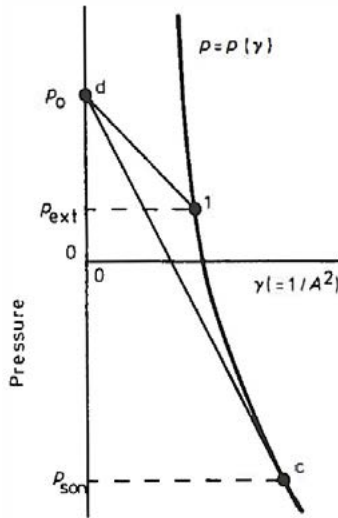
Figure 3.9 p/γ plot for a near-rigid tube. The exit pressure p_{ext}, is much higher than the pressure p_{son} at which the fluid speed would become sonic, and the flow remains subsonic (point 1).

is p_{ext}: the tube behaves as near-rigid. If, however, $p_{ext} < p_{son}$ then sonic flow can indeed occur. p is equal to p_{son} and Q is equal to Q_{max}: the distensible-tube analysis is applicable.

Thus for a given pressure head there is a critical value (p_{son}) below which the exit pressure must lie if the tube is to behave as distensible; that is, the flow is to become sonic. For a highly distensible tube the critical value is not particularly low (e.g. figure 3.3) and so sonic flow is easily attained. The less distensible the tube, the lower the critical value and the more restricted the conditions for the occurrence of sonic flow.

For a tube that is very nearly rigid the critical value is so low that sonic flow in our sense could never be attained in reality. (The 'sonic' speed

is comparable with the speed of *true* sound; were it to be approached, the compressibility of the fluid would have to be taken into account and our analysis modified.) Thus the flow is in practice always subsonic and the analysis of §3.4 is applicable.

When the flow is sonic, the fluid pressure drops suddenly from p_{son} to p_{ext} at the exit from the tube. Correspondingly the fluid accelerates (equation (3.4)), and the cross-section of the stream narrows (equation (3.3)). Because of the sudden narrowing some of our assumptions (§3.2.1) are locally not valid. Nevertheless the local narrowing seems to have no significant *overall* effect unless the distensible tube is anchored to a length of wide, near-rigid tubing at its downstream end. In that case, violent oscillations may occur (Conrad 1969, Griffiths 1977a). They are very common in models, but rare *in vivo*.

4 A Physical Approach to Flow through the Urethra: Non-uniform Tubes

4.1 Flow of an Inviscid Fluid through a Distensible Tube Having One Elastic Constriction

4. 1.1 Theory

A non-uniform distensible tube has elastic properties which differ from point to point along its length. As in §3. 1, equation (3. 1), we assume that the elastic properties can be described by a function $p(A, x)$, where x is distance measured along the axis of the tube in the direction of flow. The tube is not necessarily straight.

In this section it is assumed that, at constant cross-sectional area A, $p(A, x)$ has a single maximum within the tube at the point $x = x_c$. This is the situation in the resting female urethra (figure 2.3a). It is assumed for simplicity that the maximum occurs at the same point x for all A. It follows that, at $x = x_c$,

$$\partial p/\partial x = 0. \qquad (4.1a)$$

Since this is true for all A,

$$\partial^2 p/\partial A \, \partial x = \partial^2 p/\partial x \, \partial A = 0 \qquad (4.1b)$$

at $x = x_c$. x_c is then the position of an *elastic constriction*, so called because, if the tube were inflated at uniform pressure, the cross-sectional area would be minimum at x_c. During flow the fluid pressure is of course not uniform and the cross-sectional area is not necessarily smallest at the elastic constriction.

It is assumed further that $\partial p/\partial x$ is everywhere small. (It is zero for a uniform tube.) It then follows that the rate of change of cross-sectional area with distance, $|dA/dx|$, is small during flow (except under special circumstances; §8.2), and that the fluid velocity v and pressure p may be taken to be uniform over the cross-section of the tube. The analysis of §3.2.1, which is valid for a uniform tube, may then be applied at each point x of the non-uniform tube.

For each point a curve similar to that in figure 3.1 may be drawn. In general, all the curves are different and Q_{max} is different at different points x. In fact, from equations (3.5) and (3.9),

$$Q_{max}^2(x) = [p_0 - p(A,x)]2A^2/\rho = \left(\frac{A^3}{\rho}\right)\partial p/\partial A.$$

$$(4.2a)$$

Clearly the flow rate for given p_0 is limited to the minimum value of $Q_{max}(x)$ for the whole tube. Provided that the external (exit) pressure is sufficiently low (see §3.5), this minimum value of Q_{max} will be the flow rate that is realised:

$$Q = [Q_{max}(x)]_{min}. \qquad (4.2b)$$

Equation (4.2b) is satisfied at one particular point along the length of the tube, where equations (4.2a) are also valid, and the velocity of flow is equal to the local sonic speed, i.e.

$$v = c_0 = [(A/\rho)\,\partial p/\partial A\,]^{1/2}. \qquad (4.3)$$

The resistance relation can be determined from equations (4.2), evaluated at this one point, just as in §3.2.3. Therefore the flow rate through the tube is fixed by the elastic properties at one single point of the tube. The rest of the tube has no effect.

Location of the flow-controlling point is straightforward. Partial differentiation of equations (4.2a) with respect to x shows that both $[p_0 - p(A, x)]2A^2/\rho$ and $(A^3/\rho)\partial p/\partial A$ are stationary at $x = x_c$ under the conditions (4.1a) and (4.1b). Therefore $Q_{max}(x)$ is also stationary at $x = x_c$. Further examination shows that it normally has a minimum there, and therefore the elastic constriction is the flow-controlling point.

The reasoning may be illustrated by considering a special case, in which $p(A, x)$ is the sum of a function of x and a function of A:

$$p(A, x) = g(x) + h(A). \qquad (4.4)$$

Here the dependence of p on A is similar throughout the tube. For a fixed value of A the pressure rises and falls along the length of the tube in accordance with function $g(x)$. The elastic constriction is located where $g(x)$ is maximum, at $x = x_c$; its position is independent of the value of A, as is to be expected since equation (4.4) satisfies conditions (4. 1a) and (4. 1b).

In this special case, equations (4.2a) become

$$Q^2_{max}(x) = [p_0 - g(x) - h(A)]2A^2/\rho = (A^3/\rho)\,dh/dA. \quad (4.5)$$

Equations (4.5) are identical in form to equations (3.5) and (3.9) for a uniform tube, which together may be written:

$$Q^2_{max} = [p_0 - p(A)]2A^2/\rho = (A^3/\rho)\,dp/dA. \qquad (4.6)$$

Thus $Q_{max}(x)$ at pressure head p_0 for the non-uniform tube is precisely the same as Q_{max} at a pressure head $[p_0 - g(x)]$ for a *uniform* tube having elastic properties $p = h(A)$.

Assuming that condition (3.8b) or (3 .21c) is satisfied, Q_{max} is an increasing function of pressure head (see figure 3.2). Therefore $Q_{max}(x)$ is an increasing function of $[p_0 - g(x)]$ and so it is minimum where $g(x)$

is maximum, i.e. at the elastic constriction. Equation (4.2b) is therefore satisfied at $x = x_c$, and the flow rate is determined by the solution to equations (4.2a) at that point, the elastic constriction. The solution of equations (4.2a) and (4.3) at the elastic constriction, in order to determine the resistance relation and the sonic speed, may be performed graphically by plotting $p(\gamma, x_c)$ against $\gamma = 1/A^2$ exactly as in §3.2.3, except that the elastic properties are those at the elastic constriction and not those of the tube as a whole. In special cases the resistance relation may be found analytically.

4.1.2 Example

Suppose that

$$p(A, x) = g(x) + HA^n, \tag{4.7}$$

where H and n are nonzero constants having the same sign, $n > -2$, and $g(x)$ attains its maximum value at $x = x_0$, the elastic constriction. Equation (4.7) has the form of equation (4.4) and is a generalisation of equation (3. 11 a); see §3.2.2.

Then, following equations (3.12)-(3.16),

$$Q_{max}(x) = \left(\frac{nH}{\rho}\right)^{1/2} \left\{\frac{2[p_0 - g(x)]}{(n+2)H}\right\}^{\frac{1}{2} + \left(\frac{1}{n}\right)}. \tag{4.8}$$

Obviously $Q_{max}(x)$ is minimum where $g(x)$ is maximum, at the elastic constriction, and the resistance relation is

$$Q = \left(\frac{nH}{\rho}\right)^{1/2} \left\{\frac{2[p_0 - g(x_c)]}{(n+2)H}\right\}^{\frac{1}{2} + \left(\frac{1}{n}\right)}. \tag{4.9}$$

4.1.3. The shape of the tube

At points other than the elastic constriction the local value of $Q_{max}(x)$ is greater than the actual flow rate Q and so, as discussed in §3.2.7, two values of the cross-sectional area A are possible. The larger value of A corresponds to supersonic flow. At first sight then, the flow upstream of the sonic elastic constriction could be either sub- or supersonic, and so could the flow downstream. In fact, supersonic flow is unstable immediately upstream of an elastic constriction (§4.3.3), whereas downstream it can be stable. Thus there occurs typically a transition from subsonic flow upstream to supersonic flow downstream of the elastic constriction (§4.2). The resulting shape and pressure distribution may be determined from p/γ plots (figure 4. 1). The curve labelled x_c represents the elastic properties $p = p(\gamma, x_c)$ of the elastic constriction, and the tangent to it has slope $-\frac{1}{2}\rho Q^2$ and intercept p_0.
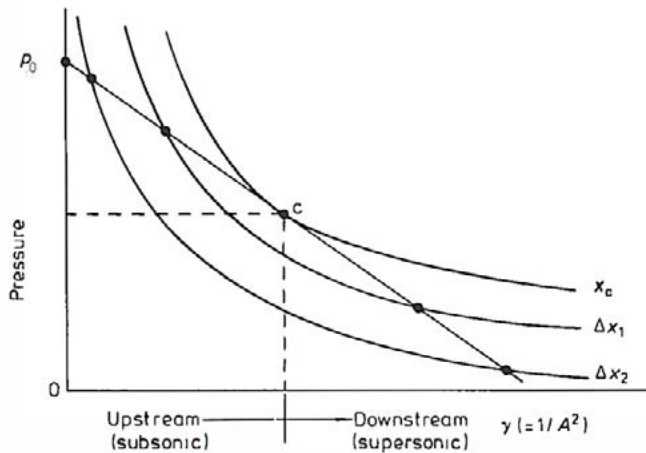
Figure 4.1 p/γ plot for a non-uniform tube. The curves represent $p = p(\gamma, x)$ at an elastic constriction (x_c) and at distances Δx_1 and Δx_2 from it.

The curves labelled Δx_1 and Δx_2 represent the elastic properties at increasing distances Δx_1 and Δx_2 from the elastic constriction. (These distances may be either upstream or downstream, if we assume for simplicity that the elastic properties are symmetrical about x_c). The intersections of the tangent to curve x_c with curves Δx_1 and Δx_2 give the values of γ ($= 1/A^2$) and p at the corresponding points. Thus p and A both become larger as one moves away from the elastic constriction in the upstream, subsonic direction, and they become smaller in the downstream, supersonic direction. The resulting shape and pressure distribution are shown in figure 4.2. Near the elastic constriction the distensible tube funnels down from wide to narrow. The smallest cross-sectional area occurs not at the elastic constriction but further downstream, where the flow is supersonic. The pressure distribution during flow is quite different from that measured at rest (e.g. figure 2.3 a). During flow, the pressure does not have a maximum at the elastic constriction. The pressure upstream of the elastic constriction is high, so tending to force that part of the tube wide open.
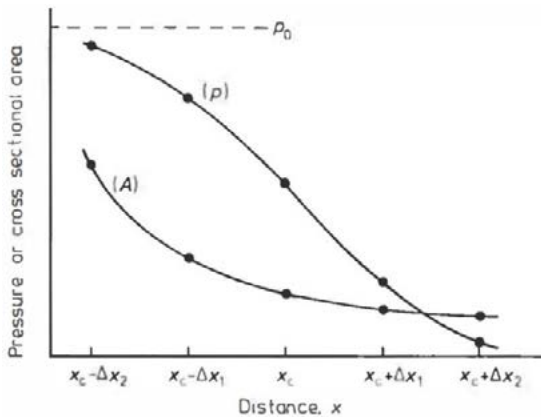
Figure 4.2 Pressure distribution (**p**) and shape (**A**) of a distensible tube near an elastic constriction(**x_c**), during flow from left to right.

In this section the questions posed in §3.1 have been answered, with certain simplifying assumptions. In particular, it is now clear that a tube with elastic properties which are symmetrical about an elastic constriction at its midpoint can take up an asymmetrical shape during flow because the flow regimes are different upstream and downstream of the midpoint.

4.2 Experimental tests

4.2.1 A simple mechanical model

The theory and the assumptions made in developing it are best tested in mechanical models. An elastic constriction is easily formed in a thin-walled collapsible tube by compressing it locally; e.g. with a block of plastic foam and an elastic band as in figure 4.3. When water is flowing, the tube takes up the expected shape, distended on the upstream side of the elastic constriction and collapsed to a small cross-sectional area on the downstream side. As in the female urethra, this asymmetrical shape arises from elastic properties which are approximately symmetrical about an elastic constriction. It is easy to verify experimentally that pressure fluctuations are not transmitted upstream through the collapsed part of the tube, confirming that the flow there is supersonic. More sophisticated measurements substantiate this observation (Elliott and Dawson 1979). Steady compression at a point downstream of the elastic constriction causes interesting shape changes but, provided it is not too severe, has no effect on the pressure head or flow rate. This situation is discussed further in §4.4.1. Alternatively, the collapsed part of the tube can be shortened by cutting part of it off; this has no effect on the resistance relation. On the other hand, extra compression exerted on the elastic
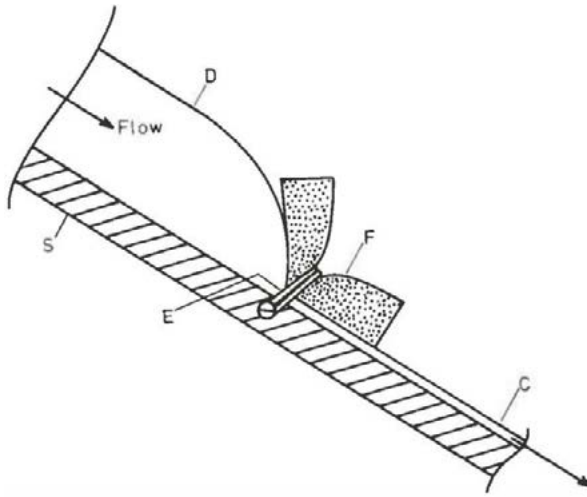
Figure 4.3 Side view of an elastic constriction formed in a collapsible tube. **D**, tube distended; **C**, tube partly collapsed; **F**, plastic foam; **E**, elastic band; **S**, rigid support.

constriction has a marked effect on the resistance relation, as it should.

To ensure that supersonic flow occurs, the collapsible tube may be inclined to the horizontal, as shown in figure 4.3. The reason for this is discussed in §4.3.2.

Thus several aspects of the theory are confirmed by this simple model: the occurrence of subsonic flow upstream and supersonic flow downstream of the elastic constriction, the importance of the elastic constriction in determining the resistance relation; the fact that changes in the elastic properties of the downstream, supersonic part of the tube do not alter the resistance relation. On the other hand, $(\partial p/\partial x)A$, and dA/dx during flow, are certainly not small in this model

as is assumed in the theory. One consequence is that the resistance relation is exceedingly sensitive to the longitudinal tension in the wall of the collapsible tube, a variable which does not appear at all in our analysis. A quantitative test of the theory is not possible with this model.

4.2.2 Quantitative tests on mechanical models

A more sophisticated model is shown in figure 4.4. It consists of a flat channel with thin polythene or latex walls, resting on a flat rigid base and compressed from above by a clamp, padded with latex foam, and so shaped that an elastic constriction is formed. By the use of clamps of different shapes, the elastic constriction can be made either more or less sharply localised, so that the assumption that dA/dx is small during flow is either less well or better satisfied.
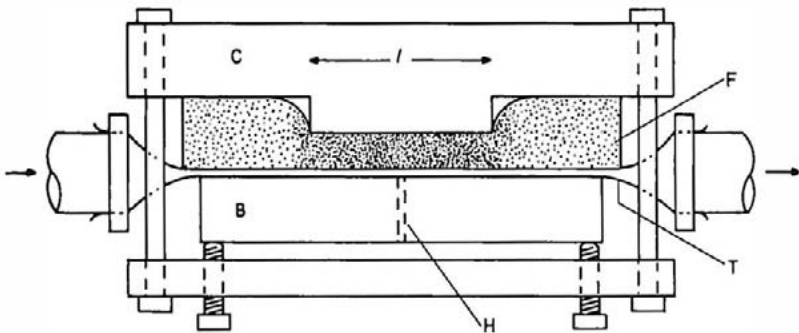
Figure 4.4 Side view of a more sophisticated model having an elastic constriction. **T**, collapsible tube; **F**, latex foam; **B**, base; **H**, hole for measuring pressure at the elastic constriction; **C**, clamp. By altering the length l the elastic constriction can be made more or less sharply localised.

The elastic properties of the elastic constriction can be measured:

(i) by static inflation of the whole channel to a series of uniform pressures, with measurement by a travelling microscope of the corresponding channel depth at the elastic constriction; or (ii) by raising or lowering the rigid base uniformly when the channel is empty, the normal stress exerted by the foam at the elastic constriction being obtained by measuring the pressure needed to force water out of a hole in the base at that position (see §5.2.2).

In method (ii) the channel actually remains closed throughout the measurements, but the raising of the base simulates a uniform increase in the depth (and cross-sectional area) of the channel. In method (i) the depth and cross-sectional area of the channel are non-uniform; each has its minimum value at the elastic constriction.

In general the elastic properties measured by the two methods differ. For a given cross-sectional area at the elastic constriction, method (ii) gives a higher pressure than method (i). This implies that the elastic properties cannot be described by a function $p(A, x)$, since at the elastic constriction p depends not just on the local cross-sectional area but on the overall configuration of the tube. Nevertheless, as the elastic constriction is made less sharply localised by increasing the length of the clamp (figure 4.4), the two sets of elastic properties approach each other. The less sharp the elastic constriction, the more closely is equation (3. 1), $p = p (A, x)$, satisfied.

The hydrodynamic theory can be tested by measuring the relation between the pressure head p_0 and the flow rate Q. Hence the elastic properties of the elastic constriction may be calculated graphically by the method explained in §§3.2.3 and 4.1.1. They may then be compared with the directly measured elastic properties.

In general the elastic properties calculated from the hydrodynamic measurements lie between those measured by methods (i) and (ii). As the elastic constriction is made less sharply localised, all three sets of elastic properties approach one another. Therefore, for the conditions under which it was derived – the existence of the function $p(A, x)$ – the hydrodynamic theory is consistent with experimental results. The existence of this function must be checked in clinical and physiological applications.

4.2.3 Experimental tests *in vivo*

A test of the applicability of the theory to the urethra is provided by some measurements made by Cass and Hinman (1971) on an anaesthetised female dog. They measured the static urethral closure
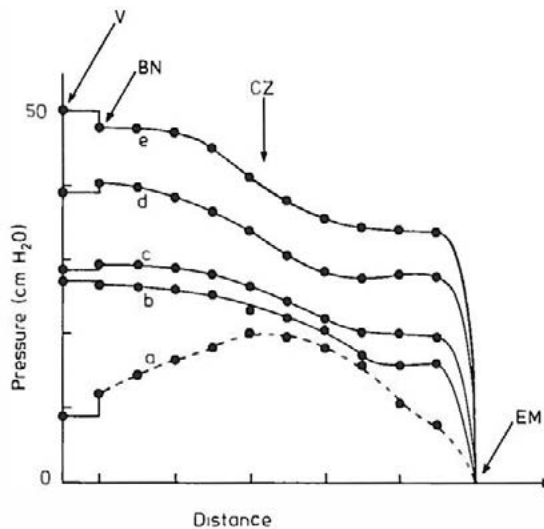
Figure 4.5 Bladder and urethral pressure distributions in a female dog. **V**, bladder: **BN**, bladder neck: **CZ**, compressive zone: **EM**. external meatus. **a**, urethral closure pressure profile at rest: **H**, pressure distributions during flow at 5, 1 0, 20 and 30 ml s^{-1}, respectively. (After Cass and Hinman 1971.)

pressure profile with a thin catheter. They measured also the pressure head p_0 and the distribution of fluid pressure along the urethra at four different flow rates Q. The situation was physiologically quite different from normal micturition, and probably the elastic properties of the urethra were similar for both the static and the flow measurements, i.e. no significant functional alterations occurred.

Figure 4.5 shows the static closure pressure profile, which is roughly symmetrical about an elastic constriction in the mid-urethra, and the pressure distributions during flow, of which the asymmetry indicates a transition from subsonic to supersonic flow. Four pairs of values of flow rate and pressure head are available from this figure. They may be plotted to give an indication of the urethral resistance relation.

Figure 4.6 is a p/γ plot made from the four pairs of values. Each line drawn has intercept p_0 on the pressure axis and slope $-\frac{1}{2}\rho Q^2$ (see figure 3.4). The envelope of the lines is drawn as well as possible, there being
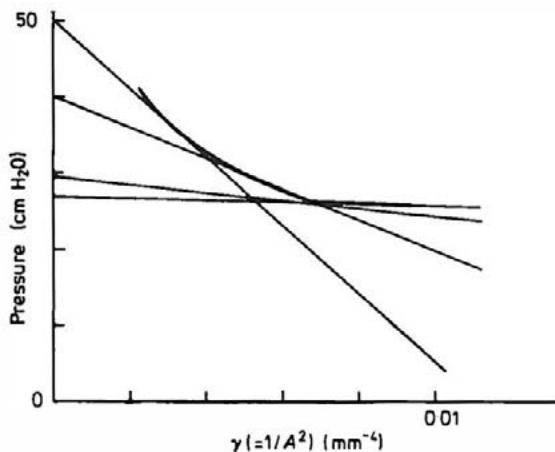
Figure 4.6 p/γ plot from the flow data of figure 4.5. The bold curve is the envelope of tangents.

a little inconsistency in the readings. Figure 4.7 is a p/A plot of the envelope, which represents the elastic properties of the elastic constriction as calculated from the hydrodynamic measurements. They appear to be consistent with static catheter measurements at the same point. Unfortunately the catheter was too small for a very precise comparison. Nevertheless the result suggests that the elastic properties of the urethra of this dog can be satisfactorily described by a function $p(A, x)$, at any rate near the elastic constriction.

The generalisation of this conclusion to the human urethra is supported by some clinical measurements on conscious males in which the peak pressure measured on the urethral closure pressure profile was compared with the pressure head necessary to force a low flow rate through the urethra (Abrams et al 1978). Such experiments are bedevilled by uncontrollable functional changes. When these were discounted there appeared to be only a small difference between the two measurements. Thus equation (3. 1) appears to be a satisfactory approximation and the theory should be applicable to flow through the urethra.

4.3 Effects of Viscosity

4.3.1 Loss of pressure head

Viscous dissipation causes the pressure head to fall monotonically in the direction of flow, the positive x direction. Therefore it makes dp_0'/dx negative, where $p_0'(x)$ is the local value of the pressure head at point x. One result is that the pressure head available locally to drive the flow through an elastic constriction, $p_0'(x_c)$, is less than the original pressure head p_0 in the upstream reservoir. The flow rate is still governed by the resistance relation of the sonic elastic constriction, but it is the flow rate corresponding to pressure head $p_0 - \Delta p_0$, where Δp_0 is the loss of head caused by viscous dissipation between the reservoir and the elastic constriction. The loss depends on the length

and cross-section of the tube upstream of the constriction. The flow rate therefore depends to some extent on the elastic properties of this upstream part of the tube, and not just on those of the elastic constriction itself. This is a significant modification to the inviscid-fluid theory given in §4.1.1. However, the upstream part of the tube tends to be wide during flow (§4.1.3). Hence the viscous loss Δp_0 is often small, so that the predictions of the inviscid-fluid theory remain a good approximation, as demonstrated by the experiments on models.

4.3.2 Positions of elastic constrictions

Another result of viscous dissipation is to shift elastic constrictions to different positions, or even to introduce new ones. It is left as an exercise to extend the argument of §4.1.1 to the case where the local pressure head p_0' is a decreasing function of x, and to show that the flow rate is then no longer controlled where $p(A, x)$ is maximum with respect to x at constant A, but where $p(A, x) - p_0'(x)$ is maximum (i.e. least negative). Thus the flow-controlling point is shifted downstream. For a pronounced elastic constriction the shift may be unimportant, but for a uniform or near-uniform tube, where $p(A, x)$ is constant or decreases only slowly with x at constant A, a more rapid decrease in
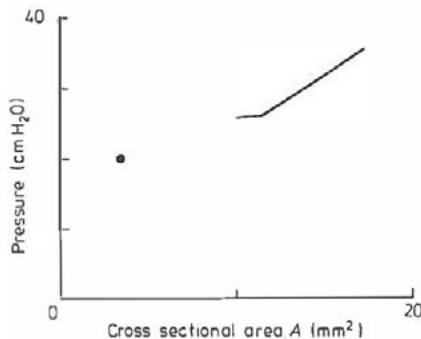
Figure 4.7 Elastic properties of the compressive zone of a dog's urethra. Curve, deduced from flow measurements (figure 4.6); point, measured at rest (curve a, figure 4.5).

p_0' (x) can produce a maximum in $p(A, x)$ - p_0' (x) at the downstream end of the tube. This was the case in §3.3. It seems to occur in the penile part of the male urethra, in which the external meatal region behaves as an elastic constriction yet no well-defined maximum is visible on the pressure profile (see figure 2.3b). All such points will be referred to as elastic constrictions, whether they satisfy the definition given in §4.1.1 or not.

In the model shown in figure 4.3, the occurrence of an elastic constriction at the downstream end is prevented by tilting. Gravity causes $p(A, x)$, which is piezometric, to decrease in the direction of flow more rapidly than p_0' (x), so that $p(A, x)$ - p_0' (x) has no maximum at the end of the tube.

4.3.3 Effects of viscosity on subsonic and supersonic flow

The experimental observations (§4.2.1) show that sub- and supersonic flow occur respectively up- and downstream of an elastic constriction. Some insight into the reason for this can be obtained by examining how the fluid pressure and the cross-sectional area vary near the elastic constriction, and especially how they are affected by viscosity. Generalising equation (3.5) to the case of a non-uniform tube with local pressure head p_0' (x),

$$Q^2 = [p_0' (x) - p(A, x)]2A^2/\rho. \qquad (4.10)$$

Differentiating with respect to x, and remembering that Q is the same for all x in steady flow,

$$Q = \frac{1}{2}A \ [dp_0'/dx - \partial p/\partial x - (\partial p/\partial A) \ dA/dx] + (dA/dx)[\ p_0' - p(A, x)].$$
$$(4.11)$$

Since, from equation (3.21a),

$$p_0' - p(A, x) = \frac{1}{2}\rho v^2 \qquad (4.12)$$

and, from equation (4.3),

$$c_0 = [(A/\rho)\, \partial p/\partial A]^{1/2}, \qquad (4.13)$$

it follows that

$$\frac{dA}{dx} = \frac{A}{\rho(c_0^2 - v^2)}\left(\frac{dp_0'}{dx} - \frac{\partial p}{\partial x}\right). \qquad (4.14)$$

Furthermore,

$$dp/dx = \partial p/\partial x + (\partial p/\partial A)dA/dx$$
$$= \partial p/\partial x + (\rho c_0^2/A)\, dA/dx, \qquad (4.15)$$

using equation (4.13). Whence

$$\frac{dp}{dx} = \frac{c_0^2}{c_0^2 - v^2}\left(\frac{dp_0'}{dx} - \frac{v^2}{c_0^2}\frac{\partial p}{\partial x}\right). \qquad (4.16)$$

In equations (4.14) and (4.16) dp_0'/dx represents the effect of viscosity. It is necessarily negative (see §4.3.1).

$\partial p/\partial x$ depends on the elastic properties of the tube. If viscosity is neglected ($dp_0'/dx = 0$), then $\partial p/\partial x$ is positive upstream and negative downstream of an elastic constriction. At the elastic constriction it is equal to zero, so that sonic flow can occur there ($v = c_0$) without dp/dx diverging (see equation (4.16)). If viscosity is allowed for, sonic flow can occur only where

$$dp_0'/dx - \partial p/\partial x = 0, \qquad (4.17)$$

since otherwise dp/dx and dA/dx diverge. Because $dp_0'/dx < 0$, equation (4.17) implies that $\partial p/\partial x$ is negative at the point where $v = c_0$. Thus the position of the elastic constriction, the point where the flow is controlled, is shifted downstream, as discussed in §4.3.2.

At the elastic constriction both $(dp_0'/dx - \partial p/\partial x)$ and $[dp_0'/dx - (v^2/c_0^2)\partial p/\partial x]$ are zero. Upstream, both expressions are negative and downstream both are positive. Hence, using equations (4.14) and (4.16), the signs of dA/dx and dp/dx may be determined both upstream and downstream of the elastic constriction and for both sub- and supersonic flow. The results are shown in table 4.1. They are consistent with the discussion in §4.1.3.

Table 4.1 The signs of dA/dx and dp/dx near a sonic elastic constriction. Flow is in the positive x direction.

	Upstream		Downstream	
	Subsonic	Supersonic	Subsonic	Supersonic
dA/dx	-	+	+	-
dp/dx	-	+	+	-

According to table 4.1, under some circumstances, dp/dx can be positive. If this is so, the fluid boundary layer may become unstable, with the result that the flow streamlines become detached from the tube wall and extra turbulent dissipation occurs; that is, dp_0'/dx becomes more negative (numerically larger) (e.g. Massey 1970, pp284-6). For *subsonic flow downstream* of an elastic constriction, the more negative dp_0'/dx, the smaller is dp/dx (see equation (4.16)). Thus there is negative feedback and the extra dissipation is self-limiting. For supersonic flow upstream of an elastic constriction, however, the more negative dp_0'/dx, the larger is dp/dx and the worse the

instability. The feedback is positive. Thus supersonic flow immediately upstream of an elastic constriction should be unstable, and is not in fact observed.

Downstream of an elastic constriction both types of flow can be stable. If the flow is sonic at the elastic constriction, supersonic flow usually occurs downstream, as discussed in §§4.1.3 and 4.2.1. If the flow is subsonic at the elastic constriction, then it remains subsonic immediately downstream (see §4.4).

Supersonic flow can develop an instability even downstream of an elastic constriction, for should a region of sufficiently high dissipation (large negative dp_0'/dx) develop, equation (4.16) shows that it can yield a large positive value of dp/dx, and so be sustained by the positive feedback discussed above. We shall meet this phenomenon in the hydraulic jump considered in the following section.

4.4 Flow through a Distensible Tube Having Two Successive Elastic Constrictions

4.4.1 The hydraulic jump

Return to the simple mechanical model described in §4.2.1. If a second elastic constriction is introduced some distance downstream of the first, and if it is not too tight, the collapsible tube takes up the shape shown in figure 4.8. There is no change in flow rate nor in the pressure head in the upstream reservoir. The overall resistance relation is thus unaffected. It is still governed by the original elastic constriction, the new one having no effect because of the intervening region of supersonic flow. A second transition from subsonic to supersonic flow takes place at the new elastic constriction, and between it and the original one a new phenomenon occurs: a localised transition from subsonic to supersonic flow, or hydraulic jump. The resistance relations for both elastic constrictions are sketched in figure 4.9. For a
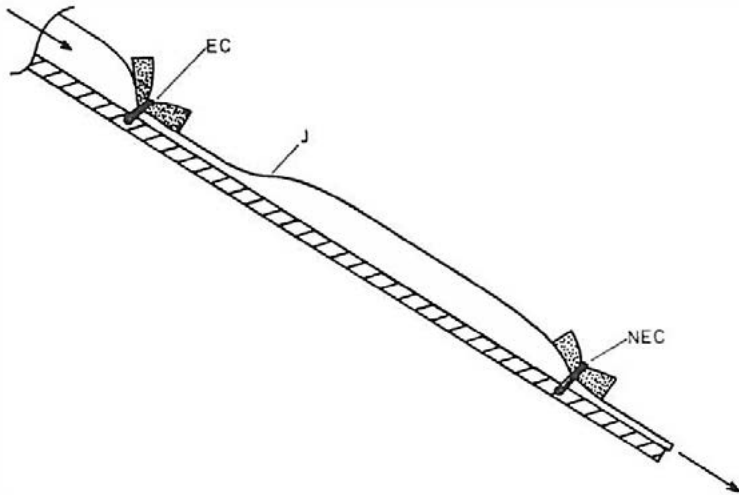
Figure 4.8 Collapsible tube with two elastic constrictions. EC, original elastic constriction (c.f. figure 4.3): NEC, new elastic constriction : J, hydraulic jump.

given upstream pressure head p_0, the resistance relation of the first elastic constriction sets the flow rate Q_A. The second elastic constriction accepts this flow rate. Since it is sonic, the necessary local pressure head p_0' is determined by its own resistance relation. Since $p_0' < p_0$, energy must be dissipated to reduce the original pressure head to p_0'. This occurs through locally turbulent dissipation at a sudden widening of the tube: the hydraulic jump. At the jump, dp/dx is positive, supersonic flow becomes unstable, and a transition to subsonic flow occurs.

If the second elastic constriction is made gradually tighter, p_0' must increase and eventually will exceed p_0, as shown in figure 4.9, curve B. In that case, p_0 is not large enough to drive the maximum possible flow rate Q_{max} for the first elastic constriction through the second.
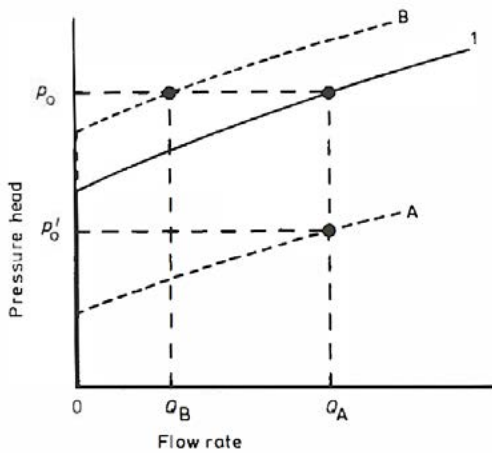
Figure 4.9 Resistance relations for two successive elastic constrictions. **1**, Resistance relation of an upstream elastic constriction: **A** and **B**, resistance relations of a second elastic constriction. When the second constriction is not tight (**A**), the flow rate is **Q$_A$**. When it is tightened (**B**), the flow rate is **Q$_B$**.

Therefore the flow rate Q_B is now determined by the resistance relation of the *second* elastic constriction, together with all the upstream pressure head losses. At the first elastic constriction, Q_B is less than Q_{max} and the fluid speed is *sub*sonic. The shape of the collapsible tube is sketched in figure 4.10.

How does figure 4.8 change into figure 4.10? As the second elastic constriction is tightened the hydraulic jump moves upstream. The supersonic region disappears when it reaches the first elastic constriction, which thereafter is subsonic. From this account one would expect the flow rate for a fixed pressure head p_0 to vary in the way shown in figure 4.11, curve A. The behaviour observed experimentally in mechanical models is similar to this (curve B), except for a sudden increase in the flow rate as the hydraulic jump reaches
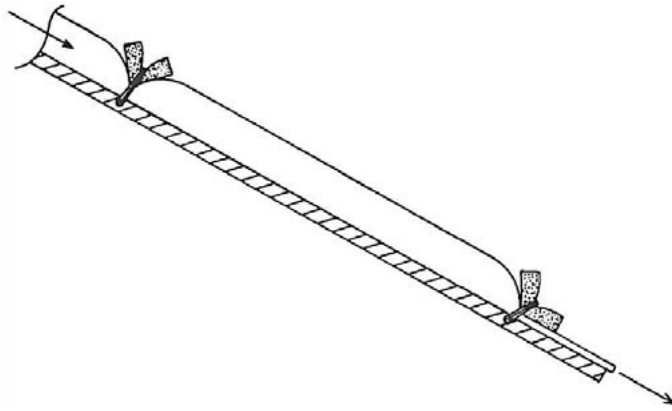
Figure 4.10 Side view of a collapsible tube with two elastic constrictions, after the downstream elastic constriction has been tightened (c.f. figure 4.8).
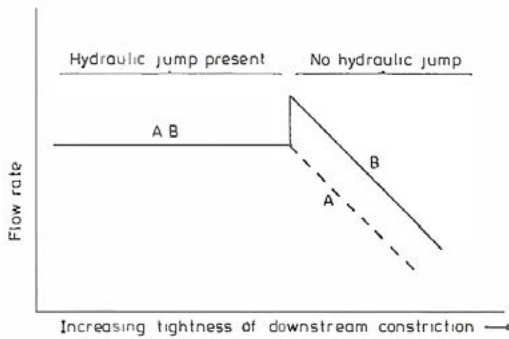
Figure 4.11 Schematic dependence of flow rate on the tightness of the downstream elastic constriction at fixed pressure head. **A**, expected; **B**, in reality.

the first elastic constriction. The behaviour occurs because, in the models, the sharply localised elastic constrictions cannot be described by a function $p(A, x)$, as discussed in §§4.2.1 and 4.2.2. The less sharply

localised the elastic constriction, the more nearly the behaviour approaches the ideal (curve A). The situation described by curve B can give rise to oscillations. However, since the elastic properties of the urethra seem to be satisfactorily described by a function $p(A, x)$, oscillations are unlikely in the urethra, and curve A is probably a reasonable approximation.

4.4.2 The criterion for the occurrence of a hydraulic jump

In the previous section it was implicitly assumed that viscous dissipation occurred only at the hydraulic jump. The loss of pressure head at the jump is then $(p_0 - p_0')$, and the criterion for the occurrence of the hydraulic jump is simply

$$p_0' < p_0, \tag{4.18}$$

where p_0 is the upstream pressure head, and p_0' is the pressure head needed to drive the set flow rate through the second elastic constriction.

In reality, viscous dissipation occurs all along the tube, and so the criterion becomes more stringent:

$$p_0' < p_0 - \Delta p_0, \tag{4.19}$$

where p_0 is now the *local* pressure head at the first elastic constriction, p_0' is the local pressure head at the second elastic constriction for the set flow rate, and Δp_0 is the loss of pressure head which would occur between the two elastic constrictions in the absence of a hydraulic jump. Since Δp_0 is here a rather imprecise concept, criterion (4.19) is not very useful in practice.

Hydraulic jumps have been considered in more detail by Oates (1975a).

4.4.3 The speed of the external stream

When a region of supersonic flow intervenes between the two elastic constrictions, alteration of the elastic properties of the second elastic constriction has no effect on the overall resistance relation. It merely alters p_0' and thus the loss of pressure head at the hydraulic jump.

p_0' is related to the speed v_{ext} of the stream which eventually emerges from the tube downstream of the second elastic constriction. The fluid pressure in the stream is equal to the external pressure p_{ext} (surface tension effects are neglected). Provided that dissipation occurring downstream of the second elastic constriction can be neglected, then from the Bernoulli equation (c.f. equation (3.34)),

$$\tfrac{1}{2}\rho v_{ext}^2 = p_0' - p_{ext}. \qquad (4.20)$$

Tightening of the second elastic constriction raises p_0' and so also v_{ext}, and vice versa. This conclusion remains valid even when some dissipation occurs between the second elastic constriction and the exit from the tube, as can be demonstrated in mechanical models.

4.5 The Limitations of a Steady-flow Analysis

The analysis given in Chapter 3 and in this chapter is strictly valid only for steady flow. A time-dependent flow, such as occurs during micturition, obviously cannot be treated as steady if the flow rate changes significantly within the time needed for the distensible tube to assume its steady configuration. A lower limit to this time is that for the pressure waves to pass along the tube from the upstream reservoir either to the exit or, if one is concerned only with the overall resistance relation, to the first sonic elastic constriction. For the urethra this lower limit is probably a small fraction of a second. Even for the long male urethra, the external stream can be observed to respond to rapid changes in the abdominal pressure within less than a

second. Therefore the slowly varying flow during a normal micturition lasting 20 s or more can probably be treated as steady. This may not always be so at the start of micturition, when the flow rate rises quite rapidly from zero (§ 11.2), nor when the external sphincter is used to interrupt and recommence voiding during the course of micturition (figure 2.1).

4.6 Flow through a Rigid Non-uniform Tube

Like §3.4, this section is a brief summary of results which may be contrasted with those just obtained for a highly distensible non-uniform tube. A rigid, non-uniform tube has a cross-section which varies along its length, and it is not necessarily straight. For brevity, near-rigid non-uniform tubes are not considered.

4.6.1 Inviscid fluid

If viscosity is neglected, the non-uniformity of the tube is unimportant. Equations (3.34)-(3.36) are valid, provided only that A_0 is taken as the cross-sectional area of the tube at the exit. The resistance relation, equation (3.36), is determined by conditions at the exit from the tube. It is of the form $Q \propto (p_0 - p_{ext})^{1/2}$ like those for rigid and near-rigid *uniform* tubes. Widening of the exit reduces the resistance to flow of the tube by raising Q for given p_0 (equation (3.36)), but leaves the speed of the external stream unchanged (equation (3.34)).

4.6.2 Viscous fluid

Once again the effect of viscosity is to cause dissipation. Equation (3.41) is valid:

$$Q = A_0[2(p_0' - p_{ext})/\rho]^{1/2}, \qquad\qquad (4.21)$$

provided that A_0 is taken as the cross-sectional area at the exit. p_0' is the local pressure head at the exit, equal to $p_0 - \Delta p_0$ where p_0 is the upstream pressure head and Δp_0 is the loss of pressure head through dissipation within the tube (equation (3.42)). Δp_0 depends on the shape and non-uniformity of the tube. The main contributions to it come from the narrow parts of the tube. There are relatively higher losses both within the narrow parts, approximately proportional to Q^2 if the flow is turbulent, and also associated with changes in cross-section from wide to narrow or vice versa (so-called minor losses), again proportional to Q^2. Thus

$$\Delta p_0 \cong KQ^2, \tag{4.22}$$

where K is constant for a given tube. Whence

$$Q = A_0[2(p_0 - p_{ext})/\rho]^{1/2}/[1 + 2KA_0^2/\rho]^{1/2}. \tag{4.23}$$

Again this resistance relation has the form $Q \propto (p_0 - p_{ext})^{1/2}$. For a given upstream pressure the flow rate is determined by the external (exit) pressure, the exit area and the value of K. Contributions to K come from all parts of the tube, but are especially associated with the narrowest parts. If K is large so that

$$2KA_0^2/\rho \gtrsim 1, \tag{4.24}$$

the resistance to flow can be significantly reduced by widening the narrowest parts of the tube. Under condition (4.24) the exit area A_0 *per se* has relatively little effect on the resistance to flow. Thus widening the exit would be expected to change the flow rate relatively little, but to reduce the speed of the external stream (equation (3.35)). This effect may be observed when the end of a garden hose is pinched and then released.

4.7 Summary

The pattern of flow through a distensible tube is determined by its elastic constrictions. An elastic constriction is essentially a point along the length of the tube where the pressure, measured at constant cross-sectional area, is maximum. Viscous losses may however shift elastic constrictions slightly downstream, or introduce a new one at the downstream end of a near-uniform distensible tube. A transition from subsonic flow (upstream) to supersonic flow (downstream) can occur only at an elastic constriction.

The overall resistance relation of a distensible tube is determined by the elastic properties of the first elastic constriction at which a transition to supersonic flow occurs, together with the viscous losses in the portion upstream of this. Elastic properties and viscous losses in parts of the tube lying further downstream have no effect on the overall resistance relation.

In the case of a distensible tube having two elastic constrictions, the first transition to supersonic flow occurs at the upstream elastic constriction if the downstream one is not too tight. An abrupt transition (a hydraulic jump) from supersonic back to subsonic flow, accompanied by dissipation, occurs between the two elastic constrictions. The downstream elastic constriction controls the speed of the external stream. If the downstream elastic constriction is sufficiently tightened, the first transition to supersonic flow occurs there; there is then no hydraulic jump.

The steady-flow theory developed in this and the preceding chapter is discussed and extended in the following: Griffiths (1969, 1971a,b, 1 975a,b,c), Oates (1975a), Elliott and Dawson (1979), Beard (1977).

Quantitative tests of the theory on models are described by Martin and Griffiths (1976a,b) and Elliott and Dawson (1977). Other observations on models have been made by Scott et al (1966).

Extensions of the theory to non-steady flow have been made by Oates (1975b) and by Reyn (1974, 1975). The theory has been applied to respiratory air flow (Dawson and Elliott 1977) and to venous blood flow (Gardner *et al* 1977).

The oscillations that occur in flow through collapsible tubes have been discussed by Conrad (1969), Brower and Scholten (1975), Griffiths (1977a), Reyn (1974, 1975), and others.
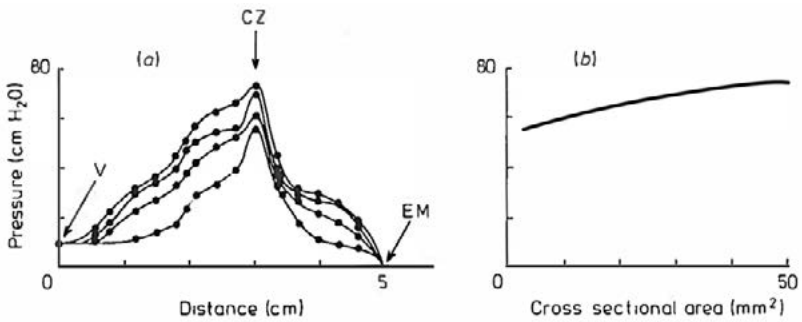
5 The Urethral Closure Pressure Profile

## 5.1 Characteristics of the Profile

5.1.1 Physical aspects

Typical urethral closure pressure profiles are illustrated in figure 2.3(a,b). In the light of the discussion in §2.2.5.1, the question arises: have these profiles any meaning? Is the urethra so distensible that one pressure measurement (at each point along its length) is representative?

One series of profiles from a female patient, measured with catheters of different sizes, is shown in figure 5.1(a). Although the measured pressure does depend on the catheter size, the dependence at the point of highest pressure is relatively slight. This is shown more clearly in figure 5.1(b), which resembles figure 2.4(b), the pressure/area relation of a highly distensible tube. Physically then, it is sensible to measure and ascribe significance to the urethral pressure, at least in the region of its maximum.

Figure 5.1 makes it clear that the point of highest pressure in the female urethra, at rest, is an elastic constriction according to the definition given in §4.1.1. Since elastic constrictions are so important in the understanding of flow, the region of high pressure has been given a special name, the *compressive zone*. The male urethra, at rest, has a similar compressive zone (see figure 2.3b). This is followed distally by a long section with fairly uniform elastic properties. It is expected that, during flow, viscous dissipation will give rise to a second elastic constriction at the downstream end of this section, near the external meatus (see §4.3.2).

Figure 5.1 (a) Urethral closure pressure profiles of a female suffering from stress incontinence, measured in the supine position with catheters of diameters 2, 4, 6 and 8 mm. **V**, bladder; **CZ**, compressive zone; **EM**, external meatus. (After Plevnik 1976.) (b) Elastic properties at the compressive zone, deduced from (a).
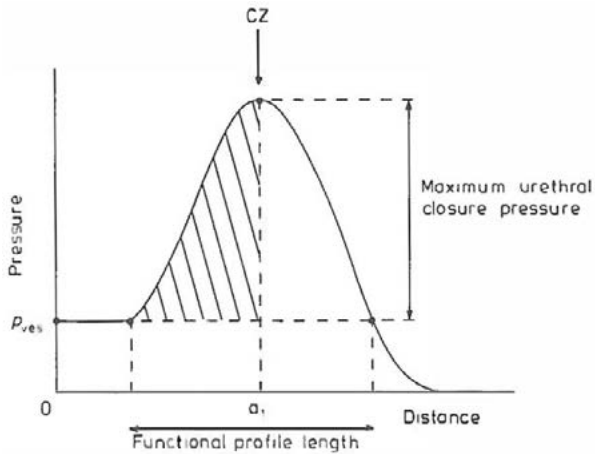
Figure 5.2 Schematic urethral closure pressure profile, showing definitions of maximum urethral closure pressure and functional profile length. The continence zone is defined as the magnitude of the shaded area (in cm H_2O.cm) up to the point a_1 , which is the point where fluid infused into the urethra begins to leave the urethra distally instead of proximally (see §5.2.2). In principle, a_1 should lie at the compressive zone (**CZ**).

In clinical practice the profile is often measured in order to assess the

ability of the urethra to prevent leakage. To reduce it to one or two manageable numbers, concepts such as the *maximum urethral closure pressure*, the *functional profile length* (International Continence Society 1976) and continence zone (Gieason et al 1974) have been introduced (see figure 5.2). Although some clinical utility is claimed for them, the problem is that, when leakage threatens, the urethra is mechanically altered (see §5.1.3). The conditions under which leakage occurs are considered more fully in the following chapter.

Under given conditions the maximum pressure recorded on the profile is quite reproducible. The standard deviation has been estimated as about 5 cm H_2O for readings repeated within a few minutes (Abrams *et al* 1978), and as 9 cm H_2O over periods of weeks or months. If the maximum pressure is monitored continuously it exhibits fluctuations (period 10-30 s) which in some individuals may be considerably greater than these averaged figures suggest. No steady decrease (or increase) has been reported, such as might be expected if the measurement was merely of a transient response to the insertion of the catheter.

5. 1.2 Relation to anatomy

5.1.2.1 Females. The most obvious feature of the female urethral closure pressure profile is the compressive zone (figure 5.2), which is located near the pelvic floor/urogenital diaphragm (see figure 1.3 and § 1.1.3.1), and is mainly muscular in origin. The muscles of the urethra itself, both smooth and striated, as well as the periurethral striated muscles of the pelvic floor probably all play a part. The general impression seems to be that the intrinsic urethral musculature dominates on the proximal side of the peak and the periurethral sphincter on the distal side.

In females the bladder neck is often open at rest and so difficult to recognise. This is the case in figure 5.1(a); the initial pressure rise at the proximal end of the urethra occurs nearer the compressive zone

with the smallest catheter, indicating that this part of the urethra is slightly open. The fall to atmospheric (zero) pressure at the distal end of the profile coincides with the external meatus.

5.1.2.2 Males. The compressive zone again lies near the pelvic floor/urogenital diaphragm (see figure 1.4 and § 1.1.3.2). It is made up of muscular contributions similar to those in the female. The bladder neck is better defined and can often be identified as a small peak immediately following the initial pressure rise (see figure 2.3b). Between the bladder neck and the compressive zone lies a prostatic region, which in older men may be several centimetres long. The long and fairly uniform section distal to the compressive zone corresponds to the less muscular penile part of the urethra, and the fall to atmospheric pressure at the external meatus is clearly defined.

5.1.3 Functional changes

Because the proximal part of the urethra lies inside the abdominal cavity, and also because it is muscular, the mechanical properties of the urethra can change greatly. During micturition, for example, the muscles forming the compressive zone normally relax, so that the compressive zone is less pronounced; i.e. the urethral pressure there, if it could be measured in the same way as at rest, would be lower (§7.2.3). There is some evidence that, in males, the region near the bladder neck may tighten during micturition (§9.5).

In order to stop flow or prevent leakage, the periurethral sphincter may be contracted, so raising the pressure near the compressive zone.

If the abdominal pressure rises, for example through change of posture or coughing, then the urethral pressure also rises in the proximal part of the urethra; that is, between the bladder neck and the compressive zone. This may be due to mechanical transmission of abdominal pressure to the intra-abdominal urethra. Recent work

seems to suggest, however, that purely mechanical transmission is confined to a region near the bladder neck and that the pressure rise near the compressive zone is mainly due to contraction of the periurethral muscles, which accompanies the raised abdominal pressure. In any event, changes in abdominal pressure greatly affect the profile.

If any of these functional changes occur during the measurement of the profile, they can cause artefacts. To help detect them, intravesical and abdominal pressures may be monitored during the measurement.

Since functional changes are so closely associated with the micturition reflex and with raised abdominal pressure, routine use of the urethral closure pressure profile to assess disorders of micturition (e.g. urethral obstruction) and leakage (stress incontinence) is difficult. However, as a research tool - for example, to assess the effect of drugs or surgery on the urethra - it has proved valuable.

5.2 The Infusion (Brown-Wickham) Method of Measuring the Urethral Pressure

5.2.1 The principal artefact

The catheter used for the measurement has either one sidehole, or two or more sideholes spaced around its circumference at one point (Abrams 1979). Liquid or gas is infused into the catheter and so forced out of the sideholes and into the urethra. The rate is usually between 1 and 10 ml min^{-1} for a liquid and much higher for a gas. The pressure head needed to do this is taken to be the urethral pressure at the site of the sideholes. Viscous losses need to be allowed for (§2.2.5.2). The measured pressure does not seem to depend significantly on the orientation of the sidehole(s) with respect to the urethra, at least near the compressive zone.

Very often the profile is recorded by withdrawing the catheter steadily through the urethra. In this case it is subject to an artefact, since there is a maximum rate of rise in pressure that the system can record. This is the rate at which the pressure rises when the sideholes are completely blocked, and is determined by the total mechanical compliance C of the catheter and pressure-measuring system, and the volume rate of infusion of fluid, Q_{inf}:

$$(dp/dt)_{max} = Q_{inf}/ C. \qquad (5.1)$$

If the catheter is withdrawn at speed v_{cat}, this maximum rate of pressure increase is translated into a maximum measurable rising pressure gradient:

$$\begin{aligned}(dp/dx)_{max} &= (1/v_{cat})\, dp/dt \\ &= Q_{inf}/Cv_{cat}.\end{aligned}$$

$$(5.2)$$

If the rising pressure gradient in the urethra exceeds the value given by equation (5.2), the profile is cut off and distorted, as shown in figure 5.3. Since Q_{inf} should not be made too large (see §5.2.2), the compliance C should be made as small as possible and the speed of withdrawal v_{cat} kept low enough to record the urethral pressure faithfully.

The rate of fall of pressure is not limited by the infusion rate. A falling pressure gradient is therefore faithfully recorded, with the result that, when distortion occurs, the recorded profile typically has the saw-tooth form shown in figure 5.3.
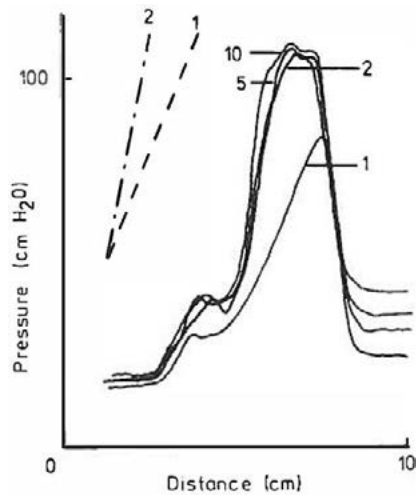
Figure 5.3 Superimposed urethral closure pressure profiles from a male subject, obtained by the infusion method with a catheter of diameter 2.5 mm, withdrawn at 7 mm s^{-1}. The infusion flow rates were 1, 2, 5 and 10 ml min^{-1}, respectively. The broken lines show the maximum measurable pressure gradients at 1 and 2 ml min^{-1}. (After Abrams *et al* 1978.)

Sometimes gas (CO_2 or air) is used instead of water. The compressibility of the gas must then be added to the compliance of the measuring system. Usually a much higher infusion rate Q_{inf} is used, so compensating in equation (5.2) for the increased value of *C*.

5.2.2 The basis of the method

It is supposed sometimes that the infusion method measures the resistance to flow of a substantial part of the urethra, rather than a local urethral pressure, and sometimes that the fluid emerging from the sidehole(s) forces the urethral wall away from the catheter to a large and unknown extent, so that the measured pressure is
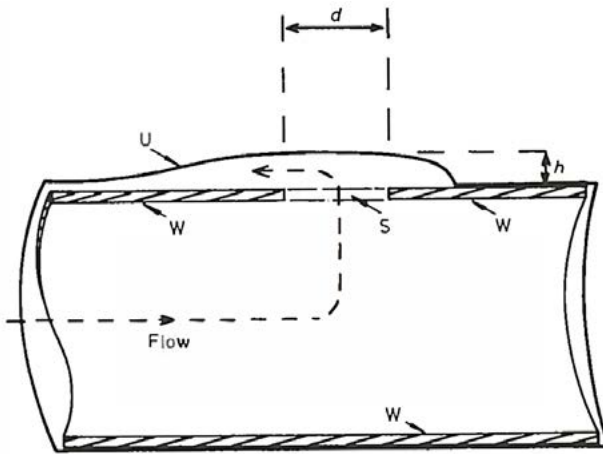
Figure 5.4 Schematic diagram of urethral pressure measurement by the infusion method. **S**, sidehole: **W**, catheter wall; **U**, urethral wall.

significantly higher than that corresponding to the cross-sectional area of the catheter. Both these ideas are a little misleading.

When the fluid emerges into the urethra it is in a channel along which there is a pressure gradient, except at a few isolated points. The fluid can escape easily in the direction of falling pressure: this is the basis of the determination of the continence zone (figure 5.2). The maximum urethral pressure experienced by the fluid is at the side-hole(s), which therefore form(s) an elastic constriction (§4.1.1). Provided viscous effects are not dominant, the escaping fluid flows supersonically. It follows that there is no accumulation of fluid just outside the sidehole(s) because this would correspond to subsonic, not supersonic flow; further, that the urethral pressure at the side-hole(s) only is important and the rest of the urethra has no effect on the measurement.

The situation is illustrated diagrammatically in figure 5.4 for the case where there is only one sidehole. The measured quantity is p_0, the pressure head within the catheter. Suppose that the urethral wall near the sidehole exerts a pressure (normal stress) G when it is just clear of the catheter wall: this is the quantity which it is desired to know. Thus the method overestimates the urethral pressure by the difference $p_0 - G$.

Suppose that, when the fluid is being infused, the urethral wall is lifted a distance h off the sidehole, which has a diameter d. Assuming that h « d, and that fluid escapes all round the circumference of the sidehole, the elastic constriction has cross-sectional area $A = \pi d h$. Thus its elastic properties are given by

$$p(A) = G + h \, dp/dh \qquad\qquad (5.3)$$

to first order in h; that is,

$$p(A) = G + [(dp/dh)/\pi d] \, A. \qquad\qquad (5.4)$$

Provided that dp/dh does not vary greatly with h, equation (5.4) is the same as equation (3.11a) with $n = 1$ and $H = (dp/dh)/\pi d$. Therefore the resistance relation of this elastic constriction is, from equation (3.16),
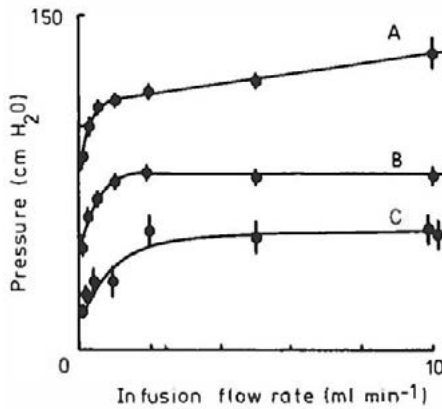
$$Q_{inf} = (H/\rho)^{1/2}[2(p_0 - G)/3H]^{3/2}. \qquad\qquad (5.5)$$

Hence the overestimate of the urethral pressure is

$$p_0 - G = (3/2)(\rho H^2 \, Q_{inf}^2)^{1/3}. \qquad\qquad (5.6)$$

This equation is strictly valid only for an inviscid fluid.

The equation has been tested in a mechanical model, using water as the infusion fluid (Martin and Griffiths 1976a). The predicted and experimental values of $p_0 - G$ are in fairly good agreement at infusion

Figure 5.5 Dependence of urethral pressure, as measured near the compressive zone by the infusion method, on infusion flow rate. Catheter 2.5 mm diameter, two sideholes 1 mm diameter. **A** and **B**, males; **C**, female. (After Abrams *et al* 1978.)

flow rates above about 1 ml min^{-1}. At rates below 1 ml min^{-1}, G is underestimated (i.e. p_0 - G is negative), and this cannot be accounted for by equation (5.6). At such low rates the predicted clearance h is very small. It is therefore important that equation (5.4) should be a good approximation down to vanishingly small values of h; that is, the wall of the distensible tube should seal perfectly round the sideholes. In practice the seal is not perfect; folds and surface imperfections allow slow leakage of fluid at pressure heads less than G.

Similar measurements made clinically (figure 5.5) strikingly resemble those made on the model (Abrams *et al* 1978). At infusion flow rates from 1 to 10 ml min^{-1} the measured pressure head p_0 apparently gives a good estimate of the pressure G exerted by the urethra near the sideholes. At 10 ml min^{-1} the overestimate p_0 - G is undetectable (less than 5 cm H_2O) in the majority of cases, but rises up to about 20 cm H_2O in a few cases (e.g. figure 5.5, curve A). At infusion flow rates

below about 1 ml min^{-1} the measured pressure head appears to fall below the urethral pressure, just as in the model, so indicating an imperfect seal between the urethral wall and the catheter.

The overestimates observed at 10 ml min^{-1} may be compared with the prediction of equation (5.6). Figure 7.3 suggests that dp/dh is about 2 cm H$_2$O/mm. If d = 1mm, then H is of order 1cm H$_2$O/mm^2. It follows that p_0- G should be of order 1 cm H$_2$O when Q = 10 ml min^{-1}. The majority of observations are indeed consistent with this estimate (figure 5.5, curves B and C), but some are not (curve A). The practical implication of these results is that measurements of urethral pressure, using an aqueous fluid, must be made at an infusion flow rate of 1ml min^{-1} or more, irrespective of the withdrawal rate. The majority of urethras are so distensible that the measurement is not sensitive to the infusion flow rate, provided it lies above this value, and so a representative result is obtained (figure 2.4b). In some urethras, however, the measurement is sensitive to the infusion flow rate. Equation (5.6) suggests that this may be a sign of reduced distensibility. The measurement is then less representative of the mechanical properties of the urethra and may begin to lose its point (figure 2.4c).

If a gas is used as the infusion fluid, the density ρ is much smaller. Since much higher infusion rates are used, however, the overestimate predicted by equation (5.6) is not greatly altered. The extent of slow leakage at pressure heads lower than the urethral pressure G has not been investigated for gas.

6 Continence and Incontinence

6.1 The Urethral Closure Pressure

The previous chapter was devoted to the urethral closure pressure profile. The urethral closure pressure is defined as the difference between the urethral pressure and the intravesical pressure. The reason for the name is that it is often considered that this is the pressure that keeps the urethra shut, i.e. resists leakage. As long as there is a positive closure pressure there should be no leakage and so the subject should be continent. This idea needs to be qualified.

On a purely mechanical level, the urethral pressure is measured with a catheter of finite diameter. The true closure pressure, without a catheter, is likely to be smaller than that with the catheter. The error is small only if the urethra is highly distensible (see §§2.2.5.1 and 5.1), but in a minority of urethras this may not be the case (see §§5.2.2 and 7.2.2). It is particularly important that the urethra should seal well, which means that at small cross-sectional areas its elastic properties should look like figure 2.4(b) and not like figure 3.6. If it does not seal well then liquid can leak through it slowly even though the measured maximum urethral closure pressure is large.

On the physiological level, it has to be realised that leakage – incontinence – commonly occurs under particular circumstances. These include:

(i) a temporary increase in abdominal pressure during coughing or other exertion, without active detrusor contraction (genuine stress incontinence);
(ii) an involuntary active contraction of the detrusor muscle;
(iii) a combination of (i) and (ii).

All these are associated with functional changes (§ 1.1.5) which can be expected to alter the maximum urethral closure pressure.

6.2 Continence Mechanisms

6.2.1 The bladder neck mechanism

When the abdominal pressure increases, not only the intravesical pressure but also the pressure in the proximal urethra rises. The pressure increases in the bladder and in the urethra close to the bladder neck are normally equal and are believed to result from purely mechanical transmission of abdominal pressure.
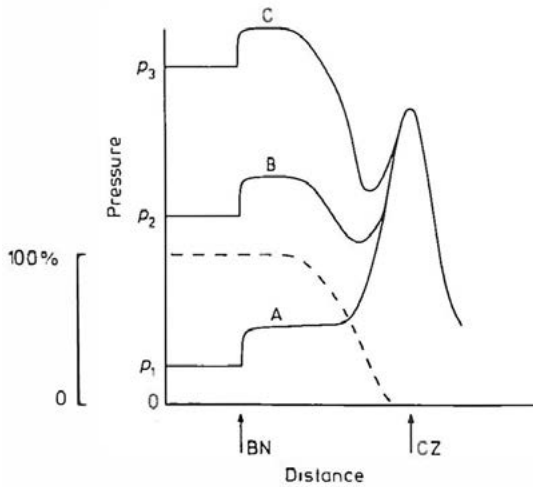
Figure 6.1 Schematic urethral closure pressure profiles, competent bladder neck mechanism. **A**, at rest, intravesical pressure p_1; **B**, intravesical pressure raised to p_2 by abdominal straining; **C**, with still more straining. The urethral closure pressure at the bladder neck (**BN**) remains unchanged. The broken curve shows the percentage transmission of abdominal pressure changes to different parts of the urethra (% scale on left).

Suppose that, at rest, the bladder neck is closed; that is, there is a non-zero urethral closure pressure at the bladder neck (even in the absence of a measuring catheter). Then, however high the abdominal pressure rises, this closure pressure is unchanged provided that there is 100% transmission to the bladder neck (figure 6.1). Therefore the bladder neck remains shut and leakage cannot occur. This mechanism is the first line of urethral defence against leakage - stress incontinence.
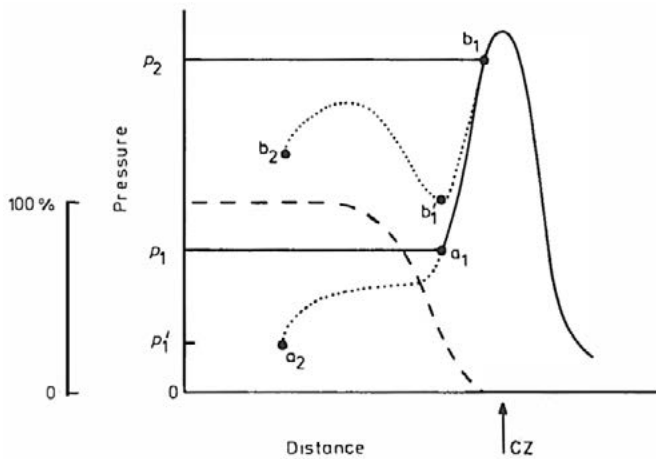
Figure 6.2 Schematic urethral closure pressure profiles, incompetent bladder neck mechanism. Initially, intravesical pressure is p_1 and the urethra is open as far as a_1. When the intravesical pressure is raised to p_2 by straining, urine penetrates further, to b_1. The result is the same whether the bladder neck lies at a_2 and is initially open, or it lies at a_1, where it is initially closed but the transmission of abdominal pressure is less than 100%. (In the latter case the segments a_1a_2 and b_1b_2 are to be ignored.) This figure also shows how a small change in detrusor pressure can affect continence. If the resting intravesical pressure were p_1', the bladder neck at a_2 would be closed at rest and competent (c.f. figure 6.1). A small rise in detrusor pressure, bringing the intravesical pressure to p_1, opens the bladder neck and makes it incompetent.

The mechanism can fail if either the pressure transmission to the bladder neck is less than 100%, or the bladder neck is open at rest so that there is no positive urethral closure pressure there. In both cases the urine in the bladder is in free communication with a part of the urethra where the transmission of changes in abdominal pressure is less than 100%. When the abdominal pressure rises urine is forced further into the urethra (figure 6.2).

In males the bladder neck is strongly developed (figure 2.3b) and the bladder neck mechanism is usually effective: it is rarely that a cough can be seen, radiologically, to force the bladder neck open. In females the bladder neck is much weaker, and a failure of the bladder neck mechanism can often be radiologically demonstrated in stress-incontinent women. Typically the bladder neck is slightly open at rest (c.f. figure 5.1(a), §5.1.2.1). When the patient coughs, it opens further. The bladder neck mechanism is extremely sensitive to functional changes in the detrusor pressure. The urethral closure pressure which keeps it shut can be extremely small. If the detrusor pressure rises even a little, it opens the bladder neck and the mechanism is no longer effective (figure 6.2). This behaviour is often observed in women, suffering from incontinence, who have unstable bladders. A single cough does not immediately open the bladder neck, but it leads after a short delay to a slight contraction of the unstable detrusor. This opens the bladder neck and subsequent coughs can result in leakage.

At first sight it may appear paradoxical that the bladder neck mechanism can prevent flow, when the compressive zone is supposed to be the point that controls the flow. If, however, transmission of abdominal pressure to the bladder neck is complete, while more distally it is less than complete, then an increase in abdominal pressure can create a new elastic constriction at the bladder neck, which controls the flow under these circumstances (figure 6.1, curve C).

6.2.2 The distal mechanism

Even if the bladder neck mechanism is ineffective, incontinence does not necessarily result, because there is a second line of defence, the distal mechanism. When the abdominal pressure rises the urethral pressure at the compressive zone rises also. The transmission of abdominal pressure to this zone may be partly neuromuscular in origin, rather than purely mechanical. If it were 100% the maximum urethral closure pressure would remain unchanged however high the abdominal pressure, and leakage would not occur (figure 6.3). In fact, the transmission is often less than 100%, but if the maximum urethral closure pressure is initially high, very large abdominal pressures are needed to reduce it to zero and so allow leakage past the compressive zone. This is the distal continence mechanism. It can be reinforced by voluntary contraction of the periurethral sphincter. For the mechanism to be effective, not only must the transmission of abdominal pressure to the compressive zone be large enough, but it must occur quickly, since during a cough, for example, the abdominal and intravesical pressures rise quickly. If these conditions are not met the distal mechanism may fail to prevent leakage when the abdominal pressure rises.
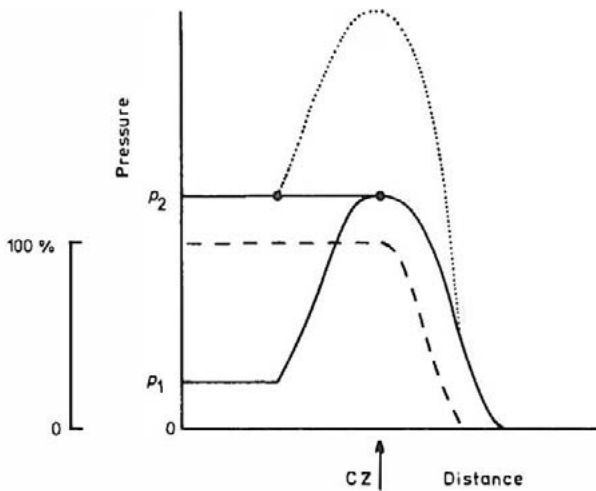
Figure 6.3 Schematic urethral closure pressure profiles: the distal mechanism. At rest, intravesical pressure is p_1 and maximum urethral closure pressure is (p_2 - p_1). If intravesical pressure is raised to p_2 by abdominal straining, maximum urethral closure pressure is unchanged (dotted curve). If, however, the intravesical pressure rises to p_2 because of detrusor contraction, maximum urethral closure pressure falls to zero (assuming no functional changes in the urethra).

Of course, if the bladder is grossly unstable, a large detrusor contraction may occur and by itself reduce the maximum urethral closure pressure to zero (figure 6.3). Leakage then occurs independently of the abdominal pressure. Under such circumstances functional changes at the compressive zone are likely to occur; e.g. voluntary contraction of the periurethral sphincter, or an involuntary relaxation of the urethral musculature, which is coupled with the detrusor through the micturition reflex.

6.2.3 Types of incontinence

The preceding discussion enables us to distinguish three types of incontinence (the list is not exhaustive):

(i)   a type in which both the bladder neck and distal mechanisms fail against raised abdominal pressure;

(ii)   a type in which the distal mechanism fails, and a competent bladder neck mechanism is overcome by an unstable detrusor contraction, perhaps very slight;

(iii)   a type in which both mechanisms are overcome by a gross involuntary contraction of the detrusor.

For further discussion of the classification of incontinence, see International Continence Society (1976), Turner-Warwick (1979), Worth (1979) and Turner-Warwick and Brown (1979).

6.3 The Opening of the Bladder Neck

Several hypotheses are current about how the bladder neck is opened for micturition (Hutch 1966, Tanagho *et al* 1966). Our discussion of the bladder neck mechanism (§6.2.1) has shown, however, that its opening is a natural consequence of a raised detrusor pressure. A small rise in the detrusor pressure is sufficient to open it (figure 6.2), and indeed to open it wide because the urethra is so distensible. During micturition then the bladder neck opens automatically as the detrusor contracts. Possible functional changes at the bladder neck form minor complications in this basically simple picture. Such functional changes might be due to relaxation or tightening of the urethral muscles, or to the mechanical action of the contracting detrusor on the bladder neck (see §9.5).

A raised abdominal pressure, on the other hand, does not normally tend to open the bladder neck. In some patients the detrusor cannot

be made to contract. They must micturate by abdominal straining or manual expression. To enable them to do so the bladder neck mechanism may have to be destroyed surgically or by means of drugs, and the distal mechanism similarly weakened.

7 The Normal Urethra during Micturition

7.1 The Compressive Zone

7 .1.1 Existence and consequences

At rest the urethra contains an elastic constriction, the compressive zone, which in the absence of functional changes would determine the urethral resistance relation during micturition. During micturition however the muscles surrounding the compressive zone relax (§7.2.3; Tanagho *et al* 1966), and so it might conceivably disappear altogether. Nevertheless, urethral closure pressure profiles measured under the influence of strong muscle relaxants still show a compressive zone. Furthermore, during micturition the urethra funnels from wide to narrow near the position of the compressive zone (figure 2.2a) and this is suggestive of a transition from subsonic to supersonic flow, implying that the compressive zone indeed governs the resistance relation. In the male, the shape of the urethra often suggests that there is a transition to supersonic flow at the compressive zone, acting as an elastic constriction, which is followed by a hydraulic jump to subsonic flow in the penile urethra (figure 2.2b) and a second elastic constriction near the external meatus. We shall therefore make the working hypothesis that, at least in the normal case, the compressive zone is present during micturition and governs the urethral resistance relation (Griffiths 1973).

It follows that the properties of the urethra distal to the compressive zone should have no effect on the urethral resistance relation, i.e. neither on the intravesical pressure nor on the flow rate. Normal male readers should be able to verify that light compression of the penile urethra causes no sustained change in flow rate, although there are interesting transient effects. (Of course, severe compression makes

the compressive zone subsonic and does alter the flow rate.) In contrast, compression of the perineum, close to the compressive zone, causes a sustained drop in flow rate.

It is worth pointing out again that the narrowest parts of the normal urethra during micturition, the external meatus in both sexes and the membranous urethra in the male, lie downstream of the compressive zone and should have no effect on the urethral resistance relation. This behaviour is in complete contrast to that of a rigid tube, in which the whole tube contributes to the resistance and the narrowest parts make the main contribution (§4.6).

7.1.2 Intravesical or detrusor pressure?

If the urethra were indeed near-rigid the pressure head governing the flow rate would be the intravesical pressure, the sum of the detrusor and abdominal components. For a distensible tube, however, this is not necessarily so, as the discussion of the conditions for leakage in §6.2 has made clear.

If the compressive zone were fully subject to changes in abdominal pressure (100% transmission; see figure 6.3), such changes would affect equally the intravesical pressure and the urethral pressure at the compressive zone and so would have no effect on the flow rate. For example, equation (4.9) of §4.1.2 shows that the flow rate Q depends on the difference between the pressure head p_0 and the (urethral) pressure $g(x_c)$ at the elastic constriction (= compressive zone). If both are increased equally the flow rate does not change. Thus with 100% transmission only the detrusor pressure would be significant.

The reality is more complicated. At rest, the transmission of abdominal pressure changes to the compressive zone is substantial but not complete, typically 70%. If this were also the case during micturition,
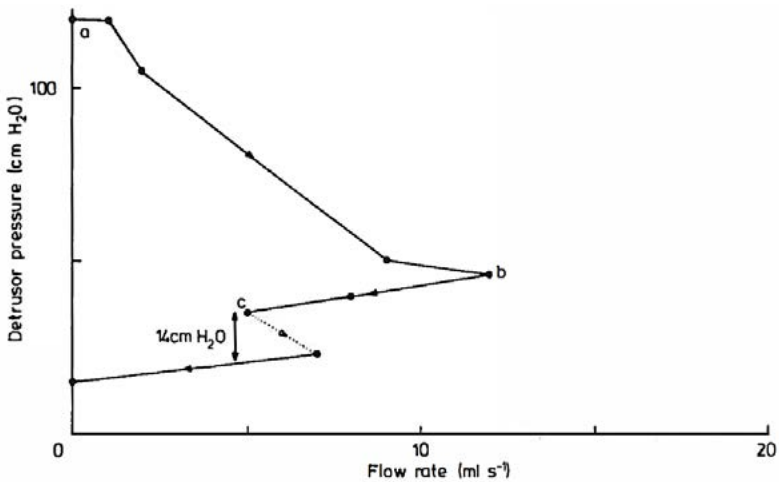
Figure 7.1 Plot of detrusor pressure against flow rate during the micturition of an 8-year-old girl. Segment ab is characteristic of a steadily relaxing urethra (see §11.3). After point b the pattern indicates a normal urethral resistance relation. At point c the abdominal pressure is raised and remains so until the end of micturition. 50 ml residual urine is left in the bladder.

abdominal pressure should affect the flow rate, but less effectively than the detrusor pressure. Since the transmission is probably partly neuromuscular in origin, it may be different during micturition and at rest. Nevertheless it is common observation that abdominal straining raises the flow rate.

During most normal micturitions there is in fact very little straining. When it does occur it is usually spasmodic and so it is difficult to measure satisfactorily the effect on the flow rate. Figure 7.1 shows the relation between detrusor pressure and flow rate (the urethral resistance relation; §7.2.1) for a micturition during which a period of sustained straining occurred. When the abdominal pressure was raised by 40 cm H_2O, the urethral resistance relation was shifted to lower

detrusor pressures by 14 cm H_2O. Thus 40 cm H_2O abdominal pressure is equivalent to 14 cm H_2O detrusor pressure in this case. The abdominal pressure has here relatively less effect on the flow rate than the detrusor pressure (35%).

This discussion has tended to suggest that the combined effect of abdominal and detrusor pressure can be reduced to a matter of percentage effectiveness. This is not so. The treatment of leakage (§6.2) has shown that the flow is governed by a complicated and nonlinear interaction between the two pressure components. An increase in abdominal pressure, by raising the urethral pressure proximally more than distally, tends to shift elastic constrictions upstream and may even create a new one (the bladder neck continence mechanism). At the same time, by exaggerating the falling pressure gradient in the distal urethra, it tends to stabilise supersonic flow, and so ensures that our basic approach remains valid.

To cut through all this complexity we shall normally neglect the effect of abdominal pressure and assume that the detrusor pressure is the pressure head driving the flow. The approximation should be good for those who micturate with little or no straining.

7.2 The Urethral Resistance Relation

7.2.1 Observations and deductions

On clinical records of normal micturition (figure 2. 1) it is striking that the detrusor pressure varies relatively little, while the flow rate varies much more widely. Therefore, if simultaneous pairs of values of detrusor pressure p_{det} and flow rate Q are plotted against each other, either by hand or online by an X-Y recorder, the slope dp_{det}/dQ of the resulting curve is very small, and the intercept on the pressure axis is finite and positive (figure 7.2, curve A). Although there are differences between the curves traced out as Q rises and then falls, they are
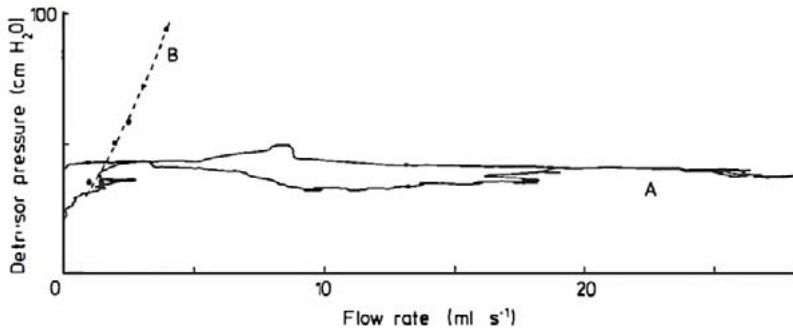
Figure 7.2 Plots of detrusor pressure against flow rate during micturition. **A**, girl without urethral obstruction ; **B**, young man, following a urethroplasty. (Data from the Clinical Urodynamic Unit, Middlesex Hospital, London.)

usually small, and may in any case be partly due to the delay in the measurement of Q (§2.2.1) . Thus functional changes in the urethral properties appear usually to be quite small during micturition. A curve such as figure 7.2 (A) is, then, a plot of pressure head against flow rate for a urethra which is behaving to a good approximation as a passively distensible tube; that is, it is the urethral resistance relation.

Our working hypothesis is that the urethral resistance relation is determined by the mechanical properties of the compressive zone, which forms an elastic constriction. According to the example described in §4.1.2, the constant features of the urethral resistance relation, its flatness and positive pressure intercept, are exactly those to be expected for a highly distensible compressive zone. This may be shown directly. Figure 7.3(a) shows an actual urethral resistance relation, recorded point by point. In figure 7.3(b) this has been transformed by the method described in §§ 3.2.3 and 4.1.1 into a plot of urethral pressure p against cross-sectional area A, the elastic properties of the compressive zone during micturition. The compressive zone is indeed highly distensible. The pressure rises quite
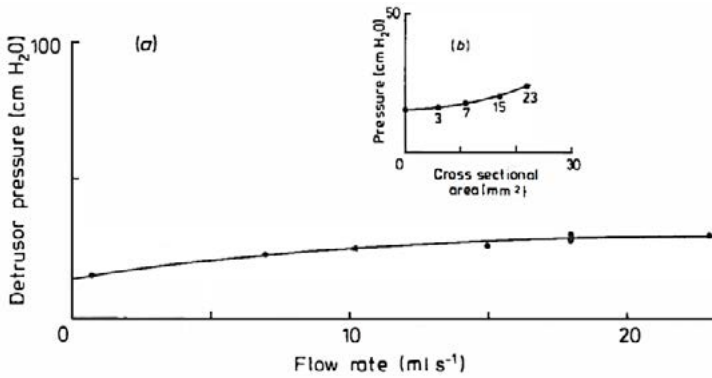
Figure 7.3 (a) Urethral resistance relation of a female subject; (b) elastic properties of the compressive zone deduced from (a). The figure beside each point indicates the corresponding flow rate in ml s^{-1}.

slowly with increasing cross-sectional area from a finite value $p(0)$ at zero cross section. The consequence, figure 7.3(a), is that the detrusor pressure must exceed $p(0)$ for flow to occur at all, but with any further increase in detrusor pressure the compressive zone distends readily, so that the flow rate increases very rapidly.

7.2.2 Lack of distensibility

The difference between a normally distensible and a more rigid urethra is made clear by figure 7.2, curve B, the urethral resistance relation of a young man as determined shortly after a urethroplasty (repair of a ruptured urethra) which involved the region near the compressive zone. The form of this resistance relation is close to that of a rigid tube, $p_0 \propto Q^2$ (§§ 3.4 and 4.6), exactly as one would expect for a narrow, scarred urethra.

7.2.3 Rest and micturition: functional changes

During flow any functional changes in urethral pressure appear normally to be quite small, so that the urethra behaves almost passively. This does not mean that it is always passive however. Relaxation and tightening of the (peri-)urethral muscles normally occur at the beginning and end of micturition, respectively (Tanagho 1971). In general, the urethral pressure at the compressive zone during micturition is considerably smaller than the maximum urethral pressure measured at rest. In the case of figure 7.3, for example, the maximum urethral closure pressure measured with a catheter of cross-sectional area 3 mm^2 was 48 cm H_2O. During micturition the urethral pressure at the compressive zone for this cross-sectional area is about 15 cm H_2O. Thus at the compressive zone the urethral pressure has fallen by about 33 cm H_2O during micturition. (Strictly, one should remember that the resting urethral closure pressure is measured with respect to the resting intravesical pressure and the urethral pressure during flow with respect to the abdominal pressure. The difference between these two zero references is small, usually less than 10 cm H_2O. Therefore our conclusion remains valid.) Thus the compressive zone relaxes for micturition. Its distensibility is probably similar at rest and micturition. Compare, for example, the slow increase in pressure with cross-sectional area during micturition (figure 7.3b) with that found at rest (figure 5.1b).

The fact that the compressive zone relaxes does not necessarily mean that the whole urethra does so (see §9.5).

7.3 Males and Females

The compressive zone and the urethral resistance relation appear to be rather similar in normal males and females. Both the maximum urethral closure pressure and the detrusor pressure during micturition tend to be slightly higher in male patients, but one must always
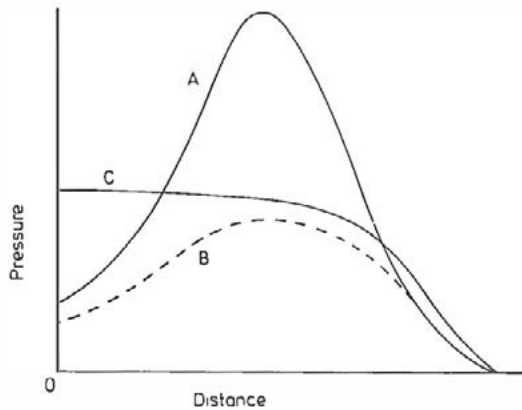
Figure 7.4 Schematic urethral pressure distributions in a female. **A**. resting urethral closure pressure profile; **B**, hypothetical profile, with uniform cross sectional area, after the compressive zone has relaxed for micturition; **C**, actual pressure distribution during micturition. Flow is from left to right.

remember that patients are a selected group. The working hypothesis is that, in both sexes, a transition to supersonic flow occurs at the compressive zone during normal micturition, so that the more distal parts of the urethra do not affect the urethral resistance relation.

In females the proximal urethra is short and normally wide open. Simple estimates suggest that the viscous losses in it must be very small, and indeed the losses in the whole of the female urethra are only about 10 cm H_2O, some 30% of the original intravesical pressure (Griffiths 1969). Therefore it is reasonable to neglect them, as in the derivation of figure 7.3(b). In the male the proximal urethra is longer and narrower. Viscous losses in it are certainly higher than in the female, and will tend to raise the detrusor pressure during micturition (§4.3.1). This may be one factor contributing to the slightly higher detrusor pressures observed in males.

The distal urethra is quite different in the two sexes. In normal females the supersonic flow appears to continue to the external meatus. The resulting urethral pressure distribution is shown schematically in figure 7.4. It differs from the resting urethral closure pressure profile, not only because the compressive zone relaxes for micturition, but also because the profile is measured at constant cross-sectional area, while during micturition the cross-section is far from uniform.

In the normal male the region of supersonic flow downstream of the compressive zone is quite short. It is followed by a hydraulic jump, a long subsonic region and a second elastic constriction.

7.4 Summary

According to our working hypothesis, in normal males and females the urethral resistance relation is governed principally by the elastic properties of the compressive zone, which corresponds to the region of maximum pressure on the resting urethral closure pressure profile. It lies near the pelvic floor and appears to be partly subject to changes of abdominal pressure, which therefore has a smaller influence than the detrusor pressure on the flow rate. Since the compressive zone is highly distensible the detrusor pressure normally varies relatively little during micturition, even for large changes in flow rate, and so the normal urethral resistance relation has a characteristic shape.

The elastic properties of the compressive zone are partly muscular in origin, and the urethral pressure there falls just before micturition. During normal, uninterrupted micturition the functional changes in the mechanical properties of the urethra are relatively unimportant.

The parts of the urethra distal to the compressive zone have no effect on the urethral resistance relation, because according to our hypothesis there is a transition to supersonic flow at the compressive zone. This transition accounts for the shape of the urethra during

micturition. In the normal case the part of the urethra proximal to the compressive zone also has little effect on the resistance relation.

8 The External Meatus in the Male

8.1 The Urinary Stream

During micturition there is apparently an elastic constriction near the external meatus of the male urethra. It controls the local pressure head p_0' in the penile urethra. Assuming that viscous dissipation downstream of the elastic constriction is small, it controls also the speed of the external stream (§4.4.3). (It is assumed that the stream exits cleanly from the external meatus, and is not interfered with by the foreskin.) With these assumptions equation (4.20) is valid. It follows that the resistance relation of the meatal elastic constriction and hence its elastic properties may be deduced from simultaneous measurements of the speed of the external stream and the flow rate. Since the meatus is not muscular it should not be subject to large functional changes. It may, however, be affected by changes in the blood supply, such as occur during erection.

The speed of the stream may be measured directly by photographing the trajectory. Alternatively, the force exerted when the stream strikes a plate may be measured. A third method depends on the break-up of the stream into drops; the frequency with which the drops pass a given point is measured. All three methods give similar information about the properties of the meatal elastic constriction.

Direct measurements of stream speed v_{ext} and flow rate Q have shown that at low flow rates Q is approximately proportional to v_{ext}, so that the cross-sectional area of the stream is a constant. Above a critical flow rate Q_c (about 10 ml s^{-1}) the cross-sectional area of the stream begins to increase. According to the theory of Chapter 4, this means that for $Q < Q_c$ the meatal elastic constriction has a constant cross-sectional area, that it becomes distended when Q is equal to Q_c, and

progressively more so as Q rises further. The less direct but more precise measurements discussed in the next section confirm that this behaviour is typical.

8.2 Measurements of the Break-up of the Urinary Stream into Drops

The fluid column in the external stream is unstable under the influence of surface tension, and breaks up into a chain of drops within a few centimetres of the external meatus. An instrument called the urinary drop spectrometer can be used to analyse, by optical and electronic means, the sizes and time distribution of the drops (Zinner *et al* 1969).

The most directly accessible variables are the mean drop frequency f and the mean drop diameter, both averaged over a short period of time. From the latter the mean drop volume can be estimated, and the product with f is then the flow rate Q. If, for one micturition, simultaneous values of f and Q are plotted against each other, the result is typically as shown in figure 8. 1. The behaviour can be idealised as

$$f = Qf_c/Q_c \quad for \quad Q < Q_c \,;$$
$$f = f_c \quad\quad for \quad Q > Q_c \,,$$

$$(8.1)$$

where f_c and Q_c are a critical frequency and flow rate, typically about 150 drops per second and 10 ml s^{-1} , respectively, for a normal male. Now

$$Q = A_{ext}\, V_{ext},$$ (8.2)

where A_{ext} is the cross-sectional area of the stream[†]. It is known that, for a stream of circular cross-section,

$$f = (\pi v_{ext}^2 / 81 A_{ext})^{1/2}. \qquad (8.3)$$

This relation seems to be valid for the much flattened urinary stream also. Therefore, eliminating f and Q from equations (8.1)-(8.3),

$$A_{ext} = (\pi Q_c^2 / 81 f_c^2)^{1/3} = A_0 \quad \text{for } Q < Q_c; \qquad (8.4a)$$

and $\qquad A_{ext} = (A_0^3 / Q_c^2) v_{ext}^2 \qquad \text{for } Q > Q_c, \qquad (8.4b)$

Equations (8.4a) and (8.4b) confirm the direct measurements discussed in §8. 1.

[†] Since the stream accelerates under gravity, A_{ext} is not uniform. The value applicable in equations (8.2) and (8.3) is that near the point where the drops are formed. In practice it differs very little from the value just outside the external meatus.
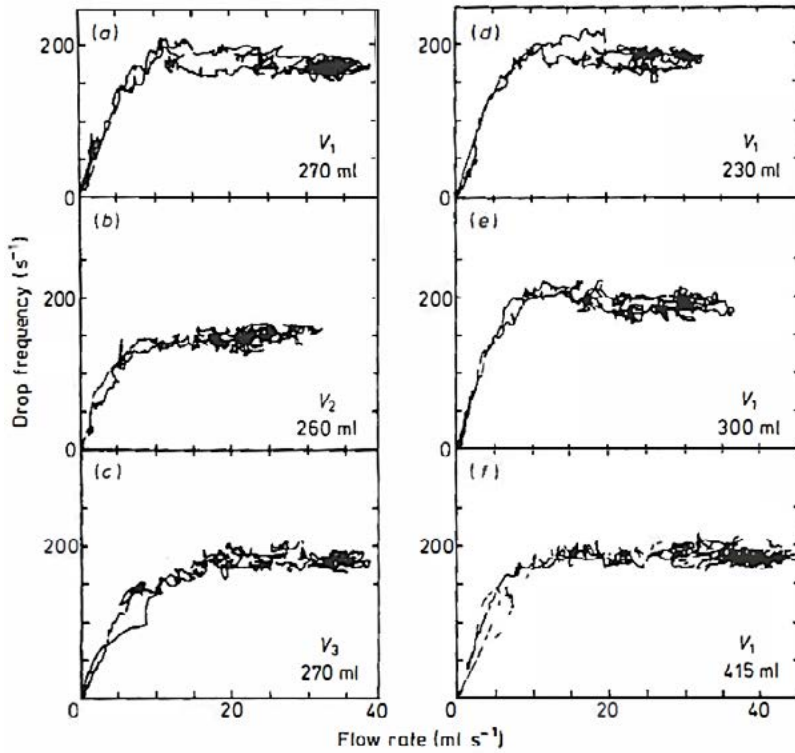
Figure 8.1 Plots of drop frequency against flow rate for six micturitions of three healthy male volunteers. The volume voided is shown in each case. (Reproduced from Sterling and Griffiths 1976 Urol. Int. 31 321-31 , by permission of S Karger AG, Basel.)

Assuming negligible viscous dissipation downstream of the meatal elastic constriction, the meatal resistance relation is identical to the relation between Q and $p'_0 = \frac{1}{2}\rho v_{ext}^2$. From equations (8.2) and (8.4),

$$Q = A_0(2p_0'/p)^{1/2} \qquad \text{for } Q < Q_c ; \qquad (8.5a)$$

And $\quad Q = (A_0^3/Q_c^2)(2p_0'/p)^{3/2} \qquad \text{for } Q > Q_c , \qquad (8.5b)$

Equation (8.5a) implies that, for $Q < Q_c$. the meatal elastic constriction behaves as a rigid nozzle of constant cross-sectional area A_0, discharging at zero (atmospheric) pressure (c.f. equation (4.21), §4.6.2). As discussed in §3.5, the flow may not become sonic under these circumstances. A comparison of equations (8.5b) and (4.9) (§4.1.2), shows that for $Q > Q_c$ the elastic properties of the meatal elastic constriction are given by

$$p(A) = HA, \qquad (8.6)$$

where $\qquad H = \rho Q_c^2/3^{3/2}A_0^3 = 3^{5/2}\rho f_c^2/\pi. \qquad (8.7)$

The corresponding p/y plot is shown in figure 8.2(a). For $Q < Q_c$, the meatal elastic constriction has constant $\gamma = 1/A_0^2$. For $Q > Q_c$. γ decreases steadily with increasing Q. At $Q = Q_c$ the value of γ changes abruptly from $1/A_0^2$ to $1/3A_0^2$. Thus the theory suggests that the meatal elastic constriction opens abruptly from area A_0 to area $3^{1/2} A_0$ as Q rises through Q_c. The abrupt opening is associated with a violation of condition (3.21c) (see §3.2.3).
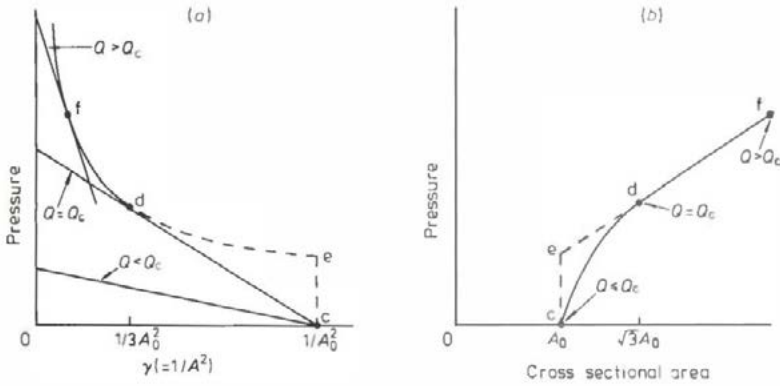
Figure 8.2 (a) p/y plot for idealised male external meatus. On curve edf, $p \propto y^{\frac{1}{2}}$ (i.e. $p \propto A$). Between c and d no points are observed. (b) p/A plot corresponding to (a). On line edf, $p = HA$.

The elastic properties are shown graphically in figure 8.2(b). For $Q < Q_c$. $p = 0$ and $A = A_o$. For $Q > Q_c$. $p = HA$, where $A > 3^{1/2}A_o$. In the region between A_0 and $3^{1/2}A_o$ there are no observable points. The curve drawn in this region corresponds to the straight line cd in figure 8.2(a}, but does not necessarily represent the real elastic properties, which might for example follow the broken lines ced in both figures. These elastic properties correspond more closely to the type shown in figure 2.4(c) than to the near-rigid or highly distensible types of figure 2.4(a) and (b).

With the typical normal values of the critical drop frequency f_c and flow rate Q_c, respectively 150 drops per second and 10 ml s^{-1}, equations (8.4a) and (8.7) become

$$A_0 = 5.6 \text{ mm}^2$$

and $\quad H = 1.1 \times 10^8 \text{ Pa m}^{-2} = 1.1 \text{ cm H}_2\text{0/mm}^2.$ $\qquad$ (8.8)

Pathological values are discussed in §9.2.2.

The interpretation of the drop spectrometer observations has been checked by means of a mechanical model with elastic properties similar to those calculated for the meatal elastic constriction (Sterling and Griffiths 1976). Observations of the relation between stream speed and flow rate (or, equivalently, drop frequency and flow rate) in the model show a striking resemblance to the behaviour of the real meatus.

When the behaviour of the model is examined near the critical flow rate, one sees that it does not open abruptly and uniformly when $Q = Q_c$, as suggested above. Instead, it develops a pronounced taper (large negative dA/dx) near Q_c, consistent with a more elaborate treatment of the hydrodynamics (Griffiths 1975b). One might expect the simple treatment (§4.1) to fail here, because one of the necessary conditions, $|dA/dx|$ small, is not fulfilled. In practice, however, it seems satisfactorily to describe the connection between the elastic properties, the resistance relation and the stream speed.

8.3 The Momentum Flux In the Urinary Stream

If the urinary stream is directed horizontally on to a vertical plate, it exerts a force which can readily be measured (e.g. Whitaker and Johnston 1966). Since in practice there is negligible splashing back from the plate, the force is equal to the momentum delivered by the stream to the plate, and there destroyed, per unit time (the momentum flux). The momentum per unit volume in the stream is ρv_{ext}. where ρ is the density of the urine. During steady flow the momentum flux F is therefore equal to the product of ρv_{ext} with Q, the volume striking the plate per unit time:

$$F = \rho Q v_{\text{ext}}. \qquad (8.9)$$

Therefore, if the flow rate is measured simultaneously, the speed of the stream can be calculated[†], and hence the local pressure head p_0' and the elastic properties of the meatus. It follows that the properties of the meatal elastic constriction determine the momentum flux for a given flow rate. It is assumed again that viscous dissipation downstream of this elastic constriction and interference with the stream by the foreskin are negligible.

In order to make the connection clear, we shall use the idealised drop spectrometer results, which are determined by the meatal elasticity, to predict the relation between momentum flow and flow rate. The prediction can then be compared with clinical observations.

The idealised result of the drop spectrometer measurement is that

$$v_{\text{ext}} = Q/A_0 \qquad\qquad \text{for } Q < Q_c ; \qquad (8.10a)$$
$$\text{and} \quad v_{\text{ext}} = QQ_c^2/A_0^3 v_{\text{ext}}^2 \qquad \text{for } Q > Q_c , \qquad (8.10b)$$

where we have made use of equations (8.2), (8.4a) and (8.4b). Since, from equation (8.7),

$$Q_c^2 = 3^{3/2} H A_0^3/\rho, \qquad\qquad\qquad (8.11)$$
$$\text{then} \quad v_{\text{ext}}^3 = 3^{3/2} HQ/\rho \qquad\qquad \text{for } Q > Q_c. \qquad (8.12)$$

_____

[†] What is measured is the horizontal component of the momentum flux. Equation (8.9) gives the horizontal component of the stream speed, and this is equal to the speed just outside the meatus provided that the stream emerges horizontally. Gravitational acceleration has no effect on the measurement.

Substituting in equation (8.9),

$$F = \rho Q^2 / A_0 \qquad \text{for } Q < Q_c ; \qquad (8.13a)$$
$$\text{and} \qquad F = 3^{1/2}(\rho^2 H Q^4)^{1/3} \qquad \text{for } Q > Q_c , \qquad (8.13b)$$

where Q_c is given by equation (8.11). Equations (8.13a) and (8.13b) show explicitly that the relation between F and Q is determined by the properties (A_0 and H) of the meatal elastic constriction, together with the urine density. Substitution of the typical normal values derived from the drop spectrometer measurements (equation (8.8)) leads to the following:

$$F = 0.021Q^2 \qquad \text{for } Q < Q_c \qquad (8.14a)$$
$$\text{and} \qquad F = 0.097Q^{4/3} \qquad \text{for } Q > Q_c , \qquad (8.14b)$$

where $Q_c = 10$ ml s^{-1}. Here Q is expressed in ml s^{-1} and F in g.wt (1 g.wt 9.8 mN). Equations (8.14a) and (8.14b) are plotted in figure 8.3, together with some clinical measurements of momentum flux and flow rate made on male patients believed to be normal (Meyhoff et al 1979). The measurements were made at maximum flow, so that the flow rate was fairly steady, as assumed in the derivation of equation (8.9). Most of the measurements fall in the range $Q > 10$ ml s^{-1}, and therefore should be described by equation (8.14b). A logarithmic regression analysis gave as a fit to the points

$$F = 0.082Q^{1.28} \qquad (8.15)$$

Clearly there is a little systematic discrepancy between equations (8.14b) and (8.15), but the powers of Q that appear in the two equations are in good agreement.

Patients with meatal stenosis are expected to have higher values of H (§9.2), and therefore should have elevated values of momentum flux

when Q exceeds Q_c (equation (8.13b)). Thus measurements of momentum flux, like those with the urinary drop spectrometer, appear to be potentially useful in the investigation of the male external meatus, and in particular whether it is obstructive or not.

Since the behaviour of the stream is so closely determined by the meatal elastic constriction, none of the measurements described in this chapter gives much information about the more proximal parts of the urethra and the bladder, apart from that already contained in the flow rate. It is obvious however, that the intravesical pressure must exceed $\frac{1}{2}\rho v_{ext}^2$ (with a gravitational correction if necessary). In the case of the drop spectrometer, although the *mean* drop frequency is determined meatally, the statistical distribution of drop frequencies is believed to contain information about turbulence introduced in the more proximal parts of the urethra, which is related to the degree and location of proximal obstruction (Ritter et al 1974)[†].
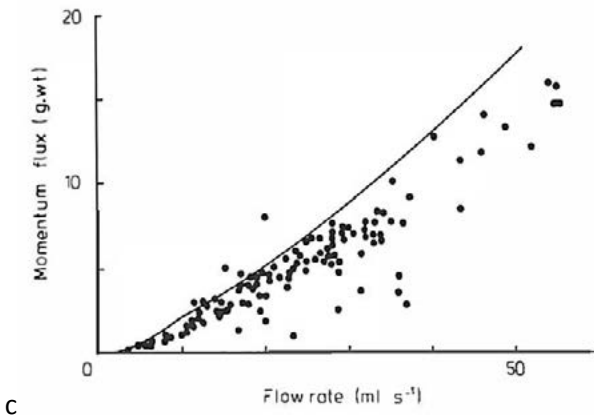
Figure 8.3 Relation between momentum flux in urinary stream and flow rate for normal males. Curve, as predicted from idealised drop spectrometer measurements; points, as directly measured at maximum flow.

9 Urethral Obstruction

9.1 Introduction

In Chapter 7 the ability of the normal urethra to pass a high flow rate at a low detrusor pressure was discussed. In many clinical conditions obstruction of the urethra is suspected. The grounds may be symptomatic, radiological or urodynamic. The pathological importance of obstruction may lie not so directly in a low flow rate as in the consequences for the bladder, which for example may cease to empty completely. The observation of residual urine in the bladder after micturition is often taken as a sign of urethral obstruction. The obstruction may be relieved surgically or by drug treatment.

From a urodynamic viewpoint, urethral obstruction exists if there is a mechanical abnormality at one or more sites in the urethra, which leads to a detrusor pressure/flow plot differing from the normal urethral resistance relation. This usually implies that the control of urethral resistance is transferred wholly or partly away from the compressive zone to another site. Two types of obstruction can be distinguished: *organic*, due to a structural narrowing or lack of distensibility in the urethra, and *functional*, due to a malfunctioning of the neuromuscular control of the urethra. For example, a near-rigid narrowing in the male penile urethra would be an organic obstruction (§9.4); a failure to relax the muscles of the compressive zone during micturition would create a functional obstruction. Obstruction of the male proximal urethra contains elements of both types (§9.5).

In clinical circles one sometimes hears of 'relative outflow obstruction,' by which is usually meant the observation of a low flow rate without a raised detrusor pressure, together with appropriate symptoms. If the urethral resistance relation were in fact of the unobstructed type, this

would be interpreted urodynamically as detrusor insufficiency rather than urethral obstruction, see § 10.3.

Some patients empty the bladder by abdominal pressure alone because the detrusor cannot be made to contract. In the normally continent urethra abdominal pressure alone will not cause emptying.

The urethra must be made abnormal (incontinent) for emptying to be possible (§6.2). The concept of urethral obstruction is therefore quite different depending on whether the bladder is emptied by detrusor contraction or abdominal straining. Only the first will be considered in this chapter.

9.2 Meatal Obstruction in the Male

9.2.1 The conditions for obstruction

According to the working hypothesis, in a non-obstructed urethra the flow is sonic at the compressive zone, which governs the urethral resistance relation. Thus the meatus is not urodynamically obstructive unless it becomes so tight that the flow at the compressive zone is no longer sonic, so that the meatal elastic constriction governs the urethral resistance relation (see §4.4). This urodynamic definition is of course quite different from the clinical definition of meatal obstruction.
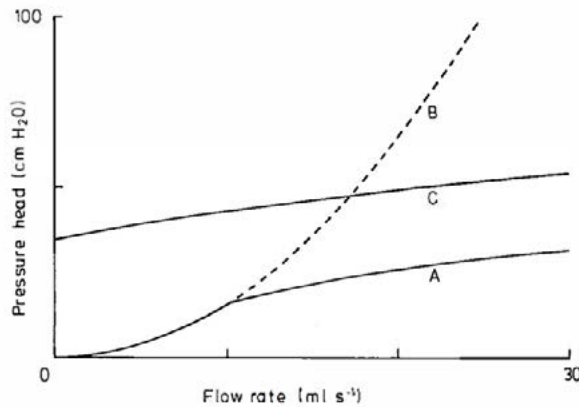
Figure 9.1 Comparison between meatal and overall urethral resistance relations (in males). A, meatal resistance relation derived from drop spectrometer results, with normal values of A_0 and H. B, meatal resistance relation for a less distensible meatus, H six or more times higher than normal. C, overall urethral resistance relation for a normal male. The pressure head is here the *intravesical* pressure, some 10-20 cm H_2O higher than the detrusor pressure which is usually plotted.

It is interesting to compare quantitatively the *meatal* resistance relation derived from the drop spectrometer observations (equations (8.5)), with an unobstructed *urethral* resistance relation. For a proper comparison the urethral resistance relation must be expressed in terms of intravesical rather than detrusor pressure, as in figure 9. 1. If the compressive zone is to remain sonic, the meatal resistance relation must certainly lie below the urethral resistance relation. In fact, the pressure difference between the two curves must exceed the irreducible dissipation between the compressive zone and the meatus (condition (4.19)). Even though the irreducible dissipation is unknown, it is clear from figure 9.1 that at high flow rates the compressive zone can govern the urethral resistance only if the meatal elastic

constriction is sufficiently distensible. It is conceivable that, even in the normal situation, the working hypothesis is incorrect at the highest flow rates and that control of the urethral resistance is then transferred to the distal parts of the urethra.

9.2.2 Clinical findings

It is well known clinically that in both sexes the meatus is the least distensible part of the urethra. The likelihood that it is obstructive is sometimes gauged by calibration. This method is appropriate for assessing the properties of a near-rigid tube (figure 2.4a). However, since within its working range the meatus is neither near-rigid nor highly distensible (figure 8.2b), neither calibration nor urethral pressure measurement is particularly appropriate.

The urinary drop spectrometer (§8.2) or measurement of the momentum flux (§8.3) offer more appropriate ways of assessing whether the meatus is obstructive. In one patient with clinically diagnosed meatal stenosis for example, the critical frequency f_c measured with the drop spectrometer was raised from the normal value of 150 drops per second to over 330 drops per second (Sterling and Griffiths 1976). Equation (8.7) shows that in this patient, the coefficient H in equation (8.6) is at least five times the normal value: the meatus is less distensible than normal. The value of A_0 is about 5 mm^2, within the normal range.

The meatal resistance relation calculated from these values is plotted in figure 9. 1. At high flow rates it crosses the unobstructed urethral resistance relation, implying that conditions (4.18) and (4.19) are violated so that the meatus must govern the flow through the urethra. Urodynamically, then, this meatus ought to be obstructive, and this is consistent with the clinical judgment.

9.3 Meatal Obstruction In Girls

Although urethral obstruction is relatively uncommon in adult females, obstructive stenosis of the external meatus is often diagnosed and surgically treated in young girls. The diagnosis usually rests on radiological evidence that the urethra is wide proximally and narrow distally during micturition, together with calibration of the meatus at a diameter significantly smaller than about 18 French gauge (6 mm). Such evidence is not really conclusive, and some believe that meatal obstruction is non-existent, the appearances being due to insufficient relaxation of the external urethral sphincter (Tanagho *et al* 1971).
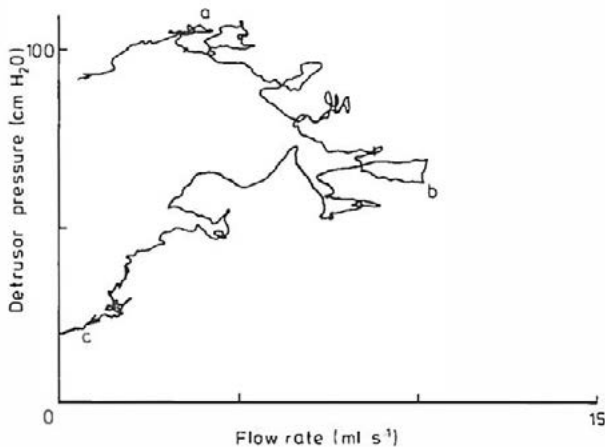
Figure 9.2 Pressure/flow plot for the micturition of a young girl with possible meatal stenosis. The segment **ab** indicates gradual relaxation of the (peri)urethral musculature. Therefore the abnormal form of segment be may not indicate organic obstruction; it is likely to result from continued urethral activity. The low maximum flow rate and high detrusor pressure are here not reliable indicators of organic obstruction (c.f. figures 7.1 and 9.5, and §1 1 .3).

Since according to our hypothesis the urine flow normally remains supersonic as it passes through the meatus, there is in the female no necessary relation between the speed of the stream and the elastic properties of the meatus. In any case the labia interfere with the stream and make satisfactory measurement difficult.

It should be possible to detect an obstructive meatus by recording the urethral resistance relation. For, if the highly distensible compressive zone governs the resistance, a normal urethral resistance relation should be obtained. If the less distensible meatus governs the resistance, the shape should be altered towards that characteristic of a more nearly rigid constriction (e.g. figure 7.2, curve B). Figure 9.2 is an example of a pressure/flow plot for a young girl. Its form indicates variable activity in the (peri)urethral musculature during micturition (see § 11.3). Plots suggesting organic meatal obstruction in girls are relatively unusual.

9.4 Distal Obstruction in the Male

Distal urethral obstruction, other than meatal stenosis (§9.2), may be caused by stricture (narrowing) of the membranous or penile parts of the male urethra (see figure 1.4). According to Chapter 7, the urethral resistance relation is independent of the properties of the distal urethra as long as the flow at the compressive zone remains sonic. Therefore moderate narrowing of the distal urethra should have no effect on flow rate or bladder pressure; i.e. it should cause no obstruction. Sufficiently severe stricture must make the flow at the compressive zone subsonic and so cause obstruction. The urethral resistance relation is altered. The flow rate and stream speed are both reduced. However, the relation between flow rate and stream speed is unchanged (§8.2), and so measurements on the stream, apart from

those mentioned at the end of Chapter 8, do not yield any additional information about the obstruction.

Unfortunately, relatively little is known of the urodynamics of this type of obstruction, which is usually examined by retrograde urethrography (§3.3), by calibration or endoscopically by direct vision. Figure 9.3 does however show the plots of detrusor pressure against flow rate for two patients with clinically established distal strictures (Nyman 1976). Both urethral resistance relations have the form characteristic of a relatively rigid constriction, confirming that the strictures are obstructive.
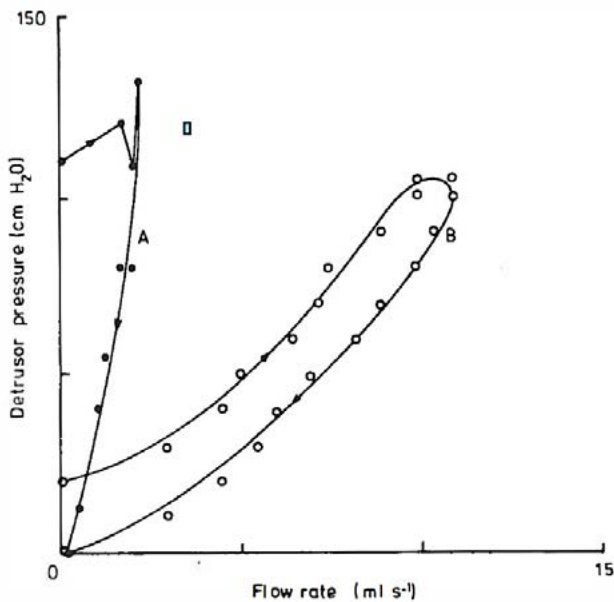
Figure 9.3 Pressure/flow plots for two patients with distal urethral strictures. **A**, in membranous urethra; **B**, just distal of membranous urethra. (Data taken from Nyman 1976.)

The plotting of detrusor rather than intravesical pressure for obstructions which are not subject to transmission of abdominal pressure is arguable. In fact both detrusor pressure and abdominal pressure are important (see §7.1.2).

9.5 Proximal Obstruction In the Male

9.5.1 The prostatic urethra

In older men the prostate gland often becomes enlarged and presses on the urethra, so causing an obstruction. A plot of detrusor pressure against flow rate in a case of severe prostatic obstruction is shown in figure 9.4, curve A. Initially the detrusor pressure is abnormally high, and then it falls gradually. The flow rate remains low throughout. In this particular case there are two separate periods of flow and some
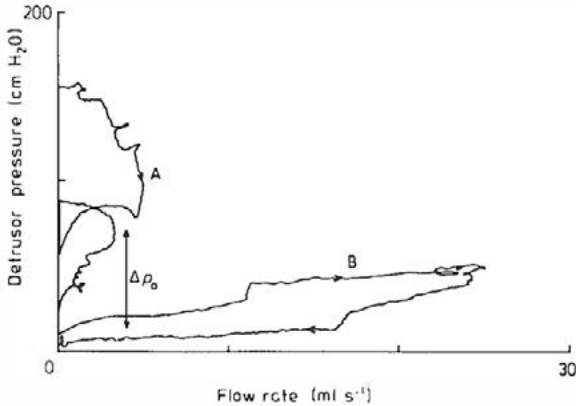
Figure 9.4 Pressure/flow plots for a male patient. **A**, with prostatic obstruction; **B**, after a transurethral operation to relieve the obstruction. The increased pressure head Δp_0 resulting from the obstruction was about 60 cm H_2O at 4 ml s^{-1}. (After Abrams and Griffiths 1979.)

functional changes in both bladder and urethra. The general shape of the plot indicates a fairly rigid obstruction; c.f. figure 7.2, curve B. After removal of part of the prostate gland the pressure/flow plot (figure 9.4, curve B), regains the form of an unobstructed urethral resistance relation.

The difference between curves A and B in figure 9.4 can be understood as being due to a narrow rigid segment in the proximal urethra. The pressure head p_0 (with respect to abdominal pressure) needed to drive a flow rate Q through the compressive zone is given by the non-obstructed urethral resistance relation (figure 9.4,B). When the obstruction is present, p_0 is less than the detrusor pressure p_{det} by the viscous dissipation Δp_0 associated with the narrow segment. Δp_0 depends on the flow rate and is probably proportional to Q^2 (see §4.6.2). Thus at each flow rate Q the detrusor pressure is increased above the unobstructed value by $\Delta p_0(Q)$. The resulting urethral resistance relation is tilted and curved (figure 9.4, A).

Simple estimates suggest that the narrow segment is usually so short that the viscous dissipation is dominated by the entry and exit losses, which are of order $\frac{1}{2}\rho v_n^2 = \frac{1}{2}\rho Q^2 / A_n^2$, where $v_n = Q/A_n$ is the fluid velocity in the narrow segment, cross-sectional area A_n. In figure 9.4, curve A, for example, Δp_0 appears to be about 60 cm H_2O (6000 Pa) when Q = 4 ml s^{-1} Therefore A_n should be about 1 mm^2, corresponding to a prostatic urethra with a diameter of about 1 mm. This seems to be consistent with the x-ray appearance. Since Δp_0 varies as 1/(diameter)^4, a prostatic urethra with a diameter of 2 mm would be only marginally obstructive, while one of 0.5 mm would allow hardly any significant flow even at a detrusor pressure of 200 cm H_2O, about the highest observed.

During micturition then, an obstructive prostatic urethra behaves like a rigid nozzle of cross-sectional area about 1 mm^2. The fluid pressure

available to distend it is essentially the detrusor pressure, about 100 cm H_2O. Thus one would expect to need a still higher pressure to force it open to a cross-section greater than 1 mm^2. At rest, on the other hand, the urethral pressures in the proximal urethra are much lower than this, perhaps 20 cm H_2O, even when the cross-sectional area of the measuring catheter is much greater, perhaps 12 mm^2. This is so whether the urethra is obstructed or not. Therefore the obstructive prostatic urethra is not passively rigid, but is tighter during micturition than at rest.

9.5.2 The bladder neck

When urethral obstruction occurs in younger men it is often caused by the bladder neck. The plot of detrusor pressure against flow rate is often curved, so suggesting that the bladder neck is acting as a rigid nozzle (c.f. figure 9.4, curve A). Sometimes the curvature is so exaggerated that the flow rate at first slowly rises as the detrusor pressure falls from an initial high value. This suggests a functional change, gradual urethral relaxation.

As in the prostatic case, the resting urethral closure pressure at the bladder neck is far lower than the fluid pressure available to distend it during micturition, implying that the bladder neck is tighter during micturition than at rest. This conclusion is consistent with §6.3, where it was pointed out that in the *absence* of functional changes the proximal urethra would automatically be opened (wide) by a raised detrusor pressure. Although technically the argument (which can be made quantitative, see Bates *et al* 1975) applies only to proximally obstructed urethras, the tightening may well occur in many male urethras, and cause obstruction only when the prostate gland or the bladder neck is too bulky.

9.6 The Quantitative Assessment of Urethral Resistance to Flow

9.6.1 Resistance factors

Since a finite bladder pressure is needed to drive fluid through a urethra, the urethra offers some resistance to flow. In general a higher pressure is needed for an obstructed than for an unobstructed urethra, at a given flow rate: the obstructed urethra has the higher resistance. One would like to quantify this idea so that a single number, a resistance factor, could be assigned to any urethra to indicate its degree of obstruction. Then one urethra could be compared with another, and the result of an operation to relieve obstruction could be quantitatively assessed. A great variety of such resistance factors has been introduced (Smith 1968, International Continence Society 1978). Usually the minimum value or the value at maximum flow has been calculated.

The main variables available to construct resistance factors are p_{ves}, p_{det}, Q and $\frac{1}{2}\rho v_{ext}^2$, the kinetic energy per unit volume in the external stream. Consider the last of these. *Physiologically* it is irrelevant, for the effect of obstruction upon the bladder is the important thing (§§ 1.2.2 and 9.1); that is, the input resistance of the urethra as expressed by the flow rate and bladder pressure(s). *Physically*, it is misleading. In the formulae it occurs in the combination $(p_{ves} - \frac{1}{2}\rho v_{ext}^2)$, the energy loss in the urethra per unit volume of fluid. A typical example is the resistance factor

$$R_1 = (p_{ext} - \frac{1}{2}\rho v_{ext}^2)/Q^2 \qquad (9.1)$$

For a distensible tube having two elastic constrictions, a tightening of the downstream constriction can raise $\frac{1}{2}\rho v_{ext}^2$ without altering p_{ves} or

Q (see §4.4.3). Thus a tightening of the tube, which might naively be expected to raise the resistance to flow, can in fact leave the input resistance unchanged, and reduce the energy loss and the resistance factor R_1. This confusing situation arises because for a distensible tube the energy loss is not closely related to the input resistance, whereas for a rigid tube the relation is close.

An example of a resistance factor not involving $\frac{1}{2}\rho v_{ext}^2$ is

$$R_2 = p_{ves}/Q^2. \qquad (9.2)$$

For a (near-) rigid tube, R_2 is approximately independent of Q. Thus each rigid tube has a unique value of R_2, as desired. Unfortunately, for a distensible tube like the urethra, p_{ves} is not proportional to Q^2 (see figure 9.1, curve C). The value of R_2 varies by a large factor according to the flow rate, which in turn depends on non-urethral variables (the behaviour of the bladder). It is not possible to assign a single value of R_2 to each urethra. The value of R_2 varies throughout the course of micturition, not because of any active, functional change in the mechanical properties of the urethra, but because of the use of an inappropriate formula, equation (9.2).

On physiological grounds one might prefer a resistance factor based on the detrusor pressure, such as

$$R_3 = p_{det}/Q^2. \qquad (9.3)$$

However R_3, like R_1 and all the other factors that have been suggested, suffers from the same fundamental defect as R_2.

9.6.2 Graphical representation

The simplest way out of the difficulty is to represent the resistance to flow of a urethra by *two* numbers, for example the maximum flow rate

attained during a micturition[†] and the corresponding detrusor pressure.

These can be displayed graphically, so that more and less obstructed urethras fall in different regions. Figure 9.5 is an example of such a graph for a group of older men with suspected prostatic obstruction. The highly obstructed and non-obstructed cases are easily picked out (and would in fact be separated by a resistance factor), but there is a substantial borderline group. It is this group, in which occur both high and low resistance factors, that makes the use of such factors so unreliable in practice: the numerical value of the factor does not show whether a case lies in the borderline region or not.

Borderline cases need to be considered carefully. For example, the complete plot of detrusor pressure against flow rate throughout micturition can be examined. Sections 9.2-9.5 have shown that in many types of obstruction the shape of the plot is altered from the highly distensible type (figure 7 .2, curve A), towards the more nearly rigid type (figures 7.2(B), 9.3 and 9.4(A)). Although there are exceptions (Abrams and Griffiths 1979), this enables one to pick out obstructed urethras with more certainty. The interpretation of pressure/flow plots is discussed further in § 11.3.

[†] The maximum flow rate is, by itself, a useful measurement. A high value rules out obstruction with a fair degree of certainty (figure 9.5). Furthermore, it is normally nearly independent of the volume voided, for volumes greater than about 150 ml (see figure 11.3).
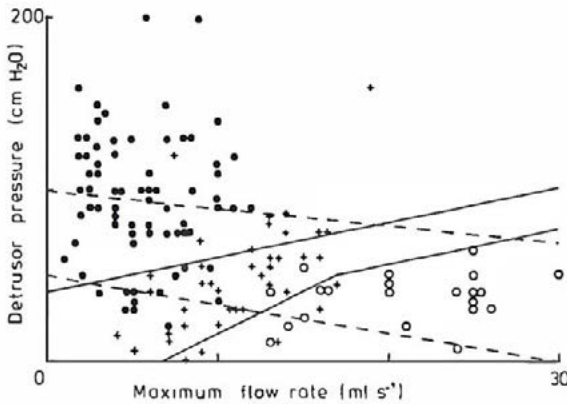
Figure 9.5 Values of maximum flow rate and detrusor pressure at maximum flow for a group of older males. Open circles, full circles and crosses, judged clinically to be unobstructed, obstructed and doubtful, respectively. The full lines divide the graph into three regions in which, on urodynamic grounds, the unobstructed obstructed and borderline cases might lie. The borderline region between the lines contains most of the crosses, as one would expect. Between the broken lines lies the region where the pressure/max. flow points should fall for bladders of normal contractility, provided the initial bladder volume is between 100 and 400 ml (see §10.3). With this proviso, points lying above and below this region correspond to hyper- and hypocontractile bladders, respectively. Many of the obstructed cases have hypercontractile bladders. (After Abrams and Griffiths 1979.)

9.7 The Obstructive Effect of a Urethral Catheter

Clinical micturition measurements are often made with a fine catheter in the urethra. In principle, this must alter the urethral resistance relation and so influence the measured pressure and flow rate.

The normal urethra is highly distensible. The effect of the catheter is to occlude part of the cross-sectional area and so raise the pressure

corresponding to a given open cross-sectional area by HA_{cat}. where A_{cat} is the cross-sectional area of the catheter, and H is the distensibility of the urethra.

For the compressive zone of the normal female or male urethra, and also for the normal male external meatus, H is of order 1 cm H_2O/mm² (see figure 7.3(b) and equation (8.8)). Therefore with a catheter of diameter 3 mm, and cross-sectional area of 7 mm², the pressure increase is about 7 cm H_2O. The urethral resistance relation will be shifted to higher pressures by this same amount. The catheter is not likely to make the meatus obstructive in the normal male.

It does not follow that the detrusor pressure will be raised by 7 cm H_2O. The detrusor responds to a higher pressure with a lower flow rate (see figures 10.7 and 11.1 (inset)). Thus the increase in detrusor pressure might be about 3.5 cm H_2O, while the flow rate might be reduced by about 3.5 ml s^{-1}. These figures agree in order of magnitude with the measurements of Smith (1968) on a normal male. Such changes are not clinically significant.

In obstruction, on the other hand, part of the urethra behaves as if it is less distensible or near-rigid, with a cross-sectional area of about 1 mm² (§ §9.2.2, 9.4 and 9.5). Thus a catheter of cross-section 7 mm² may greatly exaggerate the degree of obstruction. This fact may well be an advantage in the diagnosis of urethral obstruction.

10 The Bladder

10.1 The Collection Phase

10.1.1 Cystometry

In the working of the normal bladder two phases can be distinguished: the evacuation phase during which the detrusor contracts actively for micturition, and the collection phase during which urine accumulates in the bladder. In the collection phase, provided that there is no bladder instability (see § 1.2.2), the detrusor muscle behaves much as an ordinary non-muscular substance. Its mechanical properties in this phase will be called 'passive', even though they may depend partly on metabolic processes occurring in the muscle.

During clinical cystometry the detrusor pressure and the volume in the bladder are measured while the bladder is filled (§2.1). The main aims are to determine the capacity of the bladder and to monitor detrusor activity, especially the involuntary contractions which signify an unstable bladder. If the bladder is filled very quickly ($\gg$ 100 ml min^{-1}), the passive detrusor pressure rises to high values (40 cm H_2O or more) and a pressure decay is observed after filling has ceased. At more usual filling rates (10 -100 ml min^{-1}) and in the absence of instability, however, the detrusor pressure normally remains low during filling ($\leq$ 10 cm H_2O) and any subsequent pressure decay is masked by noise. If, exceptionally, the detrusor pressure rises substantially at a low rate of filling, with or without obvious detrusor instability, then pressure decay may be observed when the filling is stopped (c.f. figure 2. 1). In such cases it is sometimes difficult, although clinically important, to distinguish between a sustained active contraction (instability) and abnormal passive mechanical properties.
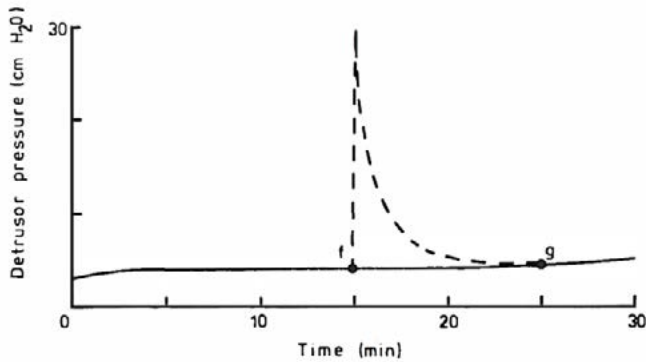
Figure 10.1 Schematic filling cystometrograms. With slow filling at 20 ml min^{-1} the detrusor pressure follows the full curve. At f the bladder contains 300 ml and at g, 500 ml. If, after slow filling to 300 ml, 200 ml is very rapidly injected into the bladder, the detrusor pressure follows the broken curve from f to g.

Thus the principal normal observations to be accounted for are as follows:

(i)   In a stable bladder, at filling rates up to about 100 ml min^{-1}, the detrusor pressure rises very little as the bladder volume increases from zero up to several hundred millilitres.

(ii)   With filling rates greater than 100 ml min^{-1} the detrusor pressure decays after filling has ceased.

(iii)   At a given bladder volume a higher detrusor pressure is attained at a very fast filling rate than at lower rates. These observations are summarised in figure 10.1.

10.1.2 Elastic behaviour of the detrusor

Observation (i) above is a natural consequence of ordinary elastic behaviour. If the bladder is treated in the simplest possible way, as a thin-walled sphere of radius R, then from equation (1.2), § 1.1.2, the detrusor pressure is given by

$$p_{\text{det}} = T/\pi R^2, \qquad\qquad (10.1)$$

where T is the total tension across the bladder circumference. For an elastic substance

$$T = T(2\pi R - 2\pi R_0), \qquad\qquad (10.2)$$

where $2\pi R_0$ is the natural, unstretched circumference of the bladder. The function $T(2\pi R - 2\pi R_0)$ depends on the elastic properties of the bladder wall. It is expected to be an increasing function for positive values of the argument, and zero for $R = R_o$. For bladder volumes smaller than that corresponding to radius R_0, the bladder wall folds up and the detrusor pressure remains close to zero. Because of the presence of R^2 in the denominator of equation (10.1), p_{det} does not necessarily increase, or increase rapidly, with increasing R. This accounts qualitatively for observation (i).

Equation (10.1) is potentially useful because it relates the detrusor pressure measured clinically to the tension in the bladder wall, which is essentially what is measured in laboratory experiments on strips of detrusor muscle[†].

[†] The majority of experiments have been carried out on strips of pig bladder, which seems to be mechanically similar to human bladder.

Together with equation (10.2), however, it suggests that the detrusor pressure is zero when $R < R_0$, that is, when the bladder volume is less than a natural, unstretched value $V_0 = 4\pi R_0^3/3$. Whether this is so, clinically, is doubtful; moreover, for the detrusor pressure during *active* contraction (§10.2.3) it is certainly incorrect. Therefore the bladder needs to be treated mathematically in such a way that the detrusor pressure does not necessarily fall to zero at small volumes. Treatment as a *thick*-walled sphere (Van Mastrigt *et al* 1978) is not sufficient.

A simple approximation which overcomes the difficulty is as follows. The bladder is treated as a sphere with a thin outer wall of radius R in which tangential tension T is developed. This wall encloses not only a volume V of fluid, but also a volume V_1 of wall tissue. The tissue is assumed incompressible but otherwise easily deformable so that it can fill up the lumen of the bladder as $V \to 0$. V_1 represents in an idealised way the volume of the non-muscular lining of the bladder wall, together with that part of the detrusor muscle itself which folds up as the bladder empties and so exerts no tangential tension. Equations (10.1) and (10.2) remain valid, but the volume of fluid in the bladder (the bladder volume) is given by

$$V = 4\pi R^3/3 - V_t. \tag{10.3}$$

Provided that $V_t > 4\pi R_0^3/3$, then $p_{det} > 0$ for all $V > 0$.

From the relation between the passive longitudinal tension F and the extension (l - l_0) of a strip of detrusor muscle (see figure 10.2),

$$F = F(l - l_0). \tag{10.4}$$
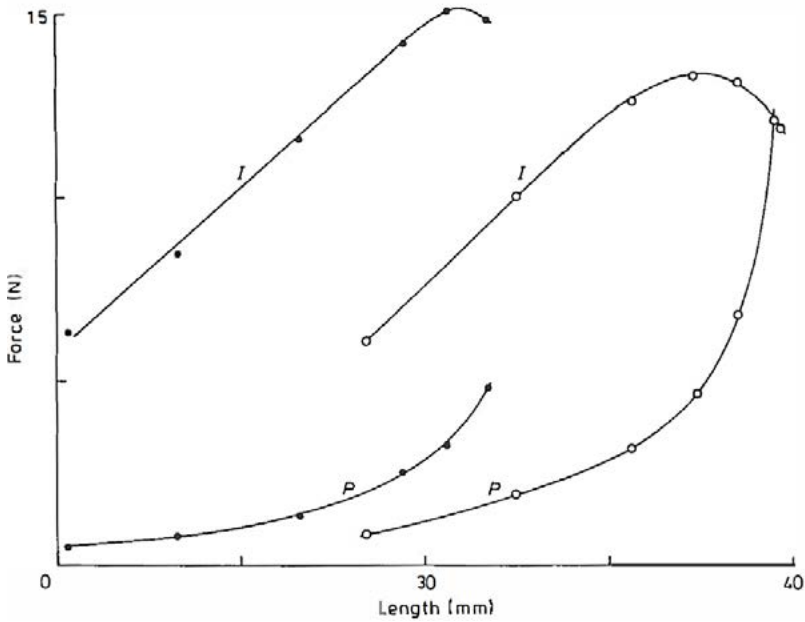
Figure 10.2 Forces exerted in vitro by a strip of pig bladder. P, passive force as a function of strip length l; I, active isometric force as a function of strip length l. Full circles, unstretched length $l_0 \cong 13$ mm; open circles, after plastic extension to an unstretched length $l_0 \cong 22$ mm. (After Griffiths *et al* 1979.)

The force/extension relation is not linear, but its slope increases approximately exponentially with the extension. This is typical of soft body tissues. Equations (10.2) and (10.4) are not identical because one refers to a strip and the other to a whole bladder.

If the length and breadth of the strip represent fractions λ and β respectively of the circumference of the bladder, then

$$2\pi R - 2\pi R_0 = (l - l_0)/\lambda, \qquad (10.5)$$

and one might expect that

$$T = F/\beta \qquad (10.6)$$

Equation (10.6) is not correct, however, because the stress is approximately uniaxial in experiments on strips and isotropic in the two surface dimensions in the spherical bladder. For small strains the tensile stress for a given axial strain is increased by a factor $1/(1 - \sigma)$ in the latter case, where σ is the Poisson's ratio of the material. For nearly incompressible materials, such as the bladder wall, $\cong 0.5$, and so the factor is approximately 2. Assuming that the same factor is applicable at large strains, equation (10.6) is replaced by

$$T = F/\beta(1 - \sigma) \cong 2F/\beta. \qquad (10.7)$$

According to equations (10.5) and (10.7), equation (10.2) can be obtained from equation (10.4), which is valid for strips, merely by scaling the tension and extension variables. The detrusor pressure can then be calculated as a function of volume from equation (10.1). The detrusor pressure calculated in this way from the experimental results shown in figure 10.2 lies close to 5 cm H_2O for bladder volumes between 50 and 600 ml, and falls to 3.5 cm H_2O at zero volume. This is consistent with cystometrograms measured clinically at low filling rates (e.g. figure 10. 1) and in particular accounts for observation (i).

10.1.3 Viscoelasticity

A purely elastic treatment yields no rate- or time-dependence and so § 10.1.2 is limited to near-static situations (slow filling). It cannot account for observations (ii) and (iii). The opposite extreme, very rapid bladder filling, has been investigated experimentally (Van Mastrigt *et al* 1978). During the filling the detrusor pressure rises rapidly and afterwards decays quasi-exponentially over times of order 1 min or more (figure 10.1). This behaviour is similar to the stress relaxation

expected of a passive viscoelastic solid. It can be quantitatively represented by a model containing elements consisting of springs and dashpots (figure 10.3). The elements possess some nonlinear characteristics, consistent with the nonlinear elastic behaviour of figure 10.2.

In the model and in practice, the pressure decay after rapid filling is the sum of three exponentially decreasing contributions with time constants of order 1- 100 s. The form of the decay and in particular the
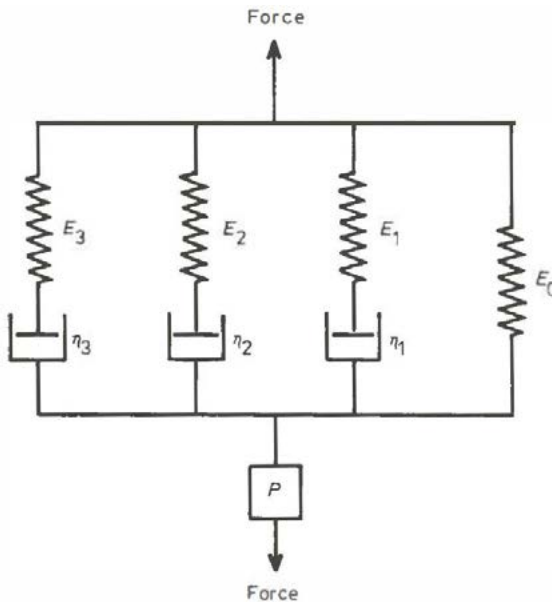
Figure 10.3 Model for the viscoelastic behaviour of a bladder strip. $E_0 - E_3$ are nonlinear elastic elements (springs); $\eta_1 - \eta_3$ are viscous elements (dashpots). The static, time-independent behaviour is governed by E_0. The three E/η series combinations describe the time-dependent behaviour. The element P yields an irreversible plastic extension when the force exceeds a critical value.

time constants are approximately independent of the bladder volume.

According to the model, after the rapid filling the pressure should decay to the static value appropriate to the new volume, as given by equations (10.1) and (10.2) (see figure 10.1). In fact this is difficult to test, because during experiments in vitro the unstretched length of the detrusor muscle continually increases, so that R_0 in equation (10.2) is uncertain. The increase of unstretched length can be incorporated in the model by including an element which flows plastically when the tension exceeds a critical level (figure 10.3).

The viscoelastic model is essentially a small-strain, linear one, slightly modified for use in large-strain, nonlinear situations. It is based on a limited class of experiments and therefore may not be quantitatively accurate in all the situations encountered clinically. Qualitatively, nevertheless, passive viscoelasticity can account for observations (ii) and (iii) in § 10.1.1.

A simple account of viscoelasticity, plastic flow and viscoelastic models is given by Hall (1968).

10.2 The Evacuation Phase

10.2.1 Striated muscle

During normal micturition there is an active contraction of the detrusor. When a muscle contracts actively its mechanical properties undergo a functional change and become quite different from those of the same muscle at rest. The behaviour of striated muscle has been studied extensively (e.g. Wilkie 1956). It is often described in terms of a model consisting of three elements (figure 10.4), which represent mathematical concepts rather than discrete structures in the muscle.

The contractile element CE is responsible for the functional change. It is under nervous control and has peculiarly muscular properties. At rest it exerts no tension. When the muscle is stimulated actively to contract, it develops an active tension. This tension depends on its speed of shortening, as well as on the extension of the muscle and the degree of stimulation. The active tension exerted at zero speed of shortening (i.e. constant length) is called the isometric tension. As the speed of shortening increases the tension exerted decreases in a characteristic way (see equation (10.8) and figure 10.5). The parallel elastic element PE exerts a tension nonlinearly dependent on its extension. During stimulation the total tension in the muscle is the sum of those in the PE and the CE. At rest, only the contribution from
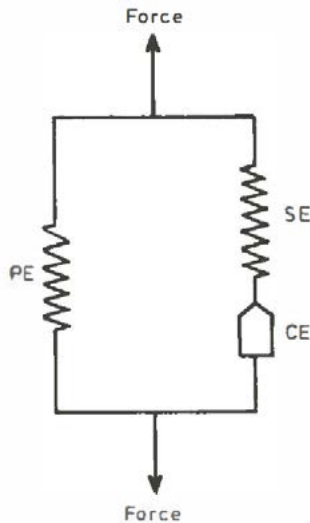
Figure 10.4 Three-element Hill model for the mechanical behaviour of striated muscle. PE and SE, parallel and series nonlinear elastic elements, respectively; CE, contractile element which exerts an active tension only when the muscle is stimulated.

the PE remains. The PE therefore represents the passive mechanical properties of the muscle. The SE is a second nonlinear elastic element in series with the CE. Because of its situation its tension is always equal to the active tension in the CE. Whenever the active tension is altered the length of the SE alters, with the result that sudden changes in the active tension are smoothed out.

10.2.2 The contractile behaviour of detrusor muscle strips

The mechanical properties of smooth muscles, such as the detrusor, are less well known. At the simplest, one might hope to represent them by a model in which the PE of figure 10.4 was replaced by the viscoelastic elements of figure 10.3. Such a model appears complicated because the passive viscoelastic behaviour is complicated. Fortunately, however, during micturition and during experiments on active contraction the passive contribution to the tension is often considerably smaller than the active contribution. During active contraction therefore the passive (viscoelastic) contribution will be neglected: only the CE and SE will be considered. This simplification is a first approximation, which may not always be valid.

The behaviour of the CE under given stimulation is described by the dependence of the tension F on the extension and on the speed of shortening u. In strips the isometric tension F_{iso} depends on the extension of the strip above its resting length, but to a first approximation the ratio F/F_{iso} depends only on the speed of shortening and is independent of the extension (Griffiths et a/ 1979). Thus the extension dependence is completely defined by the relation between F_{iso} and extension (see figure 10.2). The velocity dependence is described by the relation between F/F_{iso} and u, which follows approximately the equation first given by Hill (1938) for striated muscle, written in the form

$$(F/F_{iso} + a/F_{iso})(u + b) = (1 + a/F_{iso})b. \qquad (10.8)$$

Here b and a/F_{iso} are positive constants independent of extension. Equation (10.8) is plotted in figure 10.5. When $u = 0$, F is equal to F_{iso}. As u increases, F/F_{iso} falls monotonically, reaching zero when $u = bF_{iso}/a$.

Plastic extension of the muscle shifts the isometric tension/length relation towards greater muscle lengths (figure 10.2), but does not appreciably affect other parameters.

10.2.3 The contractile behaviour of the complete bladder

The tension developed in a strip at given extension can be related to the detrusor pressure developed by a complete bladder at given volume by means of equations (10.1), (10.5) and (10.7). Strictly, the last of these is valid only for passive elastic forces at small strains, but we assume for simplicity that it can be applied to active forces. Figure 10.6, curve A, show s values of the isometric detrusor pressure calculated in this way from the experimental results of figure 10.2. The agreement with clinical measurements of the isometric detrusor pressure is surprisingly good.

By deriving a relation between the linear speed of shortening of a detrusor strip and the rate of flow out of the complete bladder, equation (10.8) can be transformed into a pressure/flow relation for the bladder (equation (10.14) below). Let U be the speed of shortening of the outside circumference of the bladder, i.e.

$$U = -d(2\pi R)/dt = -2\pi dR/dt. \qquad (10.9)$$

Then

$$U = u/\lambda, \qquad (10.10)$$

where u is the speed of shortening of a strip whose length is a fraction λ of the circumference.

When the circumference shortens, the volume in the bladder diminishes, and therefore fluid (assumed incompressible) flows out of the bladder at a rate

$$Q = -\mathrm{d}V/\mathrm{d}t$$
$$= 2R^2U, \qquad \text{using equations (10.3) and (10.9)} \qquad (10.11a)$$
$$= 2R^2u/\lambda, \qquad \text{using equation (10.10).} \qquad (10.11b)$$

Substitution of equation (10.11b) into (10.8) yields

$$(F/F_{\mathrm{iso}} + a/F_{\mathrm{iso}})(Q + 2R^2b/\lambda) = (1 + a/F_{\mathrm{iso}})2R^2b/\lambda.$$

$$(10.12)$$

Equations (10.1), (10.3) and (10.7) imply that, at given bladder volume,
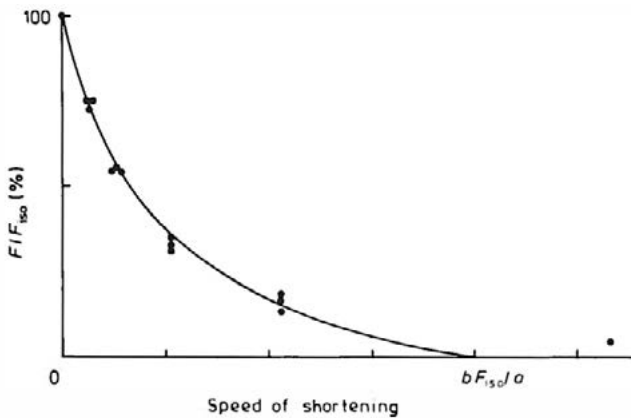
Figure 10.5 Dependence of active force (expressed as percentage of isometric force) on speed of shortening. Curve, equation (10.8), taking as F_{iso}/a as 4. Points, experimental measurements on one bladder strip.

$$F/F_{\text{iso}} = T/T_{\text{iso}} = p_{\text{det}}/p_{\text{det,iso}}, \qquad (10.13)$$

so that

$$(p_{\text{det}}/p_{\text{det,iso}} + a/F_{\text{iso}})(Q + Q^*) = (1 + a/F_{\text{iso}})Q^*. \quad (10.14)$$

Here

$$\begin{aligned}
Q^* &= 2R^2 b/\lambda \\
&= 2(3/4\pi)^{2/3}(V + V_t)^{2/3}\, B,
\end{aligned} \qquad (10.15)$$

using equation (10.3), and also writing

$$B = b/\lambda. \qquad (10.16)$$

B is the value of the velocity parameter b appropriate to a strip whose length is the whole bladder circumference. Equation (10.14) is confirmed by measurements on complete pig bladders (Van Mastrigt and Griffiths 1979). The value of the constant a/F_{iso} is approximately 0.25.
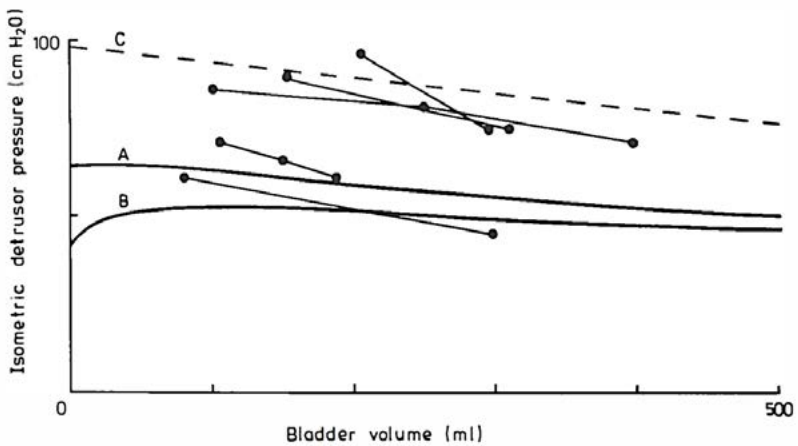
Figure 10.6 Dependence of isometric detrusor pressure on bladder volume. A, as calculated from figure 10.2, assuming an unstretched length of 4 mm. B, as calculated assuming an unstretched length plastically extended to 5 mm. C, linear approximation equation (11.4). The points show clinical measurements on five male patients, believed to be normal. Straight lines connect successive measurements on each patient. (After Griffiths and Rollema 1979.)

According to equation (10.14), at a given bladder volume the pressure generated by the detrusor depends on the flow rate out of the bladder, much as the voltage across the terminals of a battery depends on the current drawn from it because of its internal resistance. The relation between detrusor pressure and flow rate (figure 10.7), is called the bladder output relation. At zero flow rate the detrusor pressure takes its isometric value. As the flow rate increases, the detrusor pressure falls, reaching zero at a flow rate $Q^* F_{iso}/a \cong 4Q^*$. (We continue to neglect any passive contribution to the detrusor pressure.)
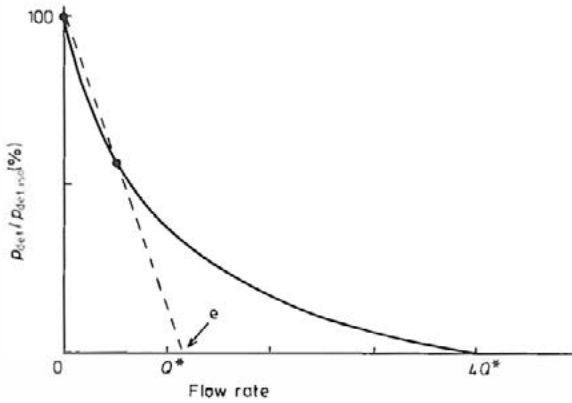
Figure 10.7 The bladder output relation, equation (11.2), with $F_{iso}/a = 4$. The two points represent measurements made immediately before and after interruption of flow by the periurethral sphincter. A straight-line extrapolation gives an estimate (e) of Q.

The bladder output relation is volume-dependent because both $p_{det,iso}$ and Q^* are volume-dependent (figure 10.6 and equation (10.15)). As we have seen, it is an automatic, geometrical consequence of the well-known relation between force and speed of shortening, equation (10.8), for muscles.

Under given stimulation, then, the contractile behaviour of the bladder is described by the bladder output relation together with the dependence of the two parameters $p_{det,iso}$ and Q^* on the bladder volume. If the degree of stimulation is altered then functional changes will occur. In particular, one may expect $p_{det,iso}$ to change.

10.2.4 Exercise

Consider a bladder for which $B = 5$ mm s^{-1} , $a/F_{iso} = 0.25$ and $V_t = 50$ ml.

(i)   Calculate $Q*$ for bladder volumes V of 462, 166 and 14 ml.
(ii)   Suppose that the bladder is initially filled to 500 ml and then contracts actively while fluid leaves it at a constant flow rate of 25 ml s^{-1}. Use figure 10.7 to estimate $p_{det}/p_{det,iso}$ for V= 462 and 166 ml. What is the result when V= 14 ml?
(iii) Hence estimate, using figure 10.6, curve A, the detrusor pressures exerted during emptying at 25 ml s^{-1} when V= 462, 166 and 14 ml. (Neglect any contribution to the detrusor pressure from the PE.)

10.2.5 The series elastic element

Relatively little is known about this element, the SE, in the detrusor. If it is assumed that its properties are purely elastic and independent of the degree of muscle stimulation, then the relation between the tension in it and its extension appears to be nonlinear and similar in form to the tension-extension relation of the PE (see figure 10.2). It can be approximately described by the equation (Van Mastrigt and Griffiths 1979)

$$T = Y \exp(\mu \Delta L)\Delta L, \qquad (10.17)$$

where Y and μ are positive parameters. ΔL is the total extension of the SE in the whole bladder circumference, and μ is approximately independent of muscle extension and is of order 25 m^{-1}. Y depends on the extension, and its order of magnitude is 100 Nm^{-1}. For simplicity we shall treat it as a constant.

When the tension T changes, ΔL and therefore the overall length of the muscle (i.e. the bladder circumference) change (see figure 10.4). Since T changes during micturition, the extension of the SE changes. This affects the course of micturition (see § 11 .2.3).

10.3 Clinical Assessment of Bladder Contractility

In the clinic there is a natural tendency to equate the contractility of a bladder with the detrusor pressure measured during micturition. The discussion of § 10.2.3 has shown however that this yields an incomplete assessment, because the pressure developed depends on the flow rate and the bladder volume through the bladder output relation.

A simple but more satisfactory method of assessment is graphically to plot a point showing the maximum flow rate and the corresponding detrusor pressure, and to see how this point lies with respect to the regions corresponding to normal, hyper- and hypo-contractile bladders. Although the bladder output relation is volume-dependent, neither $p_{det,iso}$ nor Q^* vary particularly sharply with V. Thus it is possible to mark on the pressure-flow graph a region of normal contractility corresponding to normal bladder output relations for volumes between 100 and 400 ml, as shown schematically in figure 9.5. The regions of hyper- and hypo-contractility are then obvious. Since the pressure-flow plot is the same as that suggested in §9.6.2 for the assessment of urethral obstruction, this simple method is potentially attractive.

More sophisticated assessment of contractility is possible if two points of the bladder output relation are determined. This can often be done by asking the patient to interrupt the stream before the bladder is empty (Griffiths 1977b). Usually the periurethral sphincter is quickly closed and the detrusor pressure rises to its isometric value.

Thus $p_{det,iso}$ is observed directly. Q can be determined by fitting equation (10.14) to the two points measured just before and after the sphincter is closed (see figure 10.7). More simply, a straight line can be fitted to the points. Its intercept on the flow rate axis is quite close to

$Q*$ provided that, as is usually the case, the detrusor pressure during flow is more than half of the isometric detrusor pressure.

Since, in normals, $p_{det,iso}$ is only weakly dependent on bladder volume (figure 10.6), normal values can be established without reference to the volume. The normal range appears to be about 50 to 100 cm H_2O in adults of both sexes. Values above normal are found in both some males with urethral obstruction (c.f. figure 9.5) and in some adult patients with unstable bladders and a history of persistent bed-wetting in childhood. They presumably have hypertrophied (abnormally powerful) detrusors. Values below normal have been measured in females, in whom they presumably may reflect either a weak detrusor or ineffective nervous stimulation. A fall to abnormally low values during the course of micturition indicates a functional change (failure to sustain the active contraction) and may result in residual urine (§ 11.3). The mere observation of a pressure rise to $p_{det,iso}$ is sometimes of value in showing that a detrusor which generates only a very low pressure during voiding is in fact contracting actively[†].

$Q*$ is relatively more sensitive to the bladder volume V. The theoretical volume dependence of equation (10.15) can be approximated in practice by

$$Q^*_{std} \propto V^{1/2}. \qquad\qquad (10.18)$$

[†] In principle passive viscoelasticity can produce a similar effect, but the pressure cannot rise above the passive value measured at the same volume during filling.

To establish and allow comparison with normal ranges, the value of Q^* obtained clinically at volume V should be normalised to a standard volume V_{std}:

$$Q^*_{std} = (V_{std}/V)^{1/2}Q^*. \qquad (10.19)$$

V_{std} is conveniently taken as 200 ml.

The value of Q^*_{std} so obtained is proportional to the fundamental velocity parameter B of the detrusor muscle. With V_1 taken as 50 ml, equation (10.15) suggests that

$$Q^*_{std} \cong 3B, \qquad (10.20)$$

where Q^*_{std} is expressed in ml s^{-1} and B in mm s^{-1}.

Normal values of Q^*_{std} lie between about 30 and 100 ml s^{-1} in both sexes. Q^*_{std} appears lower than normal in some males who have, or have been relieved of, urethral obstruction. Presumably such a 'slow' detrusor is the result of changes associated with detrusor hypertrophy. Q^*_{std} lies above this range in some females, who also tend to have low isometric detrusor pressures. This means that in these patients the rise to the isometric pressure on interrupting the flow is small (about 2 cm H_2O) and easy to miss. Therefore the absence of an obvious rise should not be taken as proof that there is no active contraction; it may indicate a 'fast' detrusor.

Thus, through measurement of $p_{det,iso}$ and Q^*_{std}, detrusors can be classified as powerful or weak, and as fast or slow. The possibility of functional changes during micturition, especially of $p_{det,iso}$ should be borne in mind.

10.4 Summary

In the collection phase the bladder behaves as if it were a hollow sphere of passive viscoelastic material. The small dependence of the detrusor pressure on the bladder volume, its dependence on the rate of filling, and the decay of pressure after filling ceases, can all be understood as consequences of elastic and viscoelastic behaviour.

During micturition much larger, active forces are developed in the bladder wall, and the mechanical behaviour becomes typically muscular. The detrusor pressure depends on both the bladder volume and the rate of urine flow out of the bladder. The dependence on the flow rate is described by the bladder output relation. The higher the flow rate, the lower is the detrusor pressure. This relation contains two volume-dependent parameters, the isometric detrusor pressure, and the flow rate parameter Q^*, which characterise respectively the strength and intrinsic speed of the detrusor muscle, and may be used clinically to assess bladder contractility.

11 The Course of Micturition

11.1 Fundamental Ideas

The urethra is characterised hydrodynamically by a relation between flow rate and detrusor pressure: the urethral resistance relation (§7.2). The bladder is characterised by the bladder output relation, which involves the same pair of variables together with the bladder volume (§ 10.2.3). Simultaneous solution of these two equations yields the flow rate and the detrusor pressure at any bladder volume; that is, at
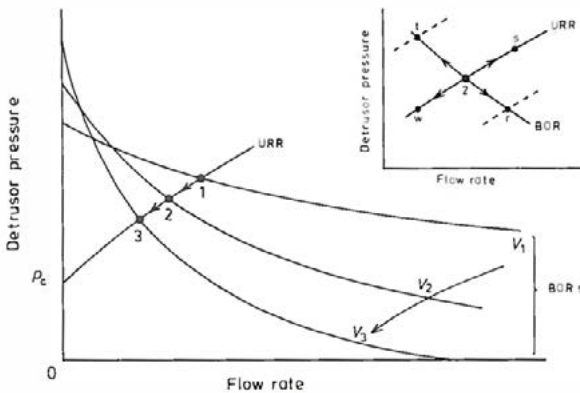
Figure 11.1 Simultaneous solution of the urethral resistance relation (URR) and bladder output relation (BOR). (The detrusor pressure is plotted directly, and not as a percentage.) As the bladder empties from V1 to V3, the flow rate and detrusor pressure normally follow the trajectory 1-2-3 along the URR. Inset: if the urethra is tightened or relaxed during micturition, the URR is altered (broken curves) and the pressure/flow point moves along the BOR to t or r, respectively. If the detrusor contraction becomes stronger or weaker, the BOR is altered and the pressure/flow point moves along the UAR towards s or w, respectively. (This movement is superimposed on the normal 1-2-3 trajectory.)

any moment during micturition (Griffiths 1973). (This statement is slightly oversimplified; see § 11.2.3). The solution is easily visualised graphically, as shown in figure 11.1.

Two different views of the solution are possible. On the one hand, the course of normal micturition can be calculated, using typical normal values of all the parameters that appear in the equations (Griffiths and Rollema 1979, see also Drolet and Kunov 1975). The calculated course is of a micturition which proceeds automatically, according to fixed equations, once the bladder has been switched on; that is, of a micturition during which no functional changes occur. The calculated course may be compared with actual observations of the micturitions of apparently normal volunteers, selected for their ability to produce consistent results. In this way one may assess the accuracy of the equations, and also whether in fact functional changes do occur in these ideally normal micturitions. This is really a test of the adequacy of the purely mechanical approach (see §11.2).

On the other hand, the variations of pressure and flow during the course of an actual, perhaps pathological, micturition may be observed, and one may try to deduce information about the urethral resistance relation, the bladder output relation, and what functional changes have occurred during the micturition, if any. This is the clinical situation (see § 11.3).

11.2 The Course of Ideal Normal Micturition, as Calculated from the Urethral Resistance and Bladder Output Relations

11.2.1 Calculation without series elastic element

If no functional changes occur during micturition, then the urethral resistance relation (URR) remains fixed, while the bladder output relation (BOR) changes as the bladder empties. Thus the point

representing the simultaneous solution of the two relations sweeps along the URR (figure 11.1). This is how the URR can be determined (§7.2.1). Only the variations in the flow rate during micturition need be considered explicitly, since the detrusor pressure is always related to the flow rate via the fixed URR.

Clinically observed normal URRs (figure 7.2, curve A) can be approximated quite well by the relation

$$Q = \alpha(p_{\text{det}} - p_{\text{c}}) \qquad \text{for} \qquad p_{\text{det}} > p_{\text{c}}; \qquad (11.1a)$$
$$Q = 0 \qquad \text{for} \qquad p_{\text{det}} < p_{\text{c}}, \qquad (11.1b)$$

where α and p_{c} are constants for a given urethra, α is the reciprocal slope of the URR, typically 1 ml s^{-1}/cm H$_2$O, and p_{c} is the opening pressure (wrt abdominal pressure) of the compressive zone, typically 25 cm H$_2$O.

The BOR is (equation (10.14))

$$(p_{\text{det}}/p_{\text{det,iso}} + a/F_{\text{iso}})(Q + Q^*) = (1 + a/F_{\text{iso}})\, Q^*. \quad (11.2)$$

Typically, $a/F_{\text{iso}} = 0.25$, and Q^* is volume-dependent. According to the model it is given by equation (10.15) as

$$Q^* = 2(3/4\pi)^{2/3}(V + V_t)^{2/3}\, B. \qquad (11.3)$$

Typically, $Q^* \cong 60$ ml s^{-1} when $V = 200$ ml (§ 10.3), so that $B = 20$ mm s^{-1} (equation (10.20)).

$p_{\text{det.iso}}$ is also volume-dependent. The clinical measurements (figure 10.6) can be well approximated by a linear decrease with increasing bladder volume. We shall suppose that

$$p_{\text{det,iso}} = p_0[1 - k(V + V_t)], \qquad (11.4)$$

taking as typical values p_0 = 100 cm H_2O and k = 5 × 10⁻⁴ ml⁻¹. V_t is included in equation (11.4) merely for convenience in solving the equations.

Substitution for p_{det} in equation (11.2) from equation (11.1a) leads to a quadratic equation for Q, with coefficients that depend on $(V + V_t)$ through equations (11.3) and (11.4). The quadratic equation can be solved for various values of $(V + V_t)$, so yielding the flow rate Q as a function of the bladder volume. (The negative root is ignored.) Figure 11.2, curve A shows the result when the typical values of the parameters are used. V_t remains arbitrary; in figure 11.2 a value of 50 ml has been selected.
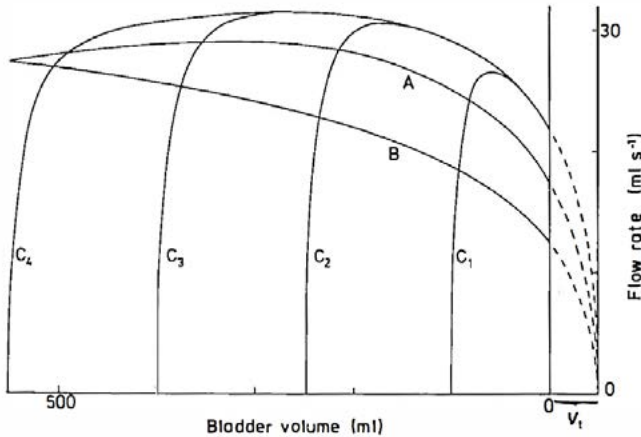
Figure 11.2 Flow rate calculated as a function of bladder volume. **A**, without SE, with typical values of other parameters; **B**, without SE, isometric detrusor pressure altered to allow for plastic extension ($p_{det,iso}$ = 70 cm H_2O, constant), C_1-C_4, with typical values of all parameters, including SE. V_t has been taken to be 50 ml.

11.2.2 Observations on normal volunteers

What is usually plotted is not flow rate against bladder volume, but flow rate against time. Provided that the bladder is emptied to completion, however, one plot is easily converted to the other, since the bladder volume at time t_i, is given by

$$V(t_i) = \int_{t_i}^{end} Q(t)dt. \tag{11.5}$$

Figure 11.3 shows 17 micturitions of one healthy male volunteer, recorded as flow rate against bladder volume. The initial bladder volume is of course different for each micturition, but otherwise the results are very consistent. After a rising leg, in nearly every micturition the flow rate follows an approximately common course; i.e. there is (approximately) one value of flow rate appropriate to each bladder volume. Micturitions from very large initial volumes do not follow the common course, however. Similar results are seen in other healthy male volunteers, although not always so consistently (Rollema *et al* 1977).
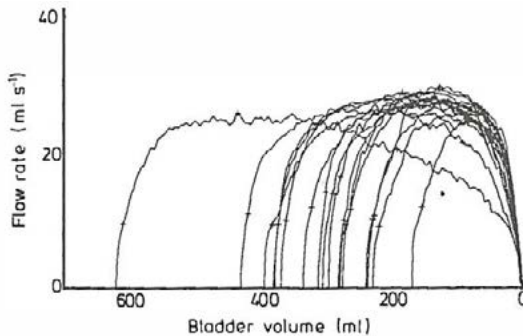
Figure 11.3 Measured flow rate as function of bladder volume: 17 micturitions of one healthy male volunteer. (Reproduced from Griffiths and Rollema 1979 Med. Biol. Engng Comput. **17** 291-300, by permission of the Int. Fed. for Med. and Bioi. Engng).

The calculation of §11.2.1 does not describe the rising legs of the flow curves. (Section 11.2.3 will show that they are the result of the series elastic element.) It does however predict that there should exist a common course. The predicted flow rate has the correct order of magnitude. The predicted shape is in qualitative agreement with the observations, except near $V= 0$. It is in this region that the bladder wall must fold up; the simple model cannot pretend to describe this process adequately.

The deviations from the common course that occur in micturitions from very large initial volumes are of considerable interest. A large initial volume implies a large passive tension prior to micturition (equation (10.1)). *In vitro*, a large passive tension causes plastic extension of the muscle (§10.1.3). If this were to occur also *in vivo*, it would alter the relation between the isometric detrusor pressure and the bladder volume (figure 10.6, curve B). $p_{det,iso}$ would be reduced, and by a greater amount at the lower than at the higher bladder volumes. In the mathematical model of §11.2.1, such an effect could be taken into account by suitably altering the parameters p_0 and k in equation (11.4). If this is done, the calculated relation between flow rate and bladder volume becomes similar to the high-volume micturitions (see figure 11.2, curve B). Thus it is feasible that plastic extension of the muscle is responsible for these deviations from the common course. The plastic extension is not truly permanent, for it disappears before the next micturition.

11.2.3 The effect of the series elastic element

If one takes into account the possibility of changes in the length of the SE, then the rate of shortening of the bladder circumference is equal to the sum of the speeds of shortening of the CE and of the SE, v and $-d(\Delta L)/dt$, respectively. Therefore the speed of shortening of the CE is not given by equation (10.9), but by

$$v = -2\pi \mathrm{d}R/\mathrm{d}t + \mathrm{d}(\Delta L)/\mathrm{d}t. \qquad (11.6)$$

Hence equation (10.11a) is replaced by

$$Q = -4\pi R^2 \, \mathrm{d}R/\mathrm{d}t \qquad (11.7a)$$
$$= -2\, R^2 [v - \mathrm{d}(\Delta L)/\mathrm{d}t]. \qquad (11.7b)$$

ΔL, the extension of the SE, satisfies equation (10.17), which with the help of equation (1.2) may be written:

$$Y \, exp \, (\mu \Delta L)\Delta L = \pi R^2 p_{\mathrm{det}}. \qquad (11.8)$$

From equations (10.8}, (10.13) and (10.16),

$$v = \frac{\left(1+\frac{a}{F_{\mathrm{iso}}}\right)B}{p_{\mathrm{det}}/p_{\mathrm{det,iso}}+a/F_{\mathrm{iso}}} - B. \qquad (11.9)$$

Elimination of ΔL, v and p_{det} from equations (11.7b)-(11 .9), together with the urethral resistance relation equation (11.1a), yields a first-order differential equation for Q in terms of V. The course of micturition can be found by numerical solution. (See Griffiths and Rollema 1979 where, however, a linear approximation to equation (11.9) is used.)

In figure 11.2, curves C, solutions are shown for which the same typical values of the parameters have been used as for curve A. For the series elastic element, values of Y and μ suggested by the experiments on pig bladders (see §10.2.5) have been used. The SE has two main effects.

(i)   It accounts for the initial rising leg of the curve where the flow rate is approaching the common course from below. On this leg the pressure is rising and the SE is being extended. Hence the flow rate is less than it would be if only the CE were present (equation (11.7b)).

(ii)   It alters the common course, raising the flow rate especially at the smaller volumes. Along the common course the volume is diminishing. Hence the tension in the muscle decreases (equation (1.2)) and the SE becomes shorter. The shortening of the SE gives an extra contribution to the flow rate, over and above that of the CE (equation (11.7b)).

The extension of the SE is maximum where the flow curve, calculated with the SE, crosses the common course as calculated without the SE (see figure 11.2). When the parameters have the values assumed for figure 11.2, curves A and C, the maximum extension of the SE is just under 25% of the corresponding bladder circumference.

Comparison of figures 11.2C and 11.3 shows that the mathematical model, without adjustment of any parameter value, accounts semi-quantitatively for the course of ideal, normal micturition. In detail, there are one or two discrepancies between model and reality. The end of micturition, where $V \lesssim V_t$ is not adequately described by the model. The actual form of the calculated flow curves is not quite correct. In the model, the flow rate rises quite rapidly to the common course, and thereafter tends to fall, so that the flow curve is distinctly skewed, the maximum occurring early in the micturition. In reality the maximum flow rate is reached typically after 45% of the initial volume has been voided (Abrams and Torrens 1979).

Thus the gross features of the flow curves can be understood as the result of the automatic, mechanical behaviour of bladder and urethra, without involving functional changes during voiding. (Of course, large functional changes occur before and after voiding (§7.2.3).) The peculiar character of voidings from very large initial volumes can be accounted for mechanically.

11.3 Pressure/Flow Plots

Clinically, one may try to make a urodynamic assessment from a flow curve (e.g. flow rate against time) alone; urologists often do so. Further information is contained in the intravesical and detrusor pressures. A plot of detrusor pressure against flow rate throughout micturition is especially valuable.

In principle, simultaneous values of detrusor pressure and flow rate are required. In practice, the flow rate measurement is smoothed and delayed (§2.2.1), and so the plot is reliable only when the variables are changing relatively slowly. Some improvement can be made by suitably delaying the pressure measurement before it is plotted. Repetition of the plot on several micturitions helps one to recognise artefacts, and to distinguish variable features, which may be due to functional changes, from constant features which may, for example, be due to an organic obstruction.

Provided that no functional changes occur in the urethra, the interpretation of the plot is straightforward. The URR remains constant, while the BOR alters. Thus the point of intersection, representing the simultaneous values of detrusor pressure and flow rate at a given instant of micturition, sweeps along the URR, so tracing it out (figure 11.1). The shape of the URR is different for unobstructed and obstructed urethras, which therefore can be distinguished (see figures 7.2, 7.3, 9.3 and 9.4). This is valuable in cases where the detrusor contraction is poor, so that assessment of obstruction merely from the *maximum* flow rate and the corresponding detrusor pressure is difficult (see §9.6.2).

The effect of tightening or relaxation of the urethra during the course of voiding is shown schematically in figure 11.1. The point representing the values of pressure and flow moves along the BOR.

The complete interruption of the flow, by which the BOR can be determined (§ 10.3), is an example of such a urethral tightening. Because the direction of movement on the plot is characteristic, functional changes of the urethra can be identified. Abdominal straining can mimic the effect of urethral relaxation (figure 7.1), but is easily recognised from the separate recording of abdominal pressure.

One common observation in both obstructed and unobstructed cases is that the detrusor pressure at a given flow rate is higher when the flow rate is rising near the beginning of voiding than when it is falling at the end. This may be partly due to a functional change – relaxation – in the urethra during voiding. The change is small in the unobstructed case (§7.2.1).

Many of the patients examined in the clinic suffer from diseases which disrupt the nervous control of bladder and urethra (see §§ 1.1.4 and 1.2.3). Consequently, functional changes occur in both organs during micturition. The resulting pressure/flow plots may be difficult to interpret, because neither the URR nor the BOR remains constant.

Very often in these cases the bladder does not empty completely, and residual urine is left. Referring to figure 11.1, residual urine can occur only if $p_{det,iso}$ falls below p_c before the bladder is empty. (The value of Q^* is unimportant, provided it is not zero.) In the normal situation not only is p_c relatively low, but also $p_{det,\ iso}$ rises as the bladder empties (figure 10.6), so that there is a double safeguard against residual urine. In pathological cases, residual urine can occur in either of two (extreme) ways.

(i)   Near the premature end of voiding, p_c may rise until it exceeds $p_{det,iso}$; i.e. voiding is terminated by a urethral spasm.

(ii)   Alternatively, $p_{det,iso}$ may fall to below p_c; i.e. voiding ceases because of an inadequately sustained detrusor contraction.

Possibilities (i) and (ii) can be distinguished by the pressure/flow plot, because the direction from which the plot approaches $Q = 0$ is different in the two cases. If there is a urethral spasm, p_{det} rises as Q falls; if the detrusor contraction fails, p_{det} falls as Q falls to zero, as shown in figure 7. 1.

Thus in principle the pressure/flow plot can be interpreted to give a history of the mechanical events that have occurred in bladder and urethra during voiding.

12 Conclusions

In this book I have tried to present, reasonably completely, a fruitful way of thinking about the lower urinary tract. It is a personal viewpoint which in some respects conflicts with the accepted wisdom concerning micturition. It would be too optimistic to expect that everything put forward here will prove to be exactly correct. Nevertheless these ideas do seem to be a sound starting point for the understanding both of clinical urodynamic measurements and of the physiology of micturition.

The mechanical approach taken in the book can account for many experimental and clinical observations. For example, the behaviour of the normal urethra and the normal bladder during micturition, and thus the whole course of micturition, can be understood almost completely in mechanical terms (Chapters 7, 10 and 11). However, it must always be remembered that the urinary tract is not a purely mechanical system, but is under neuromuscular control (Chapter 1). The control is exerted at all levels of the nervous system, conscious and unconscious – in the brain, in the spinal cord and in the urinary tract itself. Abnormal behaviour may be purely mechanical or may originate from any of these levels of control. Even when the primary abnormality is mechanical, the control system may also be disturbed. For this reason the possibility of functional changes – changes in mechanical properties which may reflect the operation of the control system – has been continually stressed. An understanding of what the mechanical behaviour would be if there were no functional changes helps one to deduce in a particular case whether such changes are occurring. So, perhaps, one can begin to identify pathological malfunctioning. Without such an understanding, behaviour which is the natural result of the given mechanical properties may be ascribed

to the operation of the neuromuscular control system, and a distorted view of both normal and pathological functioning obtained.

Further Reading

Turner-Warwick R and Whiteside C G (eds) 1979 *Clinical Urodynamics : Urologic Clinics of North America* vol 6, no. 1 (Philadelphia: Saunders)

This book gives a complementary clinical and (despite the series title) predominantly European view of urodynamics and the anatomy and function of the lower urinary tract. It contains a good deal of practical advice.

Hinman F Jr (ed) 1971 *Hydrodynamics of Micturition* (Springfield, Illinois: Thomas)

This book gives earlier and mainly American views of urodynamics, both clinical and theoretical.

International Continence Society 1976, 1977, 1978 *First, second and third reports on the standardisation of terminology of lower urinary tract function*

First report (on storage of urine in the bladder, urinary incontinence, units of measurement), Br. J. Urol. (1976) **48** 39-42, and others

Second report (on micturition, use of symbols), Br. J. Urol. (1977) **49** 207- 10

Third report (on micturition: pressure-flow relationships and residual urine), Scand. J. Urol. Nephrol. (1978) **12** 19 1-3
First, second and third reports combined: J. Urol. (1979) 121 551 -4
These reports are required reading for anyone seriously interested in urodynamics.

International Continence Society Proceedings of Annual Meetings, Urol. Int. (1974) **29** 163-236; (1975) **30** 1-108; (1976) **31** 1- 136; (1977) **32** 81 -268; (1977) **33** 1-204; (1978) **33** 277-376 New results are often reported in the Proceedings.

Rowan D 1973, 1976 Incontinence Reporter 1 nos 3 and 6 (Buckingham, UK: Vitalograph) These are useful lists of references to the urodynamic literature.

References

Abrams P H 1979 *Clinical Urodynamics* ch 10A (see Further Reading)

Abrams P H and Griffiths D J 1979 *Br. J. Urol*. **51** 129-34

Abrams P H. Martin S and Griffiths D J 1978 *Br. J. Urol*. **50** 33-8

Abrams P H and Torrens M 1979 *Clinical Urodynamics* ch 8A (see Further Reading)

Bates C P, Arnold E P and Griffiths D J 1975 *Br. J. Urol.* **47** 65 1-6

Beard A N 1977 *Med. Biol. Engng Comput*. 15 273-9

Brower R W and Scholten C 1975 *Med. Biol. Engng* **13** 839-44

Cass A S and Hinman F Jr 1971 *Hydrodynamics of Micturition* eh 12 (see Further Reading)

Conrad W A 1969 *IEEE Trans. Biomed. Engng* **BME-16** 284-95

Dawson S V and Elliott E A 1977 *J. App/. Physiol.: Respirat. Environ. Exercise Physiol*. **43** 498-5 15

Drolet R and Kunov H 1975 *Med. Biol. Engng* **13** 40-55

Elliott E A and Dawson S V 1977 *J. Appl. Physiol.: Respirat. Environ. Exercise Physiol*. **43** 51 6-22

--- 1979 *Med. Biol. Engng Comput*. **17** 192-8

Eyrick T B, Many M and Wise H M Jr 1969 *Invest. Urol*. **6** 443-65

Gardner A M N. Turner M J, Wilmshurst C C and Griffiths D J 1 977 *Med. Biol. Engng Comput.* **15** 248-53

Gleason D M, Reilly R J, Bottacini M R and Pierce M J 1974 *J. Urol*. **112** 81 -8

Gosling J 1979 *Clinical Urodynamics* ch 3 (see Further Reading)

Griffiths D J 1969 *Med. Biol. Engng* **7** 20 1-15

--- 1971a ,b *Med. Biol. Engng* **9** 58 1-8 and 589-96

--- 1973 *Br. J. Urol*. **45** 497-507

--- 1975a,b,c *Med. Biol. Engng* **13** 785-90, 791-6, 797-802

--- 1977a *Med. Biol. Engng Comput*. **15** 357-62

--- 1977b *Br. J. Urol*. **49** 29-36

Griffiths D J and Rollema H J 1979 *Med. Biol. Engng Comput*. **17** 29 1-300

Griffiths D J , Van Mastrigt R, Van Duyl W A and Coolsaet B L R A 1979 *Med. Biol. Engng Comput*. **17** 28 1-90

Hall I H 1968 *Deformation of Solids* (London: Nelson) chs 6 and 7

Hill A V 1938 *Proc. R. Soc*. **B126** 1 36-95

Huisman A B 1978 *Morfologie van de vrouwelijke urethra* Thesis, State University of Groningen, The Netherlands

Hutch J A 1966 *J. Urol*. **96** 182-8

International Continence Society 1976, 1978 First and third reports on the standardisation of terminology of lower urinary tract function (see Further Reading)

McDonald D A 1974 *Blood Flow in Arteries 2nd edn* (London: Arnold)

Martin S and Griffiths D J 1976a,b *Med. Biol. Engng* **14** 512-8 and 519-23

Massey B S 1970 *Mechanics of Fluids 2nd edn* (London: Van Nostrand Reinhold)

Meyhoff H H, Griffiths DJ , Nordling J and Hald T 1979 *Proc 9th Ann. Mtg Int. Continence Soc, Rome ed* G. Guidotti pp205-9

Netter F H 1965 *Ciba Collection of Medical Illustrations vol 2, Reproductive System* (rev. edn) (New York: Ciba Pharmaceutical Co.)

Nyman C R 1976 Scand*. J. Urol. Nephrol*. Suppl. 39

Oates G C 1975a,b *Med. Biol. Engng* **13** 773-9 and 780-4

Plevnik S 1976 *Urol. Int*. **31** 23-32

Reyn J W 1974, 1975 *Delft Prog. Rep*. F **1** 51 -67 and 69-81

Ritter R C , Zinner N R and Sterling A M 1974 *Phys. Med. Biol*. **19** 161-70

Rollema H J, Griffiths D J , Van Duyl W A, Van den Berg J and De Haan R 1977 *Urol. Int*. **32** 401-12

Scott J E S, Clayton C B, Dee P M and Simpson W 1966 *J. Urol*. **96** 763-9

Smith J C 1968 *Br. J. Urol*. **40** 125-56

Sterling A M and Griffiths D J 1976 *Urol. Int*. **31** 321 -31

Tanagho E A 1971 *Hydrodynamics of Micturition* ch 2 (see Further Reading)

Tanagho E A, Miller E R, Lyon R P and Fisher R 1971 *Br. J. Urol*. **43** 69-82

Tanagho E A, Miller E, Meyers F H and Corbett R K 1966 *Br. J. Urol*. **38** 72-84

Thomas D 1979 *Clinical Urodynamics* ch 24 (see Further Reading)

Turner-Warwick R 1979 *Clinical Urodynamics* ch 2 (see Further Reading)

Turner-Warwick R and Brown A D G *Clinical Urodynamics* ch 21 (see Further Reading)

Van Mastrigt R, Coolsaet B L R A and Van Duyl W A 1978 *Med. Biol. Engng Comput*.**16** 471-82

Van Mastrigt R and Griffiths D J 1979 Urol. Int. **34** 41 0--20

Van Schaik J C H, Sampurno S B, Sipkema P and Westerhof N 1977 *Pressure-flow Relations in Narrow Collapsible Tubes, FUPREP No. 7701* (Amsterdam: Physiological Laboratory, Free University)

Whitaker J and Johnston G S 1966 *Invest. Urol.* **3** 379-89

Wild R, Pedley T J and Riley D S 1977 *J. Fluid Mech*. **81** 273-94

Wilkie D R 1956 *Br. Med. Bull*. **12** 177-82

Worth P 1979 Clinical Urodynamics ch 20 (see Further Reading)

Zinner N R, Ritter R C , Sterling A M and Harding D C 1969 *J. Urol*. **101** 914-8

Index